International Journal of
Applied Sciences and Smart Technologies

Volume 04, Issue 01, June 2022

p-ISSN 2655-8564 & e-ISSN 2685-9432

International Journal of Applied Sciences and Smart Technologies

Volume 4, Issue 1, page i

p-ISSN 2655-8564, e-ISSN 2685-9432

CONTENTS

International Journal of Applied Sciences and Smart Technologies

Volume 4, Issue 1, page ii

p-ISSN 2655-8564, e-ISSN 2685-9432

EDITORIAL BOARD

Contact us
International Journal of Applied Sciences and Smart Technologies
Faculty of Science and Technology
Sanata Dharma University
Kampus III Paingan, Maguwoharjo, Depok, Sleman
Yogyakarta, 55282
Phone : +62 274883037 ext. 523110, 52320
Fax : +62 272886529
Email : editorial.ijasst@usd.ac.id
Website : http://e-journal.usd.ac.id/index.php/IJASST

IJASST is an open-access peer-reviewed journal that mediates the dissemination of research and studies conducted by academicians, researchers, and practitioners in science, engineering, and technology.

International Journal of Applied Sciences and Smart Technologies

Volume 4, Issue 1, pages iii-iv

p-ISSN 2655-8564, e-ISSN 2685-9432

PREFACE

Dear readers, we are delighted to serve you Volume 4, Issue 1 of *International Journal of Applied Sciences and Smart Technologies* (IJASST), which is managed and published by the Faculty of Science and Technology, Sanata Dharma University. IJASST is an open-access peer-reviewed journal that mediates the dissemination of research and studies conducted by academicians, researchers, and practitioners in science, engineering, and technology. Its scope also includes basic sciences which relate to technology, such as applied mathematics, physics, and chemistry.

In this edition, we have nine papers authored by researchers from Indonesia, India, and Palestine. Submitted papers are reviewed fairly using the open journal system (OJS) of IJASST. After the review process, accepted papers of the journal are publicly available for free at the website of IJASST.

For future issues, we are looking forward to your contributions to IJASST.

Dr. I Made Wicaksana Ekaputra
Editor in Chief
IJASST

International Journal of Applied Sciences and Smart Technologies

Volume 4, Issue 1, pages iii-iv

p-ISSN 2655-8564, e-ISSN 2685-9432

This page intentionally left blank

International Journal of Applied Sciences and Smart Technologies

Volume 4, Issue 1, pages 1-20

p-ISSN 2655-8564, e-ISSN 2685-9432

Cryptocurrencies Advantages and Disadvantages: A Review

Zaer Qaroush[1], Shadi Zakarneh[1], and Ammar Dawabsheh[1]

[1]*M.Sc. Student, Palestine Technical University- Kadoorei*

Tulkarem, Palestine

[*]*Corresponding Author: zakarnehshadi@gmail.com*

(Received 07-04-2022; Revised 08-05-2022; Accepted 21-05-2022)

Abstract

With the rapid spread of technology in life and the necessary need to increase the speed of payment processes, confidentiality, and privacy, cryptocurrencies appeared. A cryptocurrency is a virtual and intangible currency, in which transactions are made through the internet. These currencies are characterized by decentralization, transparency, and privacy. Because transactions are carried out through a cryptography process and depend on Blockchain technology it is highly protected. Blockchain generally is a distributed ledger or a decentralized database. The Blockchain architecture combines advanced cryptography, consensus mechanisms, and a complex system of incentives. In cryptocurrency, transactions are created, transferred, and verified through an integrated process called mining. Blockchain technology architecture has given cryptocurrencies many advantages and features that increase their strength and distinction from regular financial transactions such as decentralization, confidentiality, anonymity, very low fees, unrestricted by geography, transparency, protection from Inflation, and the peer-to-peer network. The misuse of powerful features in cryptocurrencies and Blockchain technology has led to many disadvantages such as the risks of lack of knowledge, the lack of wide

Volume 4, Issue 1, pages 1-20

p-ISSN 2655-8564, e-ISSN 2685-9432

acceptance, the high risk of investment, its volatile nature, and the inability to return missing payments. This study concentrates on cryptocurrencies in terms of advantages and disadvantages.

Keywords: cryptocurrency, blockchain, mining, miners, wallet, bitcoin

1 Introduction

Since ancient times, mankind has used more than one method of payment in commercial transactions, such as barter, precious metals coins, and then paper money, which is the most widespread to this day. As a result of the development in the technology market especially the internet, the human race is still looking for new methods of payment suitable to the needs and development of technology, the most recent method is cryptocurrencies which were theoretically laid by Chaum in 1983 relying on a fundamental principle not to misuse and accelerate production [1].

A cryptocurrency is a digital asset that uses cryptography to encrypt transactions and monitor the production of additional currency units as a means of exchange. Cryptocurrencies are categorized as virtual currencies and as alternative currencies [2].

Bitcoin is considered one of the most prominent cryptocurrencies, It was founded by a group that uses the pseudonym Satoshi Nakamoto [1][2]. Numerous other cryptocurrencies have been created since then. As a fusion of bitcoin derivatives, they are often referred to as 'altcoins' which are decentralized power. The decentralized control of the distributed ledger function is related to the Bitcoin Blockchain transaction database [2].

Besides users have complete control over their own money, users can even send very small payments like the so-called Satoshi, which is equal to 0.00000001BTC [3].

Bitcoin is “designed by people for people” and The rules are imposed on everyone through one another's mutual distrust [3], it has provided solutions to the double-spending problem and Byzantine Generals Problem, these innovations made the use of cryptocurrencies possible [4].

Previously before the invention of Bitcoin, it was impossible to deal electronically without a trusted third party, for example, PayPal was used as a trusted third party [4].

Volume 4, Issue 1, pages 1-20
p-ISSN 2655-8564, e-ISSN 2685-9432

To be sure that the same bitcoin has not been used or spent previously, the Blockchain is used to examine new transactions, it is a peer-to-peer network that carries out the verification process by distributing the work to all users In the network to utilize their computing power to reconcile and maintain the ledger in the Blockchain [4].

Solving the problem of double-spending presents another problem concerning the newly added nodes and the current nodes. As for the new nodes, how to make sure that it has the correct ledger?. As for the current nodes, the problem is how it knows that it is getting correct updates of the ledger?, this problem is known as Byzantine Generals Problem [4].

2 Literature Review

There are over a thousand cryptocurrency specifications as of October 2017; most are identical to and derived from the first centralized cryptocurrency, bitcoin, which was completely implemented. The mines are mutually suspicious parties, and maintain the protection, credibility, and balance of the ledger inside cryptocurrency systems: To verify the timestamp, computers belonging to members of the public are used, and they are later added to the ledge according to a firm time stamp. Most cryptocurrencies are designed to progressively reduce currency supply, Putting a final limit on the total amount of currency that will simulate the precious metals in circulation. For law enforcement agencies, cryptocurrencies in terms of seizing them or keeping them as cash in hand are more difficult than traditional currencies owned by financial companies. The leverage of cryptographic technology results in this difficulty [2].

In 1998 Wei Dai published an anonymous distributed electronic cash system 'b-money'. Shortly afterward, Nick Szabo " invented "bit gold. Which is an electronic currency scheme, including other cryptocurrencies that would follow it which allowed users to complete a proof of work feature with cryptographically put together and published solutions. The work of Dai and Szabo's was followed by Hal Finney, who later developed a reusable proof-of-work currency system [2].

Bitcoin was the first decentralized cryptocurrency developed by Satoshi Nakamoto in 2009. As its proof-of-work scheme, it used SHA-256, a cryptographic hash function. In

Volume 4, Issue 1, pages 1-20
p-ISSN 2655-8564, e-ISSN 2685-9432

April 2011, Namecoin was created as an attempt to create a decentralized Domain Name Server (DNS), which would make it very difficult to censor the Internet. Litecoin has launched in October 2011. It was the first popular cryptocurrency using Script instead of SHA-256 as its hash function. The first to use a proof-of-work/proof-of-stake hybrid was Peercoin, another prominent cryptocurrency. IOTA (Distributed Ledger Technology) was the first non-blockchain-based cryptocurrency to use the Tangle instead. While few have been popular, several other cryptocurrencies have been developed, because they brought very little technological innovation [2].

A. Reasons to use Cryptocurrency

Cash payment is characterized as an easy, effective, and fast payment method, but using this method has many disadvantages, including exposure to fraud, loss of money, and costs of managing transactions with financial institutions [5].

Many reasons encourage the trend to use cryptocurrencies, among these reasons are confidentiality and security, to maintain a high degree of security and great confidentiality, cryptocurrencies use encryption methods that use public keys and private keys in transactions and payments, as well as the cryptocurrency transactions carried out easily and quickly. Also due to cost, payment, and money transfer operations are done at the lowest possible cost, as there are no banks or intermediary monetary institutions to transfer funds between the parties [5].

B. Blockchain

Simply the cryptocurrency consist of a public and distributed ledger (distributed database) referred to as Blockchain, which users can use to record their transactions. Blockchain technology is designed to manage cryptocurrencies [6].

Blockchain is a decentralized solution for managing data and transactions. Through this solution, the data is shared and recorded in multiple data stores called a distributed ledger. They are controlled by a network of distributed servers called nodes [7].

In Blockchain, data can only be added and cannot be deleted, the data is in the form of a series of transaction blocks. To protect data and transactions, an encryption method called cryptography is used, and to create data and verify the continuous growth in the data structure, specific mathematical algorithms are used to achieve this [7].

Volume 4, Issue 1, pages 1-20
p-ISSN 2655-8564, e-ISSN 2685-9432

Depending on the practical application of the Blockchain, it is divided into two main types:

1- Permissionless Blockchain: there is no central authority to control users or to control joining or preventing anyone from joining the network. a person only needs a computer with the necessary software installed on it and thus he can join and perform the transactions he wants and store them in the decentralized ledger, an identical copy of the ledgers is distributed to all nodes in the network [7].

2- Permissioned Blockchain: for a person to join the network, approval must be made by the network validators based on specific parameters and rules that are determined by the network administrator, who defines validators and rules. The permissioned Blockchain is divided into two subcategories, (a) Private permissioned Blockchain which restricts access on the network to an administrator to update the ledger, and creates, and stores transactions. Also known as enterprise permissioned Blockchain. (b) Public permissioned Blockchain where the network can be accessed and viewed by anyone [7].

C. How the Blockchain works

Blockchain can be likened to a distributed database. Any node of the network nodes (network members) starts in addition to this database when it creates a data block, then the created data block is broadcasted in encrypted form to all network members, and the other network nodes determine the validity of the data based on the predefined validation algorithm, this method called “consensus mechanism”. After the block validation is completed, the blocks are added to the Blockchain, and then the distributed transaction ledger will be updated [8]. See Figure 1.

International Journal of Applied Sciences and Smart Technologies

Volume 4, Issue 1, pages 1-20

p-ISSN 2655-8564, e-ISSN 2685-9432

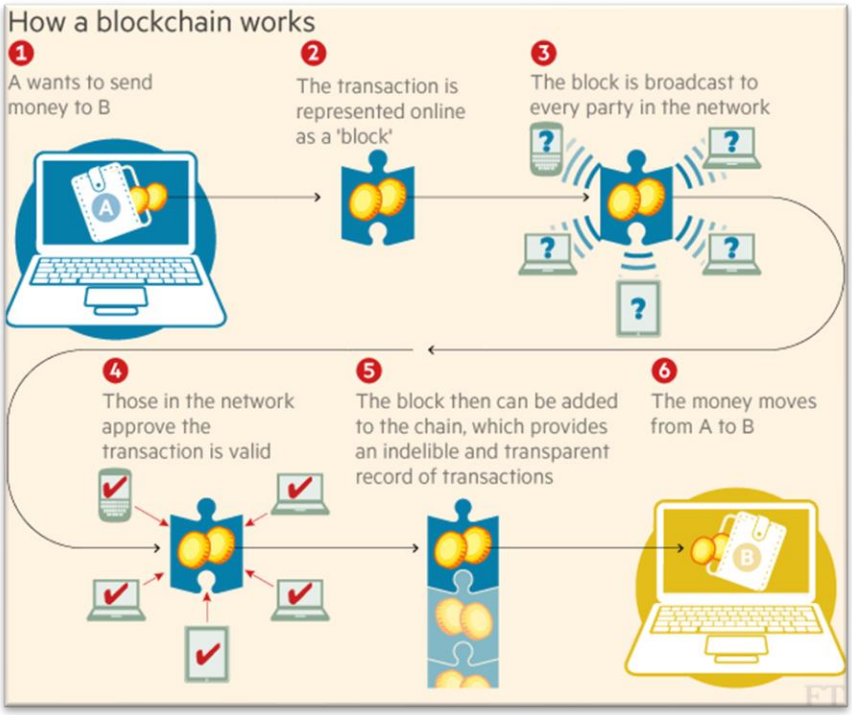

Figure 1. How Blockchain Works [8]

The Blockchain network member has two keys for his transactions public and private keys. The public key will be known to all network members and used as an address on the Blockchain and to validate the sender's identity by verifying the digital signature. The private key is used to create the transaction digital signature. These keys are kept in a digital wallet online or offline [8].

D. Blockchain consensus mechanisms

As the process of validating the added data block is done by a group of Blockchain network nodes in a decentralized manner to ensure its legitimacy, there must be an agreement between the nodes on the method of validation, this is known as the consensus mechanism, which is a predefined encrypted method within certain parameters. It ensures the correct sequence of transactions in the Blockchain. As an example of this in the case of cryptocurrencies, these mechanisms include preventing the problem of double payment [9]. The Blockchain uses a certain consensus

Volume 4, Issue 1, pages 1-20
p-ISSN 2655-8564, e-ISSN 2685-9432

mechanism based on the resources required and the expected results. Different types of consensus mechanisms used in Blockchain technology are as follows:

1- Proof of Work (PoW): it is known as mining and the network nodes are the miners. This process needs large-scale computing power to enable miners to solve complex mathematical puzzles. Many cryptocurrencies like bitcoin used this mechanism [10].
2- Proof of Stack (PoS): In this mechanism, who has the priority to produce the next block is determined, this is done through a random process. For the user to be able to produce blocks, he must become a validator, and this is done in several ways, either after the user has locked his token for a certain period, or the validator is chosen based on the Blockchain design. Another way for the user to be a validator is by keeping the coins for the largest time or owning the biggest stack gives a greater opportunity for the user to become a validator. Proof of stack is considered to be more energy efficient than other mechanisms [10].
3- Delegated Proof of Stack (DPoS): In this mechanism, delegates are chosen based on a vote from the users, where the user can share his coins and vote for a specific number of delegates, as the user's share of the coins affects the user's voting weight, more user stack mean larger vote weight. The delegate who gets the most votes has the opportunity to produce new blocks. The delegate rewards are like other Blockchain consensus mechanisms. This mechanism is one of the fastest Blockchain consensus mechanisms [10].
4- Proof of Capacity (PoC): In this mechanism, digital stores are used to store mathematical puzzle solutions. In this mechanism, users who are faster to find solutions get a chance to create a new block. This process is called plotting. In this mechanism, users with higher storage capacity have more chances to produce new blocks [11].
5- Proof of Authority: This mechanism is a modified version of the proof of stack mechanism. In this mechanism, the identities of the validators in the network are on the stack. In this mechanism, the identity is used as a correspondence between the personal identity of the validators and their official documents, to verify their identity. In the mechanism of establishing authority, the nodes that become

Volume 4, Issue 1, pages 1-20
p-ISSN 2655-8564, e-ISSN 2685-9432

validators are the only nodes that are authorized to produce new blocks. To secure and protect the Blockchain network, validators whose identity is at stack are incentivized [11].

6- Proof of Activity: This mechanism is a mixture of the Proof of Work mechanism and the Proof of stack mechanism. This mechanism relied on miners and auditors. In this mechanism, the blocks that are generated are simple blocks that contain the mining reward address and header information. Header information is used to define a random group of validators for block signature, in which case the validators with the highest stacks are the ones selected to sign the new block. The miners try to solve the puzzle and claim their reward. When the designated validators sign on, the new block becomes part of the network. The block must be signed by all validators in order not to be ignored. In this mechanism, the network fees generated by the process are distributed between the winning miner and the validators [11].

E. Mining

Mining is an integrated process in which cryptocurrency transactions are created, transmitted, and verified. Ensures a stable, safe, and secure prevalence of currency from payer to recipient. Cryptocurrencies are decentralized and work on a peer-to-peer system, and they are unlike fiat currencies that are controlled and regulated by the central authority. Banks need a huge infrastructure to generate currency and monitor transactions. But the cryptocurrency that uses the mining system overcomes this need, as it is the responsibility of miners or nodes to verify and monitor transactions [12].

When a transaction is made, details of the transaction are broadcast to all network nodes. To form a block the transactions that take place during a specific period are summarized. The system is designed to merge transparency into it, whereby all transactions made are maintained and recorded in blockchain [12].

Miners play a major role in mining, as they verify the property of currency from source to destination. Each transaction contains a previous retail transaction that was performed by and through the owner. The current position is tested for validity and thus

Volume 4, Issue 1, pages 1-20
p-ISSN 2655-8564, e-ISSN 2685-9432

validated. Miners prevent double-spending on currency through the verification process [20].

The main objective of mining is to create and issue currencies in the currency economy. After making and verifying the transactions, it is the role of the miners to collect these transactions and include them in the blocks that they are currently solving. Before the blocks are broadcast, they must be resolved and then placed in the blockchain. Solving blocks includes difficult mathematical puzzles to crack and unlock. Miner is allowed to add the block to the ledger only when solving a math puzzle, and as a result, they are awarded a reward [13].

F. Mining Requirements

Cryptocurrencies are mined using special machines for this purpose called a "Mining machine". Mining history starts from the CPU to the currently widely used ASICs. New machines with better efficiency than previously designed machines have been developed as a result of the cyclical growth of mining difficulty [12].

1- During the beginning of mining, the CPU was used efficiently with hash rates lower than or equal to 10 Mbps to mine cryptocurrencies. To deal with mining previously, having a computer with the necessary software installed on it was sufficient. But because of the increasing difficulty of mining, the use of CPUs became insufficient because the hash rates became high and thus we need advanced mining machines. cpuminer was one of the popular CPU mining software [12].

2- Since the CPU mining power did not meet the increasing requirements, the CPU was used with graphic cards for coin mining. Graphics cards contain GPUs, which are used to solve complex polygons and high mathematical functions used in games. Different hash-based algorithms are used by different cryptocurrencies to solve blocks of transactions that require high math; Therefore GPUs are considered an alternative to CPU Mining [12].

   Expanding the hash rate of cryptocurrency through GPUs is the goal of pushing the boundaries of consumer computing in amazing new ways. Despite the benefits of GPU, there are some Limitations:

   - GPUs are more expensive compared to normal CPUs [12].

Volume 4, Issue 1, pages 1-20
p-ISSN 2655-8564, e-ISSN 2685-9432

- Each GPU must be connected to a PCI-E 16x or 8x slot, of these, are relatively few on commercial motherboards [12].
- Failure to use all components such as RAM, motherboard, and hard disk in GPU mining leads to an increase in the mining cost [12].
- GPUs require a high additional power of 200-300 watts to mine effectively [12].
- Because GPU takes two slots in a motherboard, it became difficult to connect more than one GPU to a computer to get better performance [12].

3- FPGA (Field Programmable Gate Array): It has the feature to configure after manufacturing because it contains CLB, which is Configurable logical blocks that contain the property of reconfiguring, and also contains RAM and logic gates. Its power consumption is a fifth less than GPUs. It is also good at hash-based algorithms like SHA256 used in Bitcoin transactions [12].

4- ASIC (Application Specific Integrated Circuit): Bitcoin ASICs designed specifically for Bitcoin mining is effective in complex mining mathematical tasks, with high speed and efficiency [12].

G. Wallets

An electronic wallet is a type of electronic card and is used for transactions over the Internet using computers or smartphones. Its utility is the same as a debit or credit card. Cashless transaction technology has seen growth in the past year [15].

To help move away from the monetary economy e-wallets are being used. As a result of all transactions in the economy being calculated in this process, the size of the parallel economy decreases. Widespread in rural areas after the spread in urban areas of the mobile phone wallet. Hence, Wallet Funds see a very bright future very soon. In this section, we will try to study the types of electronic wallets and how to use them and talk about bitcoin as an example [14].

To pay the money the wallets collect private keys to access their Bitcoin address. They appear in various forms, especially for special types of devices. And to avoid

Volume 4, Issue 1, pages 1-20
p-ISSN 2655-8564, e-ISSN 2685-9432

placing it on the computer, paper storage can be used. It is important to have a backup copy of your Bitcoin wallet and to secure it [14].

Bitcoin has become a new way of cash, and it is starting to find acceptance among merchants as a method of payment. The mechanism of transactions and the method of creating them became known, and it remained to be known how they were stored? The money is stored in a physical wallet, and Bitcoin is stored in a wallet, but it is a digital wallet [15].

To be precise, Bitcoin is not stored anywhere. Rather, it is the protected digital keys used to access public Bitcoin addresses and sign transactions [15].

There are five main types of wallets [14]:

1. Desktop wallets

   To run a wallet you need to install the original Bitcoin Core client, and you might not even know it. This program allows you to create a Bitcoin address to obtain and transfer virtual currency, collect the private key for that as well as migrate transactions to the network. MultiBit operates on Linux, Mac OSX, and Windows. Hive is an OS X-based wallet with some features, one of which is an app store that has direct contact with bitcoin services. Some desktop wallets are specified to enhance security: Armory falls into this group. DarkWallet - It uses a lightweight browser add-on to deliver services including currency mixing where users' currencies are exchanged for others, to prevent citizens from being tracked [14].

2. Online wallets

   Web-based wallets store private keys on a computer connected to the Internet and access to it is restricted by the user. Due to the availability of these services through the Internet, and their connection to a computer and mobile phone wallets, which causes duplicate addresses between the devices used by you [15].

   - Advantages

   - The time required to complete a transaction is short [16].
   - Storing a small amount of cryptocurrency is recommended [16].

Volume 4, Issue 1, pages 1-20
p-ISSN 2655-8564, e-ISSN 2685-9432

- Some digital wallets are used to store and transfer many different cryptocurrencies between them [16].
- TOR network is used for more privacy [16].

- Disadvantages

- There is a third party that fully controls the digital wallet [16].
- When using a digital wallet it is recommended to use a personal computer and it is important to install security software [16].
- Various online fraud operations are a result of a lack of knowledge in information technologies, which exposes users to various frauds [16].

3. Mobile wallets

Using a special application on your smartphone, the wallet can save your private keys to Bitcoin addresses, and thus you can pay directly using the mobile phone. Bitcoin wallet can take advantage of near field communication (NFC), letting you tap a mobile phone versus a reader and pay with Bitcoin without ever having to provide any information [15].

- Advantages

- More useful and easier to use than other types of cryptocurrency wallets [16].
- The possibility of using the TOR network for more privacy [16].
- Provide using a QR code to scan [16].

- Disadvantages

- Because mobiles are not secure devices. The loss of the user's private encryption codes may happen in case the user's mobile was hacked [16].
- Mobile wallets are vulnerable to malware and viruses [16].

4. Hardware wallets

It is in the form of a USB device with a program, and some of it contains a screen, so the user does not need a computer to complete the transaction See Figure 2. It provides user control over the cryptocurrency with the ability to store digital assets for a long time [15].

Volume 4, Issue 1, pages 1-20

p-ISSN 2655-8564, e-ISSN 2685-9432

- Advantages
  - A USB wallet with a display screen is the most secure [16].
  - More secure than other wallets [16].
- Disadvantages
  - Too difficult to buy [15].
  - There are risks of use for beginners so it is not recommended for them [16].

Figure 2. Hardware Wallet [17]

5. Paper wallets

One of the cheapest and most impressive options for keeping your Bitcoins safe is seen in Figure 3. Many websites offer paper Bitcoin wallet services. They will create your Bitcoin address with an image containing the two QR codes: one for the public address which use to receive bitcoins; and the other for the private key, which use to pay the Bitcoins stored at this address. In a paper wallet, private keys are not stored digitally on a computer or mobile device and therefore are not subject to electronic attacks or the risk of hardware failure or loss [15].

- Advantages
  - It is kept in the user's wallet or pocket, and there is no need for a computer connection [16].
- Disadvantages
  - Need more time to complete the transaction [16].

International Journal of Applied Sciences and Smart Technologies

Volume 4, Issue 1, pages 1-20

p-ISSN 2655-8564, e-ISSN 2685-9432

Figure 3. paper wallet [18]

3 Results and Discussion

Based on previous studies and literature reviews, Blockchain is a decentralized database, each member of the network maintains a complete, synchronized, and verified copy of the database that contains all transactions. The Blockchain architecture combines advanced cryptography, distributed consensus mechanisms, and a complex system of incentives and rewards. Blockchain architecture makes it have a group of characteristics including the inability to alter transactions or fraud, and it does not require any trust in the integrity of the participants but it ensures absolute credibility in the system, it is outside of censorship. If two participants want to conduct a transaction between them, it cannot be prevented, and because of the short settlement time, which is close to zero, the speed of the final settlement and its verification leads to faster capital and increased liquidity.

The cryptocurrency is a virtual currency that exists only in electronic form on the Internet. The cryptocurrency was introduced as a digital currency for financial exchange independently of banks or financial institutions. Whereas Blockchain is the technology that underlies cryptocurrencies to conduct, secure, verify, and store transactions, these currencies gain many advantages because of their characteristics of Blockchain.

As the ledger database is distributed over the network, each member of the network has a complete copy of the ledger database. Whereas, the miners are the members of the network where the process of verifying transactions is carried out by miners. Therefore, there is no central authority to control the network and the transactions that take place on it or to individually control the database. This is what distinguishes cryptocurrencies as being decentralized. With the advantage of decentralization, the transaction cannot be prevented or controlled. Therefore, since the user has a cryptocurrency wallet, he can

Volume 4, Issue 1, pages 1-20
p-ISSN 2655-8564, e-ISSN 2685-9432

perform any number of transactions and transfers at any time and anywhere without restrictions. Thus, the cryptocurrency has unlimited transactions.

In conducting transactions in cryptocurrencies, there are no high fees. As in the case of purchase, there are very low fees for the crypto process and mining operations. Here, fees in mining operations do not go to a central authority but are distributed to the miners who have verified the reliability and validity of the transaction, and these small fees are exposed to one party of the transaction, which is the buyer. In contrast to banks that impose multiple types of fees for transactions, currency transfers, accounts, and database management. This makes cryptocurrency operations significantly lower in fees and costs compared to banks. Also As a result of the short time of mining operations and the absence of a central authority such as banks to control the transaction and make approvals, this makes the transaction progress very fast, which distinguishes the cryptocurrency by the short time in its transactions.

Since cryptocurrencies are virtual currencies and their transactions take place over the Internet, and because transactions in them are not subject to the control of a central authority, it became possible to conduct transactions between countries and outside borders without any hassles or restrictions. This is what makes cryptocurrency a cross-border currency.

Blockchain stores cryptocurrency transactions in blocks that are recorded in the distributed ledger. In cryptocurrency, each user has a crypto address, and the user can specify whether the crypto address is public or not. If the user sets their crypto address public, then other users will be able to see how much crypto is for that user. If the address is not public, then no one can know the amount of crypto for the user. This adds a transparency advantage to cryptocurrencies.

In cryptocurrencies, the user can create his wallet or any number of wallets without referring to his name, address, or any other real information. This makes anonymity another feature of the cryptocurrency to maintain and protect privacy.

By using the cryptography process, no person can perform any payment transaction from the wallet except by the owner. Cryptocurrencies use cryptography and the use of public and private keys to achieve a high level of security.

Volume 4, Issue 1, pages 1-20
p-ISSN 2655-8564, e-ISSN 2685-9432

In cryptocurrencies, transactions are carried out by a large number of distributed servers, which may be in the hundreds or more. As the cryptocurrency has no main server to control and manage transactions. The wallet software installed on users' computers in the network is part of the network. The process of exchanging transactions and payments between two or more members of the cryptocurrency network who are installed the wallet software is done directly so that neither banks nor governments can control the exchange of money in them. Thus cryptocurrency networks form a peer-to-peer network.

Since cryptocurrencies do not follow a central authority nor are they controlled by companies or governments. Cryptocurrencies are limited to use and mining, therefore there is no possibility for any party or authority to change the system or develop inflation in the system.

Accompanied by more and more expansion in the use of technology that adds to the world a lot of advantages and disadvantages that depend on how the technology is used and the purpose of its use. In addition, the use of cryptocurrencies is also expanding as the advantages of their use are accompanied by many disadvantages that depend on some of their characteristics, how they are used, and the goal of their use.

While Blockchain-based cryptocurrency technology is somewhat complex, the user needs to know about it and learn it well before starting to invest in it. The lack of knowledge about it exposes the user to the risks of hackers.

Since cryptocurrencies are still not accepted by many countries, as well as not being accepted until now in many online buying and selling sites. This makes it impractical to use it for everyday buying and selling, making it not widely accepted.

Although the cryptography and anonymity features in cryptocurrencies are considered two of its strong advantages, this gave the possibility to use it in financing illegal business and prohibited activities. In addition to the lack of a central authority to issue and supervise it, there is no legal guarantee in the event of bankruptcy. Thus, there is a high risk of investing in cryptocurrencies. As well as the volatile nature of cryptocurrencies, which increased the fear of people and companies from investing in them. As large volatilities, increase the risk of investing in the cryptocurrency.

Volume 4, Issue 1, pages 1-20
p-ISSN 2655-8564, e-ISSN 2685-9432

In cryptocurrencies, the possibility of recovery is not available, as it is not possible to recover any wrong payment without the consent of the other party only. This increases the risks of using cryptocurrencies and requires more caution and attention before conducting any transaction.

As a result of the characteristics of cryptocurrencies and the features of Blockchain technology, which is the technology on which the cryptocurrency is based, there are many advantages and disadvantages of cryptocurrencies as shown in Table 1.

Table 1. Cryptocurrency advantages and disadvantages

No.	Advantages	Disadvantages
1.	Decentralization	Lack of Knowledge
2.	Unlimited number of transactions	Not widely accepted
3.	Transactions low fees	High risk in investment in cryptocurrency
4.	Fast transaction	Strong Volatility nature
5.	Cross-border currency	Missing payment cannot be recovered
6.	Transparency	
7.	Anonymity and privacy	
8.	High security	
9.	Peer-to-peer network	
10.	No inflation	

4 Conclusion

Cryptocurrency is a virtual currency that depends on cryptography to achieve confidentiality, secrecy, privacy, speed, and low cost of transactions. Blockchain is the cryptocurrency underlying technology. Blockchain technology provides the cryptocurrency with all the abilities to achieve the decentralization mechanism. The Blockchain architecture combines advanced cryptography, distributed consensus mechanisms, and a complex system of incentives and rewards. Cryptocurrency comes to

solve the traditional currency problems to avoid the loss of time, effort, fraud, loss of physical money, and high fees in banking transactions. Cryptocurrencies with their underlying technology (Blockchain) have several advantages and features that increase their strength and distinction from regular currencies and regular financial transactions such as decentralization, high confidentiality, anonymity, speed of transactions, very low fees, unlimited number of transactions, unrestricted by geography and borders, transparency, protection from Inflation, and the peer-to-peer network. While there are these advantages to cryptocurrencies, they have many disadvantages such as the risks of lack of knowledge, the lack of wide acceptance, the high risk of investing in them, their volatile nature, and the inability to return missing payments. It is possible to overcome these disadvantages by raising awareness and training on the use of these currencies on the one hand, and on the other hand, creating regulations and laws that regulate their work and investing in them, which reduces risks, helps spread, and reduces the misuse of their potentials.

References

[1] M. Vejačka, "Basic Aspects of Cryptocurrencies," *Journal of Economy, Business and Financing*, **2**(2), 75-83, 2014.

[2] A. Okhuese, "INTRODUCING CRYPTOCURRENCY," Schemas Group, 11-12, 2016.

[3] C. Rose, "The Evolution Of Digital Currencies: Bitcoin, A Cryptocurrency Causing A Monetary Revolution," *International Business & Economics Research Journal*, **14**(4), 617-621, August 2015.

[4] E. D. a. J. Brito, "The New Palgrave Dictionary of Economics," *New Palgrave Dict. Econ.*, March 2020.

[5] M. Badar, S. Shamsi and J. Ahmed, "Blockchain: Concept and Emergence," in *Blockchain Applications for Secure IoT Frameworks: Technologies shaping the future*, Bentham Science, 19, 2020.

[6] B. Scott, "How Can Cryptocurrency and Blockchain Technology Play a Role in Building Social and Solidarity Finance?," in *Social and Solidarity Finance: Tensions, Opportunities and Transformative Potential"*, 2016.

[7] P. Mulgund, A. Sharma, A. Srivastava and L. Agrawal, "Beyond Cryptocurrency - More To Blockchain," *Cutter Business Technology Journal*, **32**(11), 8, 2019.

[8] J. Wild, M. Arnold and P. Stafford, "Technology: Banks seek the key to blockchain," Financial Times, November 2015. [Online] Available: https://www.ft.com/content/eb1f8256-7b4b-11e5-a1fe 567b37f80b64?segid=0100320#axzz3qK4rCVQP. [Accessed: 04 December 2020].

[9] R. Houben and A. Snyers, *Cryptocurrencies and blockchain*, European Parliament, 103, 2018

[10] A. Nick and L. Hoenig, "Consensus Mechanisms in Blockchain Technology," Lexology, [Online]. Available: https://www.lexology.com/library/detail.aspx?g=e30e7d54-3c7f-4ca0-8a22-478227a9b5ec. [Accessed 02 December 2020].

[11] N. JOSHI, "8 blockchain consensus mechanisms you should know about," Allerin, 23 April 2019. [Online]. Available: https://www.allerin.com/blog/8-blockchain-consensus-mechanisms-you-should-know-about. [Accessed 04 December 2020].

[12] H. Krishnan, S. Saketh and V. Vaibhav, "Cryptocurrency Mining – Transition to Cloud," *International Journal of Advanced Computer Science and Applications (IJACSA)*, **6**(9), 115-124, 2015.

[13] S. Nakamoto, "Bitcoin: A Peer-to-Peer Electronic Cash System".

[14] B. Pachpande and A. Kamble, "Study of E-wallet Awareness and its Usage in Mumbai," *Journal of Commerce & Management Thought*, **9**(1), 33-45, 2018.

[15] P. Ankalkoti and S. S G, "A Relative Study on Bitcoin Mining," *Imperial Journal of Interdisciplinary Research (IJIR)*, **3**(5), 1757-1761, 2017.

[16] S. Jokić, A. Cvetković, S. Adamović, N. Ristić and P. Spalević, "Comparative Analysis of Cryptocurrency Wallets vs Traditional Wallets," *Ekonomika*, **65**(3), 65-75, September 2017.

[17] S. Singh, April 2018. [Online]. Available: https://cryptocurrencynews.com/best-hardware-wallets/.

Volume 4, Issue 1, pages 1-20

p-ISSN 2655-8564, e-ISSN 2685-9432

[18] 30 May 2018. [Online]. Available: https://www.universidadedobitcoin.com.br/o-lancamento-da-paper-wallet-da-cardano-vem-com-recurso-de-armazenamento-offline.

[19] A. Rosic, "Blockchain Consensus: A Simple Explanation Anyone Can Understand," Blockgeeks, [Online]. Available: https://blockgeeks.com/guides/blockchain-consensus/#What_is_the_Byzantine_Generals_Problem. [Accessed 01 December 2020].

[20] Brito, J. & Castillo, A. Bitcoin: A Primer for Policymakers. 2013.

International Journal of Applied Sciences and Smart Technologies

Volume 4, Issue 1, pages 21-34

p-ISSN 2655-8564, e-ISSN 2685-9432

Impact of Online Education and Sentiment Analysis from Twitter Data using Topic Modeling Algorithms

Sulochana Devi[1, *], Chhaya Dhavale[1], Lalita Moharkar[2], Sushama Khanvilkar[3]

[1] *Department of Information Technology, Xavier Institute of Engineering, Mumbai, India*

[2] *Department of EXTC, Xavier Institute of Engineering, Mumbai, India*

[3] *Department of Computer Engineering, Xavier Institute of Engineering, Mumbai, India*

[*]*Corresponding Author: sulochana.d@xavier.ac.in*

(Received 01-05-2022; Revised 16-05-2022; Accepted 21-05-2022)

Abstract

During a pandemic, all industries suffer greatly, and every sector of the world suffers in some way, including the education sector. Internet expressions reflect users' feelings about a product or service. The polarity of information in source data toward a subject under investigation is determined by sentiment analysis processes. The goal of this study is to examine social media expressions about online teaching and learning, as online education will become a part of everyday life in the future. We collected data from Twitter using keywords related to online education and Google form from engineering undergraduate students for prototype implementation. This analysis will assist teachers, parents, and the student community in understanding the benefits and drawbacks of the education industry, allowing for further improvement in educational outcomes. We used aspect-based sentiment analysis and topic modeling to determine

Volume 4, Issue 1, pages 21-34
p-ISSN 2655-8564, e-ISSN 2685-9432

sentiment polarity and important topics for education sector stakeholders. To begin, we used TextBlob Python package to determine sentiment polarity, and Bag of Words, LDA and LSA model for discovering topics. After modeling topics from the collected data, topic Coherence is used to assess the degree of semantic similarity between high scoring words in the topic. The word cloud and LDAvis are used to visualize data. The experimental results are promising and it will assist education stakeholders in addressing the concerns that have been identified as social media expressions to work on.

Since the boom in science and technology, humans have been trying to invent machines that could reduce their efforts in day to day activities. In this paper, we develop a personal assistant robot that could pick up objects and return it to the user. The robot is controlled using an android application in mobile phones. The robot can listen to user's command and then respond in the best way possible. The user can command the robot to move to given location, capture images and pick objects. The robot is equipped with ultrasonic sensor and web camera that helps it to move to different location effectively. It is also equipped with sleds that play important role in object picking process. The robot uses a tiny YOLOv3 model which is rigorously trained on several images of the object. There are some possible improvements that can be achieved which could help this robot to be used in several other fields as well.

Keywords: coherence, education, LDA, LSA, pandemic, topic modeling, Twitter

1 Introduction

The global spread of COVID-19 altered humans daily routines of living, working, and operating in addition to their social connections. Like all other parts, the education sector grave implications related to students, instructors, and institutions across the

Volume 4, Issue 1, pages 21-34
p-ISSN 2655-8564, e-ISSN 2685-9432

world. Academic institutes were closed for formal offline face-to-face education to virtual transformation and the unprecedented upward thrust of on-line learning in the scenario of world COVID-19 lockdowns. Online learning, also known as e-learning, is learning via internet-enabled devices such as mobile phones, desktop computers, laptop computers, tablets, and so on. [1]. Within days, education was transitioned from face-to-face to online mode. All the stakeholders quickly adopted and continued with the new normal. This massive unplanned shift from traditional face-to-face learning to an online learning framework has altered the traditional ways in which educational institutions deliver knowledge to their students. Because of the abrupt transition, both teachers and students faced numerous challenges.

With video lectures and online exams, students were introduced to virtual textbooks and modules. Because of limited nonverbal communication, unstable internet access/technology, expensive equipment and devices, and a lack of technical knowledge, educators and learners faced numerous challenges in digital learning. Despite the challenges, online education provided many benefits such as continuity of studies, overall flexibility, increased information retention, extended reach of teaching, securing good grades, attendance, increased technical literacy, social interaction, accessibility, pace of learning, and no time and place restrictions.

Adoption of online learning will continue post-pandemic, and this shift will have an impact on the global education sector. A new hybrid educational model will emerge, with significant benefits. The integration of information technology in education will be accelerated, and online education will eventually become a required component of school education. Traditional offline learning and e-learning can coexist. Given the possibility of a hybrid model in which online learning will play an important role, there is a significant need to understand social media users' and learners' attitudes toward online learning in order to make online learning more effective.

This study examines students' perspectives on the positive and negative aspects of online learning, as well as the sentiments of Twitter users, who include students, teachers, and other stakeholders. During the pandemic, tweets from various education stakeholders such as teachers, students, parents, and other entities will cover the

Volume 4, Issue 1, pages 21-34
p-ISSN 2655-8564, e-ISSN 2685-9432

majority of the aspects of online learning. Data collected from students via Google forms include their perspectives on the abrupt shift from offline to online education, its impact on them, challenges encountered during the adaptation process, and their future expectations for online learning. The first tweets of education sector stakeholders were extracted using the snscrape scraper using various education-related keywords such as online education, e-learning, pandemic, and covid19. After preprocessing, sentiment analysis is done, as sentiments can be divided into positive, negative, and neutral forms, sentiment analysis processes identify the polarity of information in the source materials toward an entity. We applied the LDA model to discover topics from social media users' tweet data and students' opinions. The LDAvis tool was used for data visualization. LSA is applied to efficiently analyze the text and find the hidden topics of concerns related to education during a pandemic by understanding the context of the text. Bag of words technique is used to extract top words of concern for social media users. Same LDA, LSA and BoW techniques applied for data collected from students. [24] .

2 Research Methodology

Background work

So many researchers used twitter data for analysis. The reason could be that data can be extracted with API easily and it is one of the popular social media platforms. The collections of tweets contain useful information. Anyone can see the most recent expressions or complaints about any popular entity by combing through all of the tweets. The results of the analysis can be used to improve education performance, such as teaching and learning. Table 1 summarizes topic modeling algorithms and its applications used by various researchers. [1-3, 21,23].

Volume 4, Issue 1, pages 21-34

p-ISSN 2655-8564, e-ISSN 2685-9432

Table 1. Topic Modeling and Sentiment Analysis Review

Ref no of papers	Dataset Source	Approach	Aim/Objective	Remark
6	90,000 tweets from study area.	Naive-bayes classifier	Sentiment analysis of tweets on education during COVID-19	Topic modeling not done only sentiment analysis
7	1717 tweets from twitter	Web analytics approach	Find sentiment on educational posts	No ML
8	Online survey taken	The percentages were calculated based on the frequency of common student responses.	To know the effectiveness of online learning	Challenges and obstacles in online education at Pakistan students' perspectives
9	Data is collected with Google Forms	NLP techniques and Logistic regression classifier	Sentiment Analysis on COVID-19 Epidemic's Education	No topic modeling
10	Short Data from facebook	Topic modeling algorithm LSA, LDA, NMF, and PCA	Analysis of Topic modeling techniques	All topic modeling methods reviewed.
11	Facebook and Twitter	Topic modeling – LDA, LDAH, in the insurance domain. Sentiment analysis as well done.	Topic-aware sentiment analysis to improves, communication with customers and a better sense of the market	ML algorithms are used for text classification.
12	13,967 Tweet of Surabaya citizen	Topic modeling with LDA & LSA	Data requirement from community to support service policy,	Government made Surbaya media center.
13	1740 (Neural Information Processing Systems)	Topic modeling with LDA & LSA	Topic modeling to understand the various topics in fields of ML	Topic modeling used for detecting semantic structures in a set of research papers.

International Journal of Applied Sciences and Smart Technologies

Volume 4, Issue 1, pages 21-34

p-ISSN 2655-8564, e-ISSN 2685-9432

3 Materials and Methods

This section presents visualization and description of used datasets, description of sentiment analysis process, and the proposed methodology for performing topic modeling and sentiment analysis on the selected dataset.

Dataset Description

Two different types of data are used for this study. First dataset used for this study has been collected from Twitter through snscrape scraper using various keywords related to online education like 'onlineeducation', 'e-learning', 'pandemic', 'covid19', 'onlineclasses', 'educationincovid' etc. and contains 6000 records. Second dataset has been collected from 150 students using a google form to know their perspective about online learning, advantages, and disadvantages of online learning, difficulties and challenges faced during online learning. Table 2 presents sample tweets from the dataset with username, date and tweet content and Table 3 presents sample opinions from students' data.

Table 2. Tweet Sample from the collected dataset.

Username	Date	Tweet
Education blog	2020-10-17 14:43:06+00:00	#EDUCATION: As the #COVID19 #pandemic lingers, the impact on #highereducation is becoming clearer: #College closures, academic program terminations and institutional mergers are occurring at a pace seldom, if ever, seen before.
Paul Wusow	2020-10-16 20:23:04+00:00	The COVID-19 pandemic has changed education forever. This is how via @wef: https://t.co/owFvJYQZev #COVID19 #Pandemic #Education
Education blog	2020-10-15 15:16:23+00:00	#EDUCATION: The #COVID19 #pandemic is offering us an opportunity to rethink #accountability in education. https://t.co/jHTQ50Jrbt #schools #students #children #Teaching
panafrica nuk	2020-10-07 15:01:54+00:00	Teachers have had to move from a space in which they have years of experience to the unknown and challenging world of online, remote, correspondence and socially distanced teaching. Read more https://t.co/xhfuHRrxMh #Africa #AfricanCaribbean #COVID19 #Education #Pandemic

Volume 4, Issue 1, pages 21-34

p-ISSN 2655-8564, e-ISSN 2685-9432

Table 3. Sample Opinions from Students' dataset.

Sr. No.	Students' Opinion
1	Positive: No travel, comfortable environment, flexible Negative: No proper timeline, no proper instruments for practical for certain subjects.
2	Positive: Timings are flexible and we are doing it from the comfort of our homes, but the negative is the absence of social interaction and lack of routine'
3	Because of online education we get an opportunity to learn many new courses online and avoid the expenses of traveling.

After collecting both datasets, preprocessing is done to clean the dataset and remove unessential information. After that using TextBlob Python package polarity score of tweets is obtained. Tweets are categorized into three polarities: positive, negative, and neutral.

Methodology

This subsection explains different phases of the methodology followed and the approaches used in each phase. Aspect Based sentiment analysis and topic modeling techniques were applied on both datasets as shown in the given Figure 1.

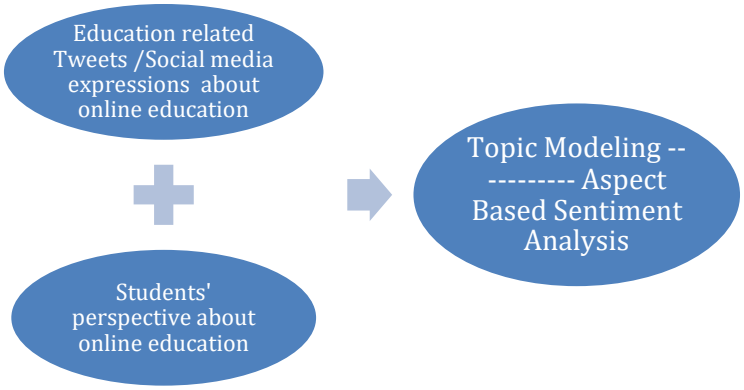

Figure 1. Proposed Work

The sequential workflow of the methodology applied on both datasets along with steps and methods is represented in the Figure 2. Workflow starts with the input phase of

Volume 4, Issue 1, pages 21-34

p-ISSN 2655-8564, e-ISSN 2685-9432

data collection from students and tweet scraping from Twitter using snscrap. In the next phase data is preprocessed to remove unnecessary and repeated words. After this phase sentiment analysis and topic modeling techniques are applied to obtain the required output.

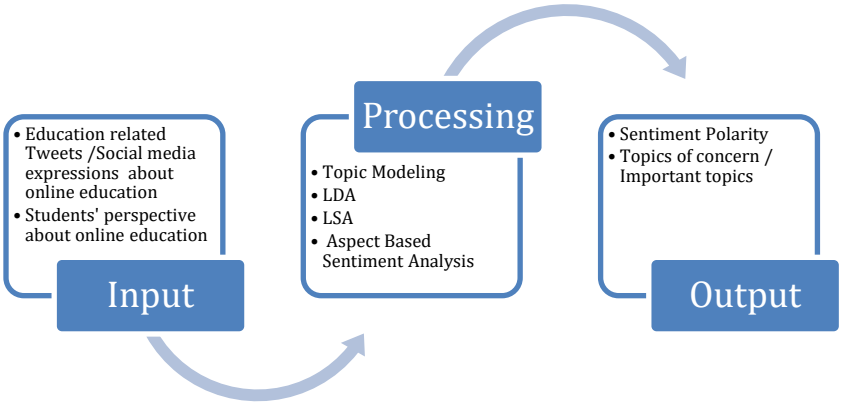

Figure 2. Processing Flow

Preprocessing of Data

Before starting data analysis process, data is preprocessed to remove non required information, this helps to increase efficiency of model and gives better accuracy. So, first step is to preprocess the data before starting encoding [3]. Python's NLP toolkit is used for preprocessing of data for this study. This is achieved by converting text into lower case, deleting URLS, removing hyperlinks and HTML tags, applying stemming, lemmatizing and finally removing stop words.

Lowercase conversion: changing the text to lowercase helps to decrease the complexity of the data as, 'data' and 'Data' are considered as different by machine learning models, so by changing all data into lower case, both words 'Data' and 'data' are considered as 'data'. Considering lower- and upper-case words as dissimilar words affects the training and classification process.

Elimination of URLs, punctuation marks, hyperlinks, HTML tags, and numbers: This type of data do not provide any additional meaning for learning models, so they do not contribute in enhancement of classification performance, also they and escalate the intricacy of feature set, so deleting them helps to bring down the feature space.

Volume 4, Issue 1, pages 21-34
p-ISSN 2655-8564, e-ISSN 2685-9432

Lemmatizing and Stemming: lemmatization and stemming is done to decrease inflectional forms and sometimes different forms of corelated words to a common base word form [4]. For example, ‘swims, ‘swimming’, and ‘swam’ are changed to the base word ‘swim’.

Elimination of Stop words: stop words do not provide any useful information for analysis. Stop words such as ‘yours’, ‘is, ‘the’, ‘a’, ‘am’ and ’an’ are removed [5].

4 Results and Discussion

TextBlob

TextBlob is a python library used for various NLP tasks such as sentiment analysis, part-of-speech tagging, paraphrase, noun phrase extraction, and sorting, etc. [14]. In our study, it is used for sentiment analyzing by providing polarity score between -1 and 1 for tweets. Tweets are assigned polarity based on polarity score, tweets having polarity score less than zero is considered as -ve, having score equal to zero is considered as neutral tweet, and having score greater that 0 will be considered as +ve tweet [15]. Table 4 presents polarity percentage of both datasets.

Table 4. Polarity Percentage

	Positive	**Negative**	**Neutral**
Dataset 1	38%	16%	46%
Dataset 2	63%	22%	15%

Feature Selection

Bag of Words (BoW) and TF-IDF are the most widely used methods for feature extraction. Bag of Words: BoW is a commonly used technique in NLP and information retrieval to extract features from preprocessed text or data [16].

BoW is used to count the appearance of a word in a text and forms a feature vector comprising the number of appearances of each unique word for text classification. The BoW is generally used to create the vocabulary of all unmatched words and train the learning models through their frequencies.

As an output of BoW, top words for dataset1 are: capacity, coffee, covid, education, experiences and for dataset 2 are: beginning, class, college, depressing, difficult etc.

Volume 4, Issue 1, pages 21-34
p-ISSN 2655-8564, e-ISSN 2685-9432

Term Frequency-Inverse Document Frequency: TF-IDF is used for feature extraction by extracting weighted features from text data. It gives the weight of each term in the corpus to enhance the performance of learning models [17].
TF-IDF score for search keywords such as education, covid, pandemic is **0.028766.**

Topic Modeling

For machine learning and natural language processing, topic modeling algorithm is used to scan large document, extract and phrase hidden patterns. Increased popularity of social media platforms makes them lucrative for researchers to extract ideas from here. Tweets contain unorganized short text topics, so it is required to uncover topics from tweet data through topic modeling.

In this paper, we have used LDA (Latent Dirichlet Allocation) and LSA (Latent Semantic Analysis) methods. LDA is an unsupervised generative probabilistic model of a corpus LDA gives topics using word probabilities. LAD has two parts, the words within documents, and probability of words is calculated related to a topic [23]. LDA is a well-known method for topic modeling. First introduced by David et al. in [22]. LSA is used to find out relation between documents and expressions. Performance of LSA is good in short sentence classification and it is demonstrated in various research works [20, 21]. Sample output obtained from LDA is given in Figure 3 & 4.

Topic Coherence is used to calculate the score of a single topic by calculating the degree of semantic similarity between high scoring words in the topic. These calculations help to discriminate topics that are semantically interpretable topics and topics that are artifacts of statistical inference. There are different coherence measures like c_v, c_p, c_uci, c_umass. We have used c_v and c_umass as given in the Table 5.

Table 5. Coherence Score

Coherence Score →	Using c_v	Using UMass
Dataset 1	0.41852	-6.95928
Dataset 2	0.33977	-2.48233

International Journal of Applied Sciences and Smart Technologies

Volume 4, Issue 1, pages 21-34

p-ISSN 2655-8564, e-ISSN 2685-9432

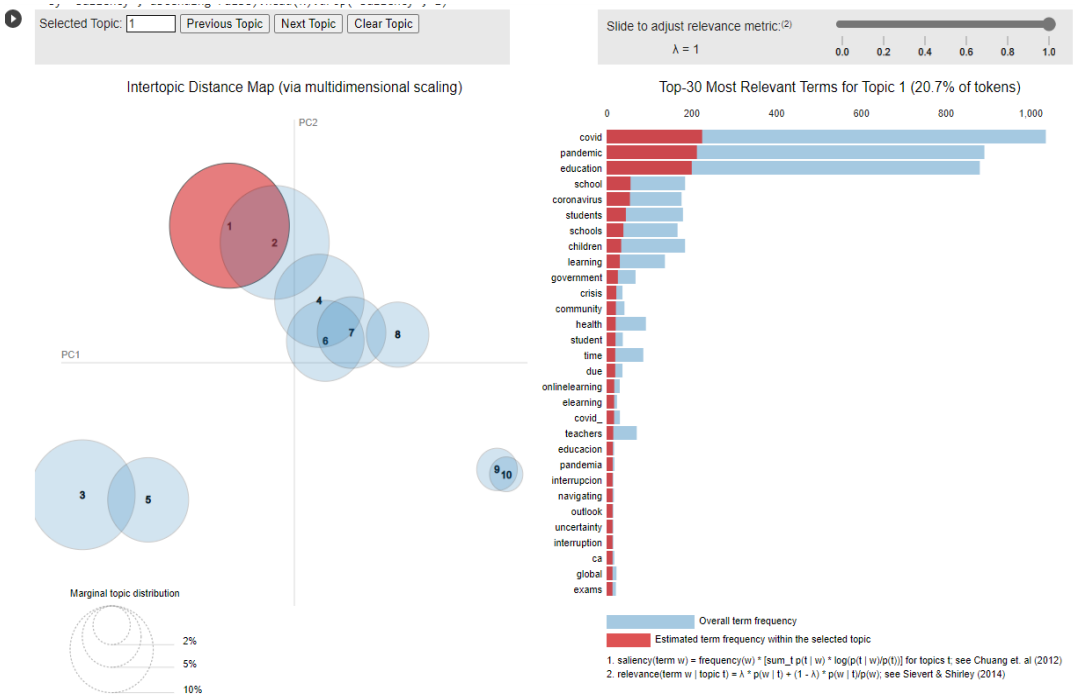

Figure 3. Top 30 Most Silent words in topic 1 twitter data

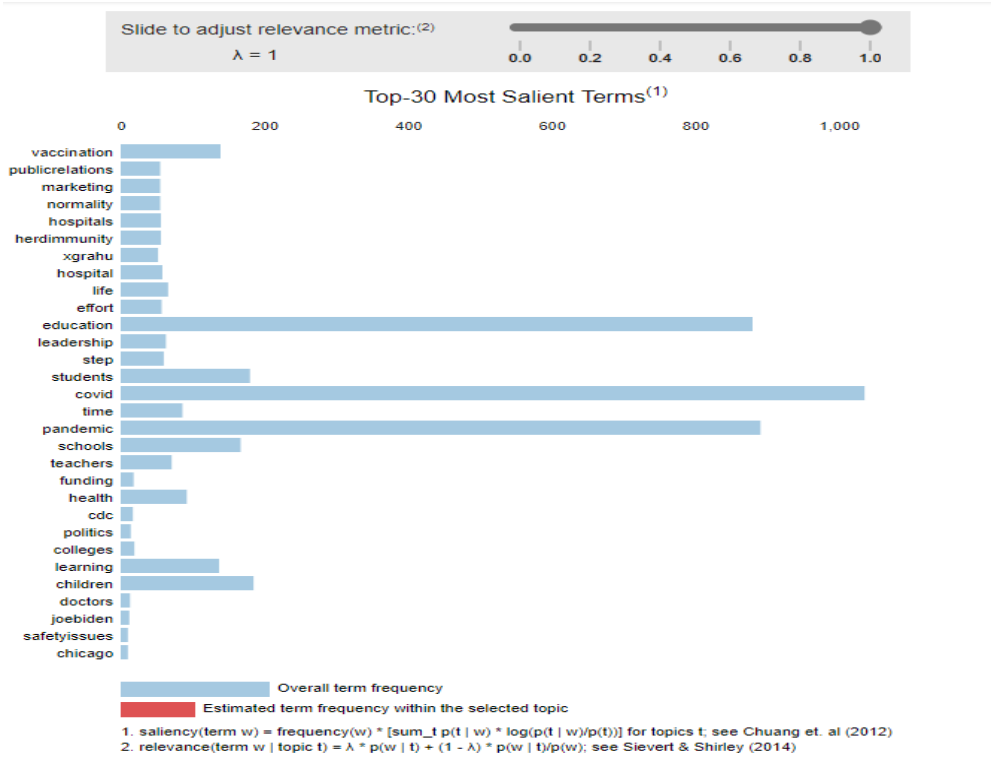

Figure 4. Top 30 Most Silent words in twitter data

Volume 4, Issue 1, pages 21-34

p-ISSN 2655-8564, e-ISSN 2685-9432

5 Conclusion

This study examines a topic related to online education during the Corona period. Polarity is calculated and analyzed as positive, negative, and neutral for the same dataset. Two datasets are created: one for Twitter data and its analysis, and the other data collected from students to understand the impact of online education on the student community. The LDA and LSA algorithms have been used successfully for topic modeling. LSA is a method for forming semantic generalizations from textual sections that uses Singular value decomposition (SVD), whereas LDA is an unsupervised machine learning algorithm. Model-generated topics are not always easy to interpret. Topic coherence calculations are thus used to differentiate between good and bad topics. The outcomes / topics can then be used to overcome challenges in the education industry, as well as to consider online education as an opportunity for the needy. We discovered clear polarity/understanding in the student dataset and mixed expressions in the social media community.

Acknowledgements

Authors are highly grateful to twitter for providing a platform for users to express their views, and thankful to Xavier Institute of Engineering, Mahim Mumbai.

References

[1] Zhu, X., & Liu, J. Education in and After Covid-19: Immediate Responses and Long-Term Visions, *Postdigital Science and Education*, **2**(3), 695–699, 2020.

[2] Mujahid M, Lee E, Rustam F, Washington PB, Ullah S, Reshi AA, Ashraf I. Sentiment Analysis and Topic Modeling on Tweets about Online Education during COVID-19, *Applied Sciences*, **11**(18), 8438. 2021.

[3] Reddy, A.; Vasundhara, D.; Subhash, P. Sentiment Research on Twitter Data, *Int. J. Recent Technol. Eng.*, **8**, 1068–1070, 2019.

[4] Jivani, A, A Comparative Study of Stemming Algorithms, *Int. J. Comp. Tech. Appl.* **2**, 1930–1938, 2011.

Volume 4, Issue 1, pages 21-34

p-ISSN 2655-8564, e-ISSN 2685-9432

[5] Armstrong, P., Bloom's Taxonomy. *Vanderbilt University Center for Teaching*. 2019.

[6] Cheeti, S. S. Twitter based Sentiment Analysis of Impact of COVID-19 on Education Globaly, *International Journal of Artificial Intelligence and Applications (IJAIA)*, **12**(3), 2021.

[7] Floradel S. Relucio and Thelma D. Palaoag. Sentiment analysis on educational posts from social media, *In Proceedings of the 9th International Conference on E-Education, E-Business, E-Management and E-Learning (IC4E '18). Association for Computing Machinery*, New York, NY, USA, 99–102, 2018.

[8] Adnan M, Anwar K., Online learning amid the COVID-19 pandemic: Students' perspectives, *Journal of Pedagogical Sociology and Psychology*. **2**(1), 45-51. 2020.

[9] Sanjok Lohar, The Impact Ofcovid-19 Pandemic On Education System, *International Journal of Emerging Technologies and Innovative Research*, **8**(4), 428-430, April 2021.

[10] Albalawi, R., Yeap, T. H., & Benyoucef, M., Using Topic Modeling Methods For Short-Text Data: A Comparative Analysis, *Frontiers in artificial intelligence*, **3**, 42, 2020.

[11] Albalawi, R., Yeap, T. H., & Benyoucef, M, Using Topic Modeling Methods For Short-Text Data: A Comparative Analysis. *Frontiers in Artificial Intelligence*, **3**, 42, 2020.

[12] Qomariyah, S., Iriawan, N., & Fithriasari, K. Topic modeling twitter data using latent dirichlet allocation and latent semantic analysis, *In AIP conference proceedings* **2194**(1), 020093. AIP Publishing LLC, December 2019.

[13] Slimane Bellaouar, Mohammed Mounsif Bellaouar, and Issam Eddine Ghada. Topic Modeling: Comparison of LSA and LDA on Scientific Publications. *In 2021 4th International Conference on Data Storage and Data Engineering DSDE Association for Computing Machinery*, New York, NY, USA, 59–64. 2021.

[14] Loria, S. textblob Documentation. Release 0.15. **2**, 269, 2018.

[15] Sohangir, S., Petty, N., & Wang, D, Financial Sentiment Lexicon Analysis, *IEEE 12th International Conference on Semantic Computing (ICSC)*, 286-289, 2018.

[16] Eshan, S.C., & Hasan, M.S., An application of machine learning to detect abusive Bengali text, *20th International Conference of Computer and Information Technology (ICCIT)*, 1-6, 2017

[17] Zhang,W.; Yoshida, T.; Tang, X. A comparative study of TF* IDF, LSI and multi-words for text classification, *Expert Syst. Appl.* **38**, 2758–2765, 2011.

[18] Robertson, S., *Understanding inverse document frequency: on theoretical arguments for IDF*, Journal of Documentation, **60**(5), 503-520, 2004.

[19] George, M., Soundarabai, P.B., & Krishnamurthi, K., Impact Of Topic Modelling Methods And Text Classification Techniques In Text Mining: A Survey, 2017.

[20] Salloum, S.A., Al-Emran, M., Monem, A.A., Shaalan, K, Using Text Mining Techniques for Extracting Information from Research Articles. *In: Shaalan, K., Hassanien, A., Tolba, F. (eds) Intelligent Natural Language Processing: Trends and Applications. Studies in Computational Intelligence*, **740**. Springer, Cham. 2018.

[21] Deerwester, S.; Dumais, S.T.; Furnas, G.W.; Landauer, T.K.; Harshman, R. Indexing by latent semantic analysis. *J. Am. Soc. Inf. Sci.* **41**, 391–407, 1990.

[22] David M. Blei, Andrew Y. Ng, and Michael I. Jordan, Latent dirichlet allocation. *J. Mach. Learn. Res.* **3**, 993–1022, 2003

[23] Hamed Jelodar, Yongli Wang, Chi Yuan, Xia Feng, Xiahui Jiang, Yanchao Li, and Liang Zhao. Latent Dirichlet allocation (LDA) and topic modeling: models, applications, a survey. *Multimedia Tools Appl*, **78**, 15169–15211. 2019.

[24] Mujahid M, Lee E, Rustam F, Washington PB, Ullah S, Reshi AA, Ashraf I. Sentiment Analysis and Topic Modeling on Tweets about Online Education during COVID-19, *Applied Sciences*. **11**(18), 8438, 2021.

International Journal of Applied Sciences and Smart Technologies

Volume 4, Issue 1, pages 35-46

p-ISSN 2655-8564, e-ISSN 2685-9432

Determining the Coefficient of Restitution Through the "Bouncing Ball" Experiment using Phyphox

Jesi Pebralia[1, *]

[1]*Department of Physics, Universitas Jambi, Jambi, Indonesia*
[*]*Corresponding Author: jesipebralia@unja.ac.id*

(Received 13-04-2022; Revised 26-04-2022; Accepted 26-04-2022)

Abstract

This study aims to determine the restitution coefficient based on the reflected sound from the "bouncing ball" experiment. The experiment used a Phyphox-based smartphone. The produced sound came from a reflection between marble and the floor. Theoretically, the value of the coefficient of restitution is obtained based on the square root of the final height of the object's reflection divided by its initial height. In this study, the determination of the height of the bounce from the "bouncing ball" was measured using the Phyphox application, which was analyzed based on the sound of the bouncing ball and the time interval of the reflection. The results show that the value of the coefficient of restitution for each marble were 0.93, 0.92, and 0.92, while the average error were 0.65%, 0.85%, and 1.43%, respectively. Furthermore, the average error value of the overall measurement is 0.97%. This error is highly dependent on the shape of the object. The rounder a thing is, the higher the level of accuracy will be. In this study, the determination of the coefficient of restitution was carried out in two ways: by comparing the height of the ball's bounce and the time intervals for the n and n+1 bounce. The value of the coefficient of restitution generated by these methods was identic. Thus,

Volume 4, Issue 1, pages 35-46
p-ISSN 2655-8564, e-ISSN 2685-9432

this study had confirmed that the bounce ball experiment using the Phyphox indicated valid data well so that it could be implemented for determining the coefficient of restitution.

Keywords: bouncing ball, coecficient of restitution, Phyphox, smartphone

1 Introduction

The coefficient of restitution is a value that states the level of elasticity of objects in the collision phenomenon. Particularly, the coefficient of restitution is a characterization of the degrees of freedom in the inelastic collision and dimensionless [1]. The value of the coefficient of restitution depends on the ratio of the final height and initial height of the collision particles, which is mathematically expressed by the Equation (1):

$$e = \sqrt{\frac{h_2}{h_1}}. \quad (1)$$

Determining the value of the coefficient of restitution is very useful for developing various sub-fields of physics. The coefficient of restitution has become an essential part of granular hydrodynamics and the kinetic theory of gas [2], [3], computation of granular matter [4], and even in agriculture, especially for the development of agricultural techniques [5]. The coefficient of restitution provides information on the energy lost during the collision process [6]. It could be necessary for dry granular modelling and multi-phase flow models.

Research in determining the value of the coefficient of restitution has been carried out using different techniques. These are determining the coefficient of restitution using a robot and piezoelectric sensor [7], determining the coefficient of restitution using a high-speed camera [6], [8], determining the coefficient of restitution using the double pendulum method [9], determining the coefficient of restitution using high-speed video [10], and others [11]–[14].

One of the experiments that can be used to determine the value of the coefficient of restitution is the “bouncing ball” experiment [15]. A bouncing ball is a bounce event from a ball dropped without initial velocity from a certain height above the earth’s surface and hits a particular surface. In the bouncing ball phenomenon, an inelastic collision occurs where the ball will bounce up and until the ball stops at a specific time. The process of

Volume 4, Issue 1, pages 35-46
p-ISSN 2655-8564, e-ISSN 2685-9432

the bouncing ball illustrates many aspects that could be observed from the principles of mechanics, including the phenomenon of collisions when the ball hits the floor surface [16].

According to the studies that have been carried out, the technique for determining the value of the coefficient of restitution is expensive, complex, and challenging to carry out independently by students. In this study, a cheap and practical technique for determining the coefficient of restitution will be introduced using a smartphone. Generally, using advanced technology in this era, smartphones have been equipped with sophisticated sensors that can support the implementation of science practicums, especially physics. In Addition, this is also supported by the existence of practical support applications that can be downloaded and run freely on smartphones. One application that can be used for physics experiments is the Phyphox.

Several studies using the Phyphox application include research on determining spring constants on spring oscillation events [17], free-fall motion experiments using the stopwatch acoustic feature [18], pendulum motion experiments [19], and others [20], [21]. The value of the coefficient of restitution can be determined by using the Phyphox application, by finding the ratio of the object's speed between two adjacent bounce [22]. In this study, we provide a method to determine the value of the coefficient of restitution of bouncing ball by using Phyphox based on two approaches. The first approach is through the ratio of the height of marbles in two adjacent bounce. While the second approach is through the ratio of time intervals between two adjacent bounce.

2 Research Methodology

In this study, the value of the coefficient of restitution between the marble and the floor would be calculated through the bouncing ball experiment. Based on equation (1), the value of the restitution coefficient could be determined if the initial height and final height of the following bounce process were known. The object used in this study were three marbles with different diameters. The purpose is to evaluate the effect of the size of marble.

International Journal of Applied Sciences and Smart Technologies

Volume 4, Issue 1, pages 35-46

p-ISSN 2655-8564, e-ISSN 2685-9432

The experiment design is illustrated in Figure 1. The first process was setting the initial height of the marbles using a ruler. It was 15 cm from the floor. The smartphone was placed on the floor in a position close to the bounce of the marbles. To find the value of the bounce marbles' height, a smartphone was installed with the Phyphox. After that, the ball was dropped without initial velocity and allowed to bounce. The sound produced by the marble's bounce would be detected and recorded by the smartphone sensor. Then it would be processed and converted to generate data on interval time, height, and energy of the bounce. Furthermore, the data would be displayed on the smartphone's LCD. The number of bounces produced in this experiment was five times.

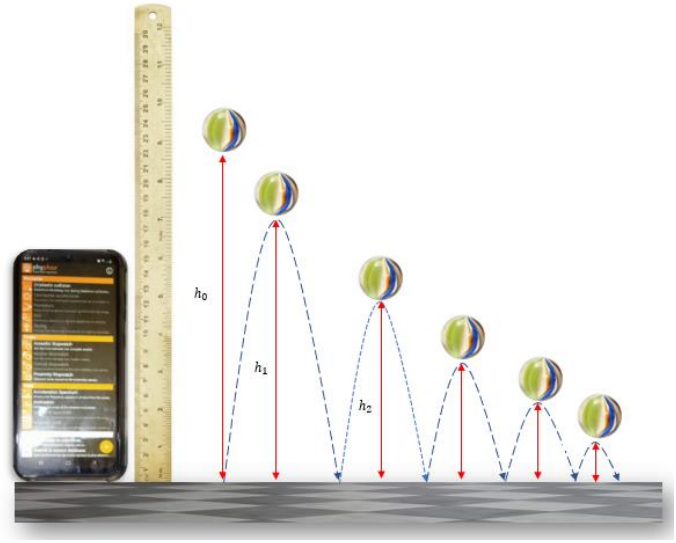

Figure 1. Experiment design in determining the coefficient of restitution

In the next stage, the accuracy of the obtained data needs to be declared because it is related to the error value of a measurement. The smaller the measurement error value, the greater the level of research accuracy. So, it might be stated that the data experiment was valid. The measurement error value is calculated through the Equation (2),

$$error = \left|\frac{m_{standard} - m_{experiment}}{m_{standard}}\right| \times 100\%, \quad (2)$$

where $m_{standard}$ represents the actual value measured through standard measuring instruments and $m_{experiment}$ represents the value displayed by the smartphone.

International Journal of Applied Sciences and Smart Technologies
Volume 4, Issue 1, pages 35-46
p-ISSN 2655-8564, e-ISSN 2685-9432

The error value was attained from the initial height measurement read by the smartphone compared to the actual height. In this study, the arisen error should be under 2%. Therefore, if the error value is less than 2%, the data collection process could be continued, while others would repeat the experiment process.

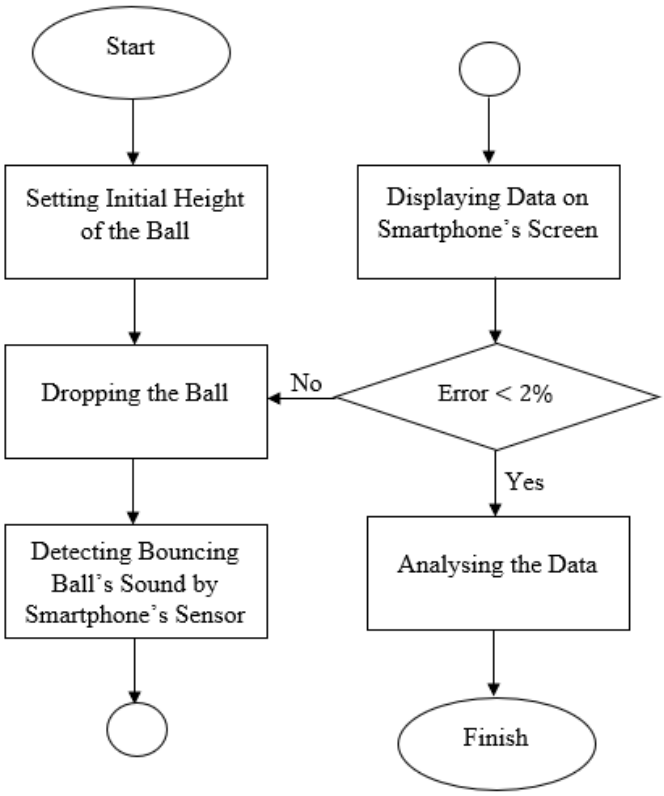

Figure 2. Flowchart of Detecting the coefficient of restitution by Using Phyphox

After determining the error value, the data generated by the smartphone would be analyzed to determine the coefficient of restitution and standard deviations. The calculation of the standard deviation value follows the Equation (3),

$$Ds = \frac{1}{n}\sqrt{\frac{n\sum_{i=1}^{n} x_i^2 - \left(\sum_{i=1}^{n} x_i\right)^2}{(n-1}}, \quad (3)$$

where n represents the number of measurements and x_i represents the measurement results in the i^{th} experiment.

International Journal of Applied Sciences and Smart Technologies

Volume 4, Issue 1, pages 35-46

p-ISSN 2655-8564, e-ISSN 2685-9432

3 Results and Discussion

In this study, three types of marbles with different diameters were used in the experiment. They were labelled with marble 1, having a diameter of 14.1 mm, marble 2, having a diameter of 15.2 mm, and marble 3, having a diameter of 27.4 mm. To obtain the valid data, the experiment was done and repeated five times. The experiment results are shown in Figure 3.

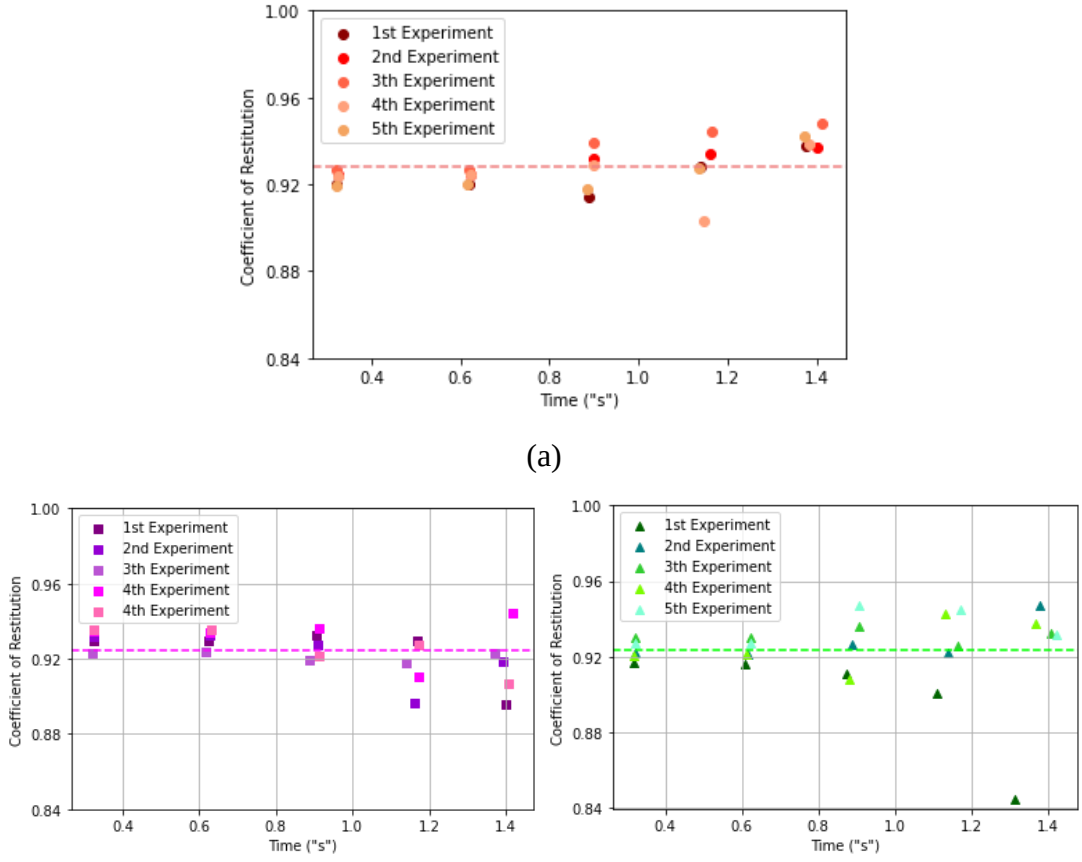

(a)

(b) (c)

Figure 3. The experiment results of the coefficient of restitution for (a) marble 1, (b) marble 2, and (c) marble 3

Figure 3 shows the bounce ball experiment results using marble with various diameters. The initial height of the marble is set at 15 cm from the floor. In this experiment, the

Volume 4, Issue 1, pages 35-46
p-ISSN 2655-8564, e-ISSN 2685-9432

coefficient of restitution for marble 1 was 0.90 to 0.95, while for marble 2, the coefficient of restitution was 0.90 to 0.94, as well as the coefficient of restitution for marble 3 was in the range of 0.84 to 0.95. The dash line in each figure indicate the average value of the coefficient of restitution. The average value of the three marbles respectively are 0.9282, 0.9247, and 0.9237. Based on equation (2), average error value of the three marbles respectively are 0.65%, 0.85%, and 1.43%, respectively. Moreover, the average coefficient of restitution for collisions in this experiment was displayed in Table 1.

Analytical calculation

The coefficient of restitution is a significant empirical parameter in any physical modelling where there is energy loss caused by particle collisions [23]. One of the essential factors that influence the factor determining the value of the restitution coefficient is the velocity value immediately after the n^{th} reflection [24],

$$v_n = v_0 e^n, \tag{4}$$

where v_0 is the velocity of the ball just before the collision. The time interval between adjacent collisions (n^{th} to $(n+1)^{th}$) is expressed by the Equation (5),

$$\begin{aligned} T_n &= \frac{2v_n}{g} \\ T_n &= \frac{2v_0 e^n}{g} \\ T_n &= T_0 e^n. \end{aligned} \tag{5}$$

where g is the gravitational acceleration and $T_0 = 2v_0/g$. Then, from the equation 5, it could be obtained that the coefficient of restitution could also be determined through the time interval of the bouncing ball,

$$e^n = \frac{T_n}{T_0}. \tag{6}$$

Time interval (T_n) of bouncing marble was show in Figure 4.

International Journal of Applied Sciences and Smart Technologies

Volume 4, Issue 1, pages 35-46

p-ISSN 2655-8564, e-ISSN 2685-9432

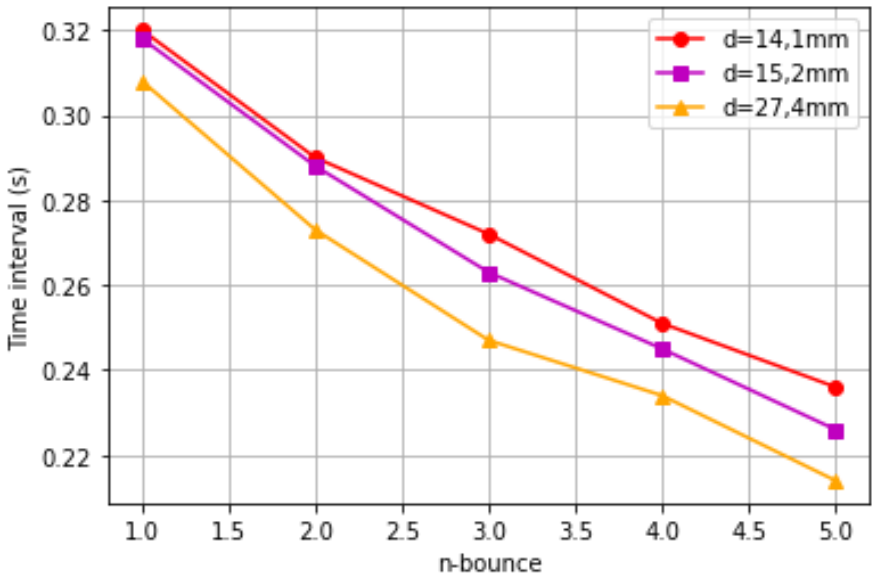

Figure 4. The time interval vs *n*-bounce for each marble

From Figure 4, it is obtained that for marble 1, when $n = 1$, then the value of $h = 0{,}1497\ m$, dan $T_n = 0{,}322s$. So, substituting those data to T_0, it could be determined the coefficient of restitution,

$$T_0 = (2v_0/g)$$
$$T_0 = \left(2\sqrt{2gh}/g\right)$$
$$T_0 = \left(\sqrt{\frac{8h}{g}}\right)$$
$$T_0 = \left(\sqrt{\frac{8(0{,}1497m)}{9{,}8\ m/s^2}}\right)$$
$$T_0 = 0{,}3496s, \qquad (7)$$

Thus, for $n = 1$ the coefficient of restitution of marble 1 is

$$e^1 = \frac{0{,}322s}{0{,}3496\ s}$$

$$e_1 \approx 0{,}92. \qquad (8)$$

The coefficient of restitution of marble 2 dan marble 3 could be found by applying the same method. Those are $e_2 \approx 0{,}93$ and $e_3 \approx 0{,}92$.

Volume 4, Issue 1, pages 35-46

p-ISSN 2655-8564, e-ISSN 2685-9432

The last step in this study was comparing values of the coefficient of restitution. The purpose was to see the validity of the data between the experimental and analytical methods. The data is shown in Table 1.

Table 1. Comparison of the coefficient of restitution between analytical and experimental method

Marble	Coefficient of Restitution	
	Experimental	**Analytical**
d1 = 14,1 mm	$e \approx 0{,}93$	$e \approx 0{,}92$
d2 = 15,2 mm	$e \approx 0{,}92$	$e \approx 0{,}93$
d3 = 27,4 mm	$e \approx 0{,}92$	$e \approx 0{,}92$

Table 1 shows that the coefficient of restitution between the experiment and analytical approach is not the same but very identic. Many factors could cause this. The measurement of the restitution coefficient value is highly dependent on the shape and material of the object, the level of surface roughness of the reflection, the level of sphericity of the thing, and the measurement error. However, the small measurement error may cause a shift in energy to the translational or rotational components [23]. Furthermore, since there was no change in the coefficient of restitution for three kinds of marble, it could be stated that there is no effect from the diameter of the marble to determine the coefficient of restitution. Thus, this study confirmed that bounce ball experiment using the Phyphox indicates valid data well so that it could be implemented to determine the coefficient of restitution.

4 Conclusion

This research has succeeded in determining the coefficient of restitution. The method was cheap and practical through the phenomenon of bouncing balls and smartphones integrated with the Phyphox application. The value of the coefficient of restitution for each marble was 0.93, 0.92, and 0.92, while the average error was 0.65%, 0.85%, and 1.43%, respectively. Moreover, the average error value of the overall measurement is 0.97%. This error is highly dependent on the shape of the object. The rounder an object is, the higher the level of accuracy will be. In this study, the determination of the coefficient of restitution was carried out in two ways: by comparing the height of the

ball's bounce and the time intervals for the *n* and *n*+1 bounce. The value of the coefficient of restitution generated by these methods was identic. Thus, this study had confirmed that the bouncing ball experiment using the Phyphox indicated valid data well so that it could be implemented for determining the coefficient of restitution

References

[1] M. Heckel, A. Glielmo, N. Gunkelmann, and T. Pöschel, "Can we obtain the coefficient of restitution from the sound of a bouncing ball?," *Phys. Rev. E*, **93**(3), 1–10, 2016.

[2] D. Serero, N. Gunkelmann, and T. Pöschel, "Hydrodynamics of binary mixtures of granular gases with stochastic coefficient of restitution," *J. Fluid Mech.*, **781**, 595–621, 2015.

[3] T. Pöschel, N. V. Brilliantov, and T. Schwager, "Long-time behavior of granular gases with impact-velocity dependent coefficient of restitution," *Phys. A Stat. Mech. its Appl.*, **325**(1–2), 274–283, 2003.

[4] T. Schwager and T. Pöschel, "Coefficient of restitution and linear-dashpot model revisited," *Granul. Matter*, **9**(6), 465–469, 2007.

[5] B. Feng, W. Sun, L. Shi, B. Sun, T. Zhang, and J. Wu, "Determination of restitution coefficient of potato tubers collision in harvest and analysis of its influence factors," *Nongye Gongcheng Xuebao/Transactions Chinese Soc. Agric. Eng.*, **33**(13), 50–57, 2017.

[6] M. C. Marinack, R. E. Musgrave, and C. F. Higgs, "Experimental investigations on the coefficient of restitution of single particles," *Tribol. Trans.*, 56(4), 572–580, 2013.

[7] M. Montaine, M. Heckel, C. Kruelle, T. Schwager, and T. Pöschel, "Coefficient of restitution as a fluctuating quantity," *Phys. Rev. E - Stat. Nonlinear, Soft Matter Phys.*, **84**(4), 3–7, 2011.

[8] B. Crüger *et al.*, "Coefficient of restitution for particles impacting on wet surfaces: An improved experimental approach," *Particuology*, **25**, 1–9, 2016.

[9] J. Hlosta, D. Žurovec, J. Rozbroj, Á. Ramírez-Gómez, J. Nečas, and J. Zegzulka, "Experimental determination of particle–particle restitution coefficient via double pendulum method," *Chem. Eng. Res. Des.*, **135**, 222–233, 2018.

[10] D. B. Hastie, "Experimental measurement of the coefficient of restitution of irregular shaped particles impacting on horizontal surfaces," *Chem. Eng. Sci.*, **101**, 828–836, 2013.

[11] X. Li, M. Dong, D. Jiang, S. Li, and Y. Shang, *The effect of surface roughness on normal restitution coefficient, adhesion force and friction coefficient of the particle-wall collision*, **362**, Elsevier B.V, 2020.

[12] S. Singh, D. Tafti, and V. Tech, "Gt2013-95623 Predicting the Coefficient of Restitution for Particle Wall," 1–9, 2013.

[13] Z. Jiang, J. Du, C. Rieck, A. Bück, and E. Tsotsas, "PTV experiments and DEM simulations of the coefficient of restitution for irregular particles impacting on horizontal substrates," *Powder Technol.*, **360**, 352–365, 2020.

[14] H. Tang, R. Song, Y. Dong, and X. Song, "Measurement of restitution and friction coefficients for granular particles and discrete element simulation for the tests of glass beads," *Materials (Basel).*, **12**(19), 2019.

[15] P. Müller, M. Heckel, A. Sack, and T. Pöschel, "Complex velocity dependence of the coefficient of restitution of a bouncing ball," *Phys. Rev. Lett.*, **110**(25), 1–5, 2013.

[16] R. Cross, "Behaviour of a bouncing ball," *Phys. Educ.*, **50**(3), 335–341, 2015.

[17] H. A. Ewar, M. E. Bahagia, V. Jeluna, R. B. Astro, and A. Nasar, "Penentuan Konstanta Pegas Menggunakan Aplikasi Phyphox Pada Peristiwa Osilasi Pegas," *J. Kumparan Fis.*, **4**(3), 155–162, 2021.

[18] I. Boimau, A. Y. Boimau, and W. Liu, "Eksperimen Gerak Jatuh Bebas Berbasis Smartphone Menggunakan Aplikasi Phyphox Infianto," in *Seminar Nasional Ilmu Fisika dan Terapannya*, 67–75, 2021.

[19] J. Pebralia and I. Amri, "Eksperimen Gerak Pendulum Menggunakan Smartphone Berbasis Phyphox: Penerapan Praktikum Fisika Dasar Selama Masa Covid-19," *JIFP (Jurnal Ilmu Fis. dan Pembelajarannya)*, **5**(2), 10–14, 2021.

Volume 4, Issue 1, pages 35-46

p-ISSN 2655-8564, e-ISSN 2685-9432

[20] S. Yasaroh, H. Kuswanto, D. Ramadhanti, A. Azalia, and H. Hestiana, "Utilization of the phyphox application (physical phone experiment) to calculate the moment of inertia of hollow cylinders," *J. Ilm. Pendidik. Fis. Al-Biruni*, **10**(2), 231–240, 2021.

[21] Y. F. Ilmi, A. B. Susila, and B. H. Iswanto, "Using accelerometer smartphone sensor and phyphyox for friction experiment in high school," *J. Phys. Conf. Ser.*, **2019**(1), 2021.

[22] D. Dahnuss, P. Marwoto, R. S. Iswari, and P. Listiaji, "Marbles and smartphone on physics laboratory: An investigation for finding coefficient of restitution," *J. Phys. Conf. Ser.*, **1918**(2), 2021.

[23] J. E. Higham, P. Shepley, and M. Shahnam, "Measuring the coefficient of restitution for all six degrees of freedom," *Granul. Matter*, **21**(2), 2019.

[24] C. E. Aguiar and F. Laudares, "Listening to the coefficient of restitution and the gravitational acceleration of a bouncing ball," *Am. J. Phys.*, **71**(5), 499–501, 2003.

International Journal of Applied Sciences and Smart Technologies

Volume 4, Issue 1, pages 47-58

p-ISSN 2655-8564, e-ISSN 2685-9432

Weft Computation of *Endek* Weaving

Nyoman Dewi Pebryani[1,*], Putu Manik Prihatini[1],

Tjok Istri Ratna C.S[1]

[1] *The Indonesian Institute of The Arts Denpasar, Bali, Indonesia*

[*]*Corresponding Author: dewipebryani@isi-dps.ac.id*

(Received 18-05-2022; Revised 27-05-2022; Accepted 29-05-2022)

Abstract

Endek is a textile produces in Bali with a single ikat technique, specifically weft ikat. Weft ikat means that the pattern is created or drawn on the weft threads before ikat or tying process. The weft threads are transferred into a frame; a frame consists of tens to hundreds of bundles or called traditionally as *bulih*. Drawing a pattern on a frame requires special expertise as the pattern maker has to translate a two-dimensional pattern into a shape that is distorted on the wide side. Indirectly, this special requirement confines the pattern maker as they have to visualize a distortion shape to be able to draw in the frame. To provide easiness in design exploration, providing various templates and multiplier to automatically distort the template are substantial. Therefore, understanding the manual process on site is important before simulating the formula of weft computation including are templates and multiplier. With this computation, the pattern makers or anyone who has an enthusiast in designing *Endek* patterns may involve in the design process.

Keywords: *bulih*, computation, *Endek*, pattern, weft

International Journal of Applied Sciences and Smart Technologies

Volume 4, Issue 1, pages 47-58

p-ISSN 2655-8564, e-ISSN 2685-9432

1 Introduction

Traditional textile is created through a process of weaving, where the warp and weft threads intersect in a loom. *Endek* as one of the Balinese traditional textiles is produced with the weft ikat technique. According to Schaublin et al "ikat (Indonesian "bundle," *mengikat* "to tie") is a complicated and time-consuming resist dye technique in which undyed yarns are mounted on a frame in bundles" [1]. The pattern that appears in *Endek* is created on the weft threads. To create a pattern on the weft threads, the pattern maker needs to have proficiency in visualizing two-dimensional shapes into distorted shapes on the wide side. In addition to that, the pattern maker also needs to decide the number of round threads or bundles to set in the frame (called *penamplikan* traditionally). The number of bundles (called *bulih* traditionally) is varied from one design to another, mostly between fifty to hundreds of *bulih* in one frame.

The expertise of creating the pattern in the weft threads passes from generation to generation verbally and is not well documented. To preserve this cultural creation, transforming it into digital formats is essential. Defined according to the Guidelines for the Preservation of Digital Heritage as "texts, databases, still and moving images, audio, graphics, software, and web pages, among a wide and growing range of formats" [2]. There are challenges in keeping this digital heritage usable and available, especially for the community that owns the tradition. Today, globalization poses significant challenges to the survival of many traditions, one of which is traditional forms of craftsmanship design. Young people in communities may find the required, sometimes-lengthy apprenticeships too demanding, though they are necessary to learn the many traditional forms of the craft. This knowledge may disappear if family or community members are not interested in learning them.

The process of transforming an oral tradition into a digital form involves careful decoding to avoid misinterpretation. According to Pebryani, "the resulting cultural creation produced is based on the cultural knowledge owned by the local people in a specific area" [3]. This cultural knowledge entails indigenous algorithms consisting of the grammar and computation used by the artisans to create their textile. Hence, investigating the pattern design and computation of the weft threads in the process of

Volume 4, Issue 1, pages 47-58
p-ISSN 2655-8564, e-ISSN 2685-9432

designing *Endek* will provide complete documentation on *Endek* weft ikat design process.

2 Research Methodology

The research methodology used in this study is to explore and explain the cultural knowledge and indigenous algorithm in the process of patterning *Endek* textiles. The methodology includes descriptive and simulation, meaning the study is divided into several stages. According to Sommer, "the steps involved in conducting a simulation include formulating the model, simulating the event, and analyzing the results" [4]. Therefore, as shown in Figure 1, this study is divided into three stages: (1) investigating *Endek* textile patterns on-site, (2) simulating the weft computation, (3) assessing the weft computation into the actual threads.

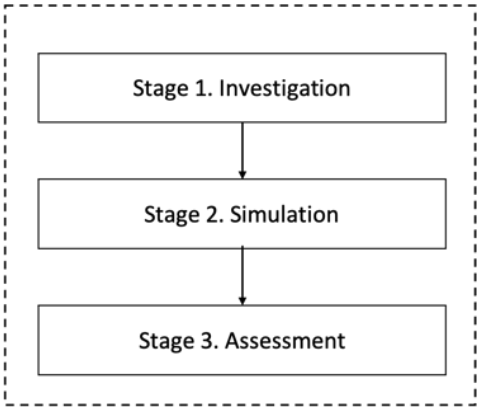

Figure 1. Stages in understanding the weft threads computation

The data was collected from interviews and participant observations with five pattern makers and weavers from various weaving centers. The participant observation allowed the researcher to see and infer information that people may not have mentioned during an interview. The researcher made appointments with participants, including the pattern makers and weavers. Both the interviews and observations took place while participants worked and lasted 60 minutes each. The researcher observed the activities of the participants, including pattern making, the steps involved in creating the patterns, and other phases of the process. The data achieved from the on-site investigation is

Volume 4, Issue 1, pages 47-58
p-ISSN 2655-8564, e-ISSN 2685-9432

necessary to be used as a guideline to conduct the second stage to avoid misinterpretation in decoding the patterns design of *Endek* textile. As well as the information from the first and second stage are significant to be used in the assessment stage.

3 Results and Discussion

The data from the site was analyzed and discussed in three sub-topics: investigation, simulation, dan assessment. Investigation discusses how the process of creating *Endek* on-site including the process of counting threads and patterns. Simulation examines formula of bundles on frame related with the pattern on *Endek* textile. Assessment tests the formulas into the actual *Endek* design process.

Investigation. Creating *Endek* textiles follows several steps. Warp and weft threads are treated with a different procedure. Procedure for warp threads: coloring or dyeing the warp threads, putting the warp threads into a non-machine weaving loom. According to Pebryani, "the treatment and procedure of the warp and weft yarns in the *Endek* weaving consist of approximately 14 stages" [5]. Procedure for weft threads as shown in Figure 2, consists of splitting weft threads, transferring weft threads into a frame, drawing patterns on the weft threads, tying the weft threads, dyeing weft threads, coloring the second and third different colors on the weft threads. After both threats are processed, then both are ready to weave with a non-machine weaving loom as shown in Figure 2.e.

(a) (b)

International Journal of Applied Sciences and Smart Technologies

Volume 4, Issue 1, pages 47-58

p-ISSN 2655-8564, e-ISSN 2685-9432

(c)

(d)

(e)

(f)

Figure 2. (a) splitting weft threads; (b) transferring weft threads into a frame, (c) drawing pattern on a weft threads frame, (d) tying patterned weft threads frame, (e) coloring weft thread frame, (f) weaving on a non-machine weaving loom

The weft threads are stored on a frame prior to drawing the pattern on the threads. A frame consists of several *bulih*, and a *bulih* contains several round threads. One round thread consists of 28 to 30 strands of yarn. The number of *bulih* is vary depending on the desired pattern to be created, approximately around fifty to hundreds of *bulih* in one frame. An experienced pattern maker has already computed the number of *bulih* during the process of transferring the weft, based on the pattern which the pattern maker desired. Hence, the pattern design needs to be decided before transferring weft threads to the frame. Figure 3. shows the size of the frame, 108 x 100 centimeters. In the width size of 108 cm, 7 cm and 1 cm on both left and right of the frame are reduced, leaving 92 cm for the drawing area. The distance between *bulih* is 1 cm.

International Journal of Applied Sciences and Smart Technologies

Volume 4, Issue 1, pages 47-58

p-ISSN 2655-8564, e-ISSN 2685-9432

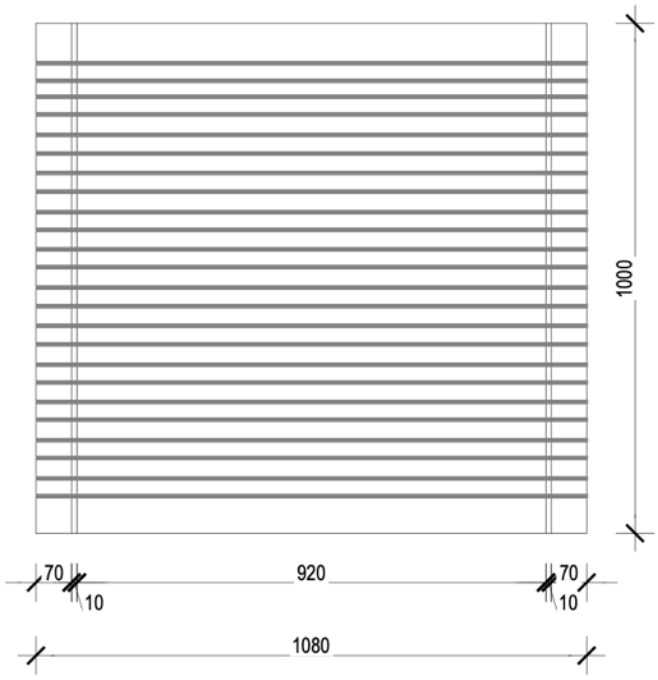

Figure 3. A frame of weft threads

As shown in Figure 3, the pattern maker draws in the area of 92 cm x 100 cm. After the frame is prepared, the pattern maker draws helper lines vertically every 2 cm or so. These lines will assist the pattern maker in dividing space or area on the weft threads. The drawing process uses a marker in navy or red color. The downside of this process is difficult to undo or erase lines that have been created. Hence, not many junior pattern makers are able to explore new designs in the weft threads. They mostly follow images or patterns they have already drawn before.

Designing a pattern for *Endek* in frame is different compared to designing a pattern in a template. When designing a pattern in frame, the pattern maker has to visualize a two-dimensional shape into a distortion shape on the wide side. It limits the pattern maker during design exploration. To provide easiness for beginner pattern makers or experienced pattern makers, transferring this knowledge into a digital format is essential.

Simulation. Paulus Gerdes using the study of mathematics in culture found that the craft art created by the indigenous people involves calculations (or hidden logic) that

Volume 4, Issue 1, pages 47-58

p-ISSN 2655-8564, e-ISSN 2685-9432

indigenous people pass on from generation to generation [6]. Thus, to understand indigenous algorithms on weft computation is through studying and involving in local activity of designing Endek textile. Knowledge gathered across interviews and participant observations from several pattern makers and weavers are simulated to acquire a formula for the template as well as *bulih* computation. One frame consists of tens to hundreds *bulih*, in one *bulih* consist of several bundles (where one bundle consists of two-time thread pulling), bundles traditionally called "as". One-time thread pulling consists of 28 strands of yarns, where 28 strands of yarns create a 1 cm length of textiles. Therefore, 28 becomes a divider in order to seek a multiplier as shown in Table 1. The formula for the multiplier is:

$$1.\, Multiplier = \frac{28}{bundles\ x\ 2}$$

Table 1. Multiplier computation

bundles (As)	Multiplier
2	7
3	4.6
4	3.5
5	2.8

The template for designing the pattern has a fixed height with distinctive widths. As shown in Figure 4.a., a design created on a template with a size of 92 x 28 cm. Then in Figure 4.b, the pattern's design in Figure 4.a. is transformed into a weft threads frame. To identify the size of designated weft threads frame, the width size of a template times with the multiplier from the bundles that preferred. As shown in Figure 4.b, the width size is altered from 28 to 98, that comes from 28 times to 3.5 (multiplier from bundles four).

International Journal of Applied Sciences and Smart Technologies

Volume 4, Issue 1, pages 47-58

p-ISSN 2655-8564, e-ISSN 2685-9432

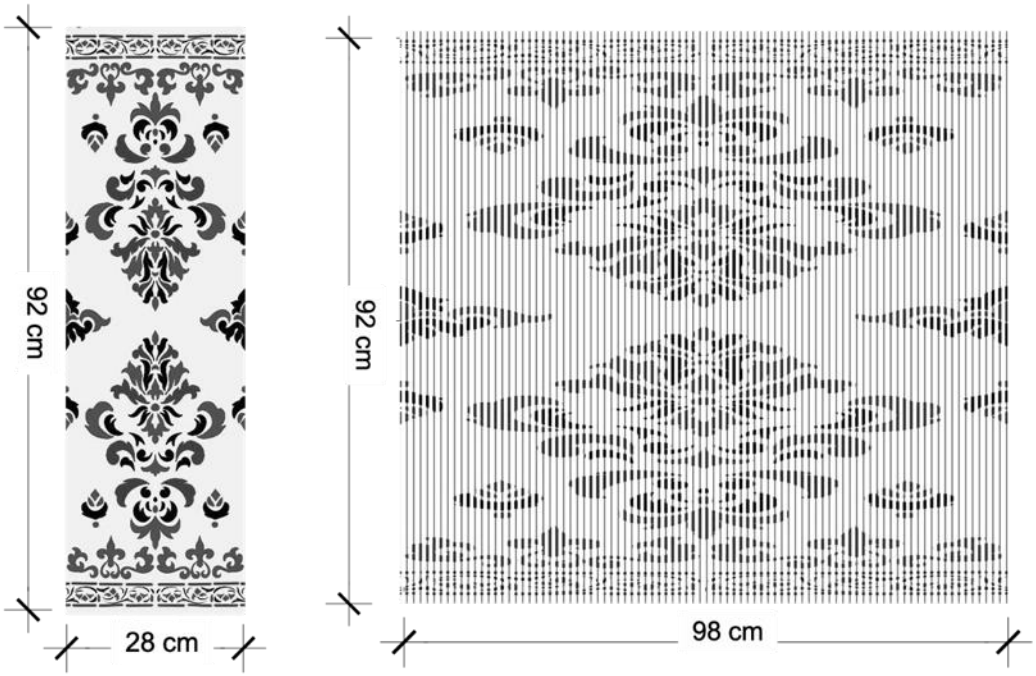

Figure 4. (a) left: *Endek's* pattern design in a template; (b) right: *Endek's* pattern design in a frame

$$2.\ Bulih = multiplier\ x\ the\ width\ of\ the\ template$$

Subsequently, knowing the number of *bulih* and the bundles can be used to compute the length of *Endek* textiles (as shown in Table 2) with the formula as follow:

$$3.\ \text{The textile length} = \frac{30}{28}\ x\ bulih\ \text{x (bundles x2)}x\ 2$$

Table 2. The width, *bulih*, and the result

The width of the template	*Bulih* for *As* 4	*Bulih* for *As* 3	*Bulih* for *As* 2	result
28 cm	98	128	126	1680 cm
26 cm	91	120	182	1560 cm
24 cm	84	110	168	1440 cm

Volume 4, Issue 1, pages 47-58

p-ISSN 2655-8564, e-ISSN 2685-9432

22 cm	77	101	154	1320 cm
20 cm	70	92	140	1200 cm
18 cm	63	83	126	1080 cm
16 cm	56	74	112	960 cm
14 cm	49	64	98	840 cm
12 cm	42	55	84	720 cm
10 cm	35	46	70	600 cm
…	…	…	…	…

Assessment. Theorems need to be presented through illustration or graphs in order to see how the theorems or formulas have been proven [7]. The frame as shown in Figure 4.b. is printed with a scale of 1:1 and created holes on it as a mold to allow ink to permeate on the weft threads frame as shown in Figure 5.a. The signed ink on the weft threads frame then is tied as shown in Figure 5 b.

Figure 5. (a) left: the weft threads frame that have been patterned; (b) right: the weft threads frame that the patterns have been tied

After the weft threads have been tied according to the patterns, the next process is coloration basic dye followed by desired colors. Later, the threads are split into a

Volume 4, Issue 1, pages 47-58

p-ISSN 2655-8564, e-ISSN 2685-9432

shuttle. This shuttle of weft threads passes the warp threads horizontally or from right to left and reverse, until an *Endek* textile is materialized as shown in Figure 6.

Figure 6. *Endek* textile pattern as the result from the design on the left side

4 Conclusion

The computation of weft threads provides easiness in designing the patterns for *Endek* textiles by providing various template dimensions. In addition to that, with the multiplier, the template can automatically stretch on the wide side to transform it into *bulih*. The *Endek* design pattern created through this computation has been assessed until it created a textile. The computation of weft threads contributes a benefit in transforming the manual process into a digital process in designing *Endek* patterns as well as encouraging the pattern maker more explorative.

Acknowledgements

This research is supported by the Ministry of Education, Culture, Research, and Technology and the Education Fund Management Institute (LPDP) through the 2021 Applied Science Research Program Funding Program. Also, we would like to express

our gratefulness to *Astiti* Weaving Center which are willing to be partners in this research process.

References

[1] Schaublin, Kartaschoff, & Ramseyer. Balinese Textile, British Museum Press, London, 1991.

[2] National Library of Australia. Guidelines for The Preservation of Digital Heritage. 2003. Retrieved from https:// unesdoc.unesco.org/ark:/48223/pf0000130071

[3] Author. Culturally Specific Shape Grammar: Formalism of Geringsing Textiles Patterns through Ethnography and Simulation, *All Dissertations*, 2387. https:/tigerprints.clemson.edu/all_dissertations/2387

[4] Sommer B & Sommer R. A Practical Guide to Behavioral Research: Tools and Techniques. Oxford University Press. 1991.

[5] Author. Digital Transformation in Endek Weaving Tradition. Mudra Jurnal Seni Budaya, **37**(1), 78-85.

[6] Gerdes, P. Reflections on ethnomathematics. *For learning of mathematics,* **14**(2), 19-22, 1994.

[7] Herawati, M.V.A., Henryanti, P.S., Aditya, R. Indentity Graph of Finite Cyclic Groups. *International Journal of Applied Sciences and Smart Technologies*, **3**(1), 101-110.

Volume 4, Issue 1, pages 47-58

p-ISSN 2655-8564, e-ISSN 2685-9432

This page intentionally left blank

International Journal of Applied Sciences and Smart Technologies

Volume 4, Issue 1, pages 59-74

p-ISSN 2655-8564, e-ISSN 2685-9432

The Effect of Motor Parameters on the Induction Motor Speed Sensorless Control System using Luenberger Observer

Bernadeta Wuri Harini[1,*]

[1] *Department of Electrical Engineering, Sanata Dharma University, Yogyakarta, Indonesia*

[*] *Corresponding Author: wuribernard@usd.ac.id*

(Received 08-04-2022; Revised 27-05-2022; Accepted 29-05-2022)

Abstract

The sensorless control system is a control system without a controlled variable sensor. The controlled variable is estimated using an observer. In this investigation, the sensorless control system is used to control induction motor speed. The observer that is used is the Luenberger observer. One of the drawbacks of the sensorless control system is precision motor parameter values. In this research, the effect of induction motor parameters in a speed sensorless control system, i.e. resistance and inductance motor, will be investigated. The differences in induction motor parameters between the controller and the actual value affect the system response. The value differences of Rr and Rs that can be applied are a maximum of 50%. However, the small differences in the inductance value greatly affect the system response. To get a good response, the value differences of Ls and Lr are between -5% to +5%, while the difference in the value of Lm is between -3% to +3%.

International Journal of Applied Sciences and Smart Technologies

Volume 4, Issue 1, pages 59-74

p-ISSN 2655-8564, e-ISSN 2685-9432

Keywords: inductance, induction motor, Luenberger observer, resistance, sensorless

1 Introduction

A control system without a controlled variable sensor, often known as "sensorless control," is one controller that is still being researched. Sensorless control systems evolved to overcome the challenges of sensor installation that sensor-based control systems faced. Sensor-based control systems are widely used by researchers, such as those of Z. Alpholicy X., et al [1] and Y. E. Loho, et al [2]. Sensors will drive up prices and complicate installation [3]. The controlled variable in this system is approximated from the plant's current input using an observer rather than being measured directly by a sensor [4]. The stator current is used to estimate the motor speed using an observer. Sensorless control will be used to control the speed of the Induction Motor in this investigation.

The induction motor is one of the Alternating Current (AC) motors. The phase angle, as well as the modulo current (current vector), must be controlled while driving an AC motor [4]. It is not the same as a DC motor. The torque and flux that produce the AC motor current are decoupled in vector control so that they can be controlled independently.

Precision motor parameter values are one of the drawbacks of the sensorless control approach for controlling motor speed. For this sensorless speed control to work properly, parameter values must be clearly understood. As a result, a variety of approaches for determining induction motor parameter values have been offered by different researchers [5][6]. The importance of induction motor parameters is also underlined in the paper[7]. The disparity in parameter values causes inaccuracies in motor speed, according to this article. However, it is not indicated in these trials how much variances in motor parameter values will affect the speed controller. A motor speed error will occur if the motor parameters deviate from the real parameter [8]. In that research, it is used MRAS observer to estimate the Permanent Magnet Synchronous Motor (PMSM).

International Journal of Applied Sciences and Smart Technologies

Volume 4, Issue 1, pages 59-74

p-ISSN 2655-8564, e-ISSN 2685-9432

In this research, the effect of induction motor parameters in a speed sensorless control system, i.e. resistance and inductance motor, will be investigated. To estimate the motor speed, it is used the Luenberger observer.

2 Research Methodology

This section provides the research methodology that we use in this work.

2.1. Induction Motor Sensorless Control System

The block diagram of the system is shown in Figure 1. Each part is explained below.

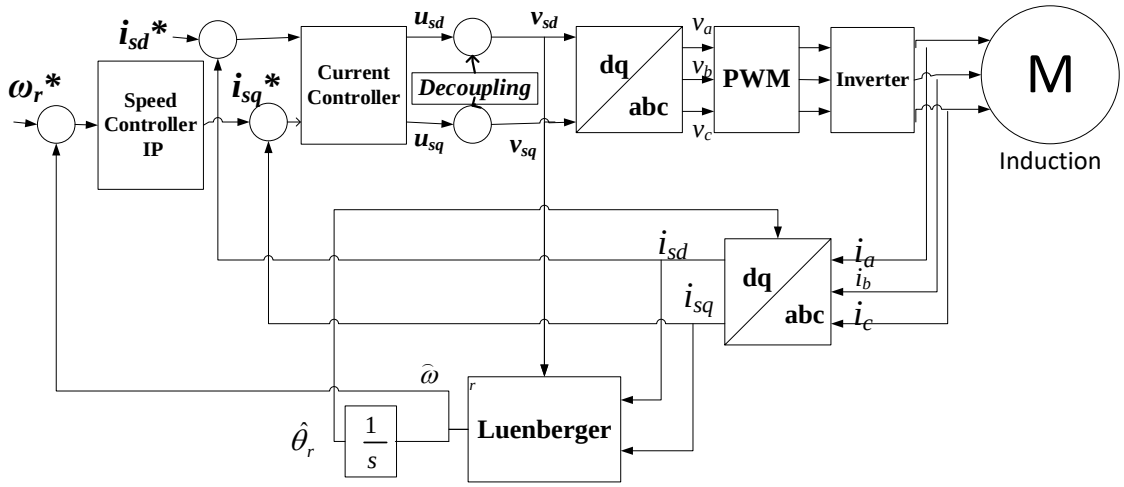

Figure 1. Block diagram of the system

2.1.1. Induction Motor Mathematic Model

Using Clarke and Park transforms, the three-phase mathematical model of the induction motor will be transformed into a two-phase mathematical model. The Clarke transformation converts balanced three-phase values ($V_{sa,sb,sc}$) into a two-phase stationary reference frame (α,β,0) using equation [9]:

$$\begin{bmatrix} v_{s\alpha} \\ v_{s\beta} \\ v_0 \end{bmatrix} = \sqrt{\frac{2}{3}} \begin{bmatrix} 1 & -\frac{1}{2} & -\frac{1}{2} \\ 0 & \frac{\sqrt{3}}{2} & \frac{-\sqrt{3}}{2} \\ \frac{1}{2} & \frac{1}{2} & \frac{1}{2} \end{bmatrix} \begin{bmatrix} v_{sa} \\ v_{sb} \\ v_{sc} \end{bmatrix} \quad (1)$$

where $V_{s\alpha}$ and $V_{s\beta}$ are the stator voltage in α,β reference frame.

International Journal of Applied Sciences and Smart Technologies

Volume 4, Issue 1, pages 59-74

p-ISSN 2655-8564, e-ISSN 2685-9432

The Park transformation transforms a stationary reference frame into a rotating reference (*d*, *q*, 0) frame using the equation

$$\begin{bmatrix} v_{sd} \\ v_{sq} \end{bmatrix} = \begin{bmatrix} \cos\theta_e & \sin\theta_e \\ -\sin\theta_e & \cos\theta_e \end{bmatrix} \begin{bmatrix} v_{s\alpha} \\ v_{s\beta} \end{bmatrix} \quad (2)$$

where θ_e is the electric angle of the motor, while V_{sd} and V_{sq} are the stator voltage in *d*-*q* reference frame.

The induction motor mathematical model in *d*-*q* frame [10] is

$$\frac{d}{dt} i_{sd} = \frac{1}{\sigma L_s} V_{sd} - \left(\frac{R_s}{\sigma L_s} + \frac{(1-\sigma)}{\sigma \tau_r}\right) i_{sd} + \frac{(1-\sigma)}{\sigma \tau_r} i_{rd} + \frac{(1-\sigma) N_p \omega_r}{\sigma} i_{rq} + \omega_e i_{sq} \quad (3)$$

$$\frac{d}{dt} i_{sq} = \frac{1}{\sigma L_s} V_{sq} - \left(\frac{R_s}{\sigma L_s} + \frac{(1-\sigma)}{\sigma \tau_r}\right) i_{sq} + \frac{(1-\sigma)}{\sigma \tau_r} i_{rq} + \frac{(1-\sigma) N_p \omega_r}{\sigma} i_{rd} + \omega_e i_{sd} \quad (4)$$

$$\frac{d}{dt} i_{rd} = -\frac{R_r}{L_r} i_{rd} + \frac{R_r}{L_r} i_{sd} + \left(\omega_e - N_p \omega_r\right) i_{rq} \quad (5)$$

$$\frac{d}{dt} i_{rq} = -\frac{R_r}{L_r} i_{rq} + \frac{R_r}{L_r} i_{sq} - \left(\omega_e - N_p \omega_r\right) i_{rd} \quad (6)$$

$$\frac{d}{dt} \theta_e = N_p \omega_r + \frac{i_{sq}}{\tau_r i_{mr}} \quad (7)$$

$$\frac{d}{dt} \omega_r = \frac{1}{J} (T_e - T_L - B.\omega_r) \quad (8)$$

$$\frac{d}{dt} \theta_r = \omega_r \quad (9)$$

Where i_{sd} is stator current in *d*-frame, i_{sq} is stator current in *q*-frame, i_{rd} is rotor current in *d*-frame, i_{rq} is rotor current in *q*-frame, θ_e is voltage vector angle, and ω_r is rotor speed. Table 1 shows the parameter values of the induction motor that is used in this paper. The parameters are shown in Figure 2 [11].

Table 1. Parameter Values of Induction Motor

Symbol	Description	Values	Unit
Np	Pole pairs	2	pairs
R_r	Rotor resistance	2.9	Ω
R_s	Stator resistance	2.76	Ω
L_s	Stator inductance	0.2349	H
L_r	Rotor inductance	0.2349	H
L_m	Mutual inductance	0.2279	H

International Journal of Applied Sciences and Smart Technologies

Volume 4, Issue 1, pages 59-74

p-ISSN 2655-8564, e-ISSN 2685-9432

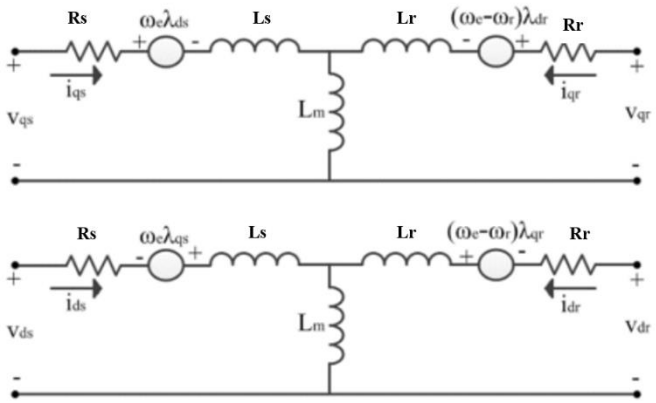

Figure 2. Equivalent Circuit in *d-q* frame

2.1.2. Observer Luenberger

Luenberger observer is one of observer that uses adaptive method to estimate the controlled variable [12]. The equations of the estimation [10] are

$$\frac{d}{dt}\hat{\imath}_{sd} = -\left(\frac{R_s}{\sigma L_s} + \frac{(1-\sigma)}{\sigma\tau_r}\right)\hat{\imath}_{sd} + \omega_e\hat{\imath}_{sq} + \frac{L_m}{\sigma L_s L_r \tau_r}\hat{\varphi}_{rd} + \frac{L_m N_p \omega_r}{\sigma L_s L_r}\hat{\varphi}_{rq} + \frac{1}{\sigma L_s}v_{sd} + g_1(i_{sd} - \hat{\imath}_{sd}) - g_2(i_{sq} - \hat{\imath}_{sq}) \quad (10)$$

$$\frac{d}{dt}\hat{\imath}_{sq} = -\omega_e\hat{\imath}_{sd} + \frac{1}{\sigma L_s}\left(-R_s - \frac{L_m^2}{\tau_r L_r}\right)\hat{\imath}_{sq} - \frac{L_m N_p \omega_r}{\sigma L_s L_r}\hat{\varphi}_{rd} + \frac{L_m}{\sigma L_s L_r \tau_r}\hat{\varphi}_{rq} + \frac{1}{\sigma L_s}v_{sq} + g_2(i_{sd} - \hat{\imath}_{sd}) + g_1(i_{sq} - \hat{\imath}_{sq}) \quad (11)$$

$$\frac{d}{dt}\hat{\psi}_{rd} = \frac{R_r}{L_r}L_m\hat{\imath}_{sd} - \frac{1}{\tau_r}\hat{\varphi}_{rd} + (\omega_e - N_p\omega_r)\hat{\varphi}_{rq} + g_3(i_{sd} - \hat{\imath}_{sd}) - g_4(i_{sq} - \hat{\imath}_{sq}) \quad (12)$$

$$\frac{d}{dt}\hat{\psi}_{rq} = \frac{L_m}{\tau_r}\hat{\imath}_{sq} - (\omega_e - N_p\omega_r)\hat{\varphi}_{rd} + \frac{1}{\tau_r}\hat{\varphi}_{rq} + g_4(i_{sd} - \hat{\imath}_{sd}) + g_3(i_{sq} - \hat{\imath}_{sq}) \quad (13)$$

where

$$g_1 = \frac{(k-1)}{k}\left(-\frac{R_s}{\sigma L_s} - \frac{R_r}{\sigma L_r}\right) \quad (14)$$

$$g_2 = -\frac{(k-1)}{k}N_p\omega_r \quad (15)$$

$$g_3 = \frac{(k-1)}{k(\tau_r^2 N_p^2 \hat{\omega}_r^2 + 1)}\left(\frac{R_s R_r \tau_r + L_s R_r - \sigma\tau_r L_s L_r N_p^2 \hat{\omega}_r^2}{L_m}\right) \quad (16)$$

$$g_4 = \frac{(k-1)}{k(\tau_r^2 N_p^2 \hat{\omega}_r^2 + 1)}\left(\frac{(R_s L_r \tau_r + L_s R_r \tau_r - \sigma L_s L_r) N_p^2 \hat{\omega}_r}{L_m}\right) \quad (17)$$

Volume 4, Issue 1, pages 59-74

p-ISSN 2655-8564, e-ISSN 2685-9432

The estimation speed ($\hat{\omega}_r$) is then calculated using equation

$$\hat{\omega}_r = K_p\left(\hat{\psi}_{rq}e_{isd} - \hat{\psi}_{rd}e_{isq}\right) + K_i\int\left(\hat{\psi}_{rq}e_{isd} - \hat{\psi}_{rd}e_{isq}\right)dt \quad (18)$$

where

$$e_{isd} = i_{sd} - \hat{\imath}_{sd} \quad (19)$$

$$e_{isq} = i_{sq} - \hat{\imath}_{sq} \quad (20)$$

2.2. Decoupling and Current Sensor

The direct-axis stator current i_{sd} (the rotor flux-producing component) and the quadrature-axis stator current i_{sq} (the torque-producing component) must be controlled separately for rotor flux-oriented vector control. The equations for the stator voltage components, on the other hand, are linked. u_{sd}, the direct axis component, and u_{sq}, the quadrature axis component, are both dependent on i_{sd}. For the rotor flux and electromagnetic torque, the stator voltage components u_{sd} and u_{sq} cannot be regarded as disconnected control variables. If the stator voltage equations are decoupled and the stator current components i_{sd} and i_{sq} are indirectly controlled by manipulating the induction motor's terminal voltages, the stator currents i_{sd} and i_{sq} can only be adjusted individually (decoupled control) [13]. The currents i_{sd} and i_{sq} are then controlled by Proportional Integral (PI) current sensor. The output current sensors are determined using equation [14]

$$u_{sd} = \left(K_{idp} + \frac{K_{idi}}{s}\right)\left(i_{sd}^{*} - i_{sd}\right) \quad (21)$$

$$u_{sq} = \left(K_{iqp} + \frac{K_{iqi}}{s}\right)\left(i_{sq}^{*} - i_{sq}\right) \quad (22)$$

where

$$i_{sd} = \frac{1}{T_d s+1} i_{sd}^{*} \quad (23)$$

$$i_{sq} = \frac{1}{T_d s+1} i_{sq}^{*} \quad (24)$$

International Journal of Applied Sciences and Smart Technologies

Volume 4, Issue 1, pages 59-74

p-ISSN 2655-8564, e-ISSN 2685-9432

2.1.3. Speed Controller

The reference current in *q*-reference frame (i_{sq}^{*}) in (24) is controlled by the Integral Proportional (IP) speed controller. The equation of IP speed controller [15] is

$$i_{sq}^{*} = \int K_i(\omega_r^{*} - \omega_r)dt - K_p\omega_r \tag{25}$$

where K_p and K_i are the speed controller gain.

2.2. Testing Method

The system is tested using Matlab – Simulink – Cmex [16]. The simulation block diagram is shown in Figure 3.

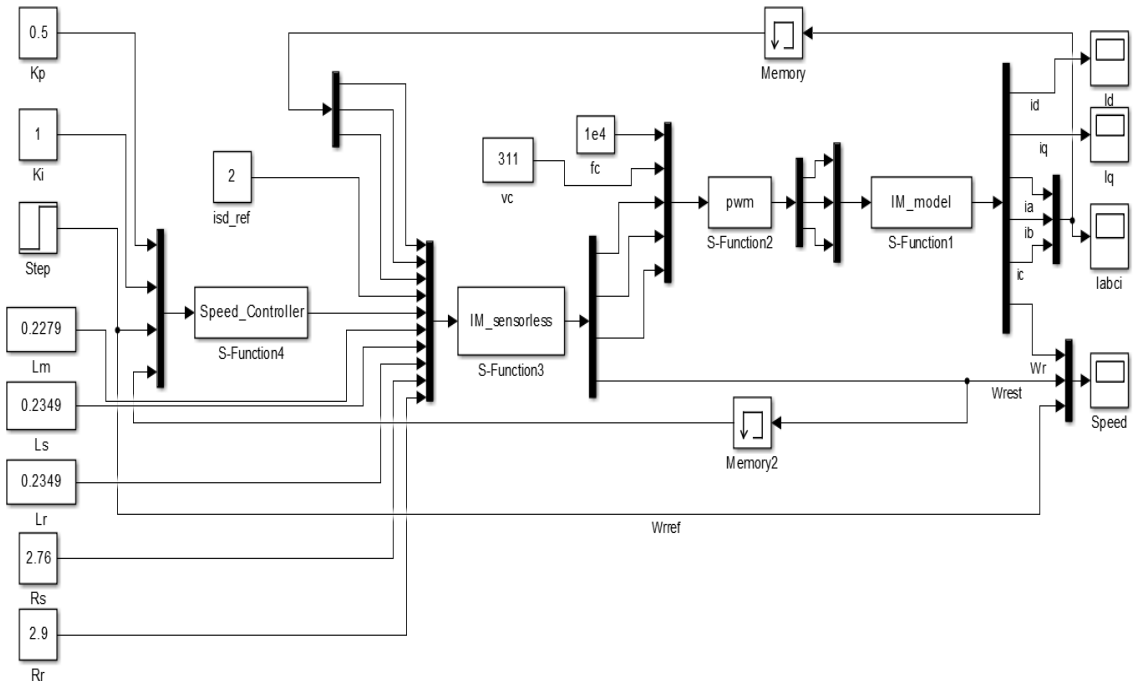

Figure 3. Simulation system

The values of the various parameters are inputted to the current controller using the input port in the figure. With the control parameters K_p=0.5 and K_i=1, the reference speed is 100 rad/s. The stator and rotor resistance, stator and rotor inductance, and mutual inductance characteristics are all employed. In this test, the values of motor parameters in the controller vary as shown in Table 2, so they are different from the actual motor parameters.

Volume 4, Issue 1, pages 59-74

p-ISSN 2655-8564, e-ISSN 2685-9432

Table 2. Variation Parameter Values of Induction Motor

Parameter	Percentage change (%)	Values	Unit
R_s	-50	1.38	Ω
	-90	0.276	
	+50	4.14	
	+90	5.244	
R_r	-50	1.45	Ω
	-90	0.29	
	+50	4.35	
	+65	4.785	
L_s	-4	0.225504	H
	-5	0.223155	
	+5	0.246645	
	+10	0.25839	
L_r	-4	0.225504	H
	-5	0.223155	
	+5	0.246645	
	+10	0.25839	
L_m	-2	0.223342	H
	-3	0.221063	
	-5	0.216505	
	-10	0.20511	
	+2.5	0.233598	
	+3	0.234737	

3 Results and Discussion

The simulation result of the system using the right parameters is shown in Figure 4. It is shown that the actual speed (ω_r) can reach the reference speed (ω_r^*), i.e. 100 rad/s. Although the estimated speed at the transient is slightly different from the actual speed, the estimated speed has the same value as the actual and reference speed at a steady-state. This means that the sensorless control system is working well. The simulation result of the system using various parameters values are described in Figures 5 - 9.

International Journal of Applied Sciences and Smart Technologies

Volume 4, Issue 1, pages 59-74

p-ISSN 2655-8564, e-ISSN 2685-9432

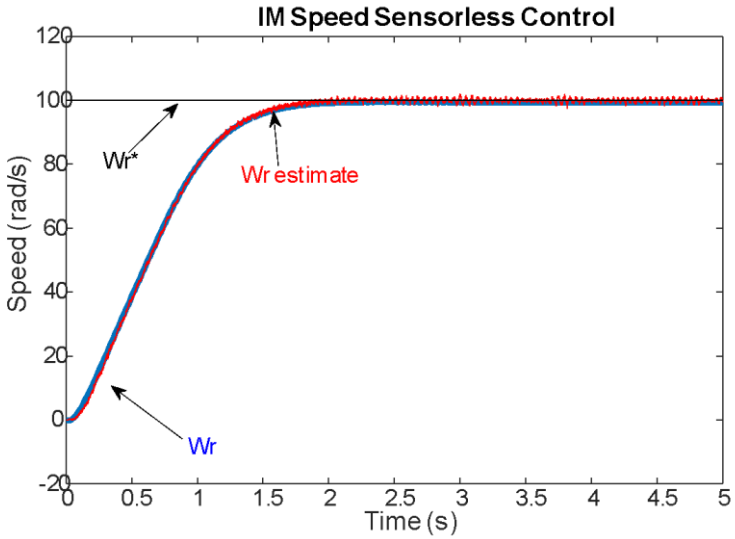

Figure 4. Simulation result with normal parameter values

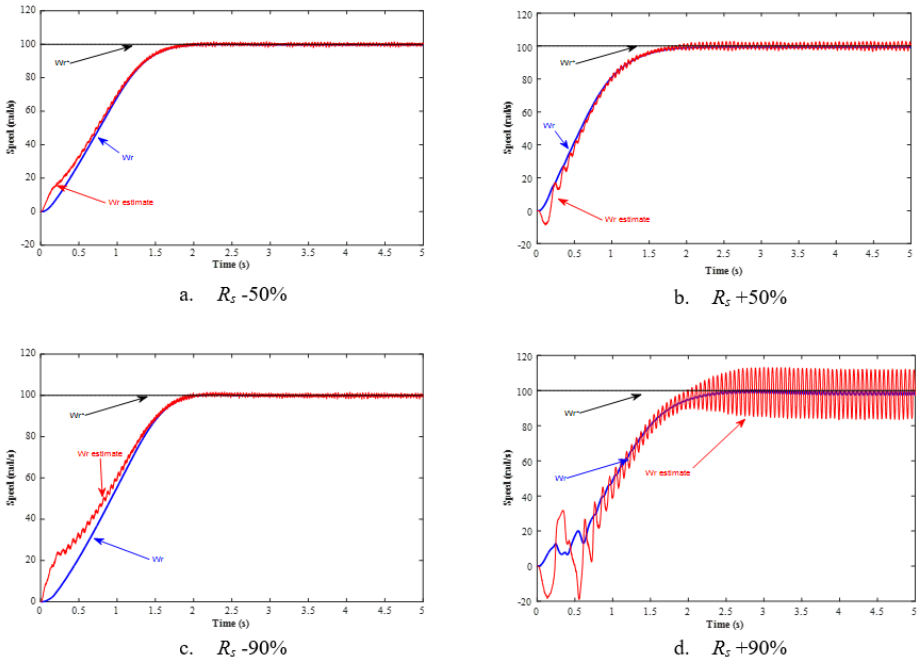

Figure 5. Simulation result with the variation of R_s parameter values

Figure 5 shows the value of R_s on the controller being varied. The figure shows that when the value of R_s in the controller is reduced to 90% (Figures 5.a and c), the actual speed can reach the reference speed, which is 100 rad/s, although there are differences in the transient conditions. When R_s is enlarged by 50% (Figure 5.b), the actual speed can

Volume 4, Issue 1, pages 59-74

p-ISSN 2655-8564, e-ISSN 2685-9432

reach the reference speed, even though the estimated speed is oscillating. However, if the value of R_s is enlarged again, a steady state error occurs, where there is a difference between the actual and the reference speed, although only slightly (Figure 5.d). In this condition, the estimation speed oscillates with increasing amplitude. Thus, to get a good response, the difference in the value of R_s that can be applied is a maximum of +50%.

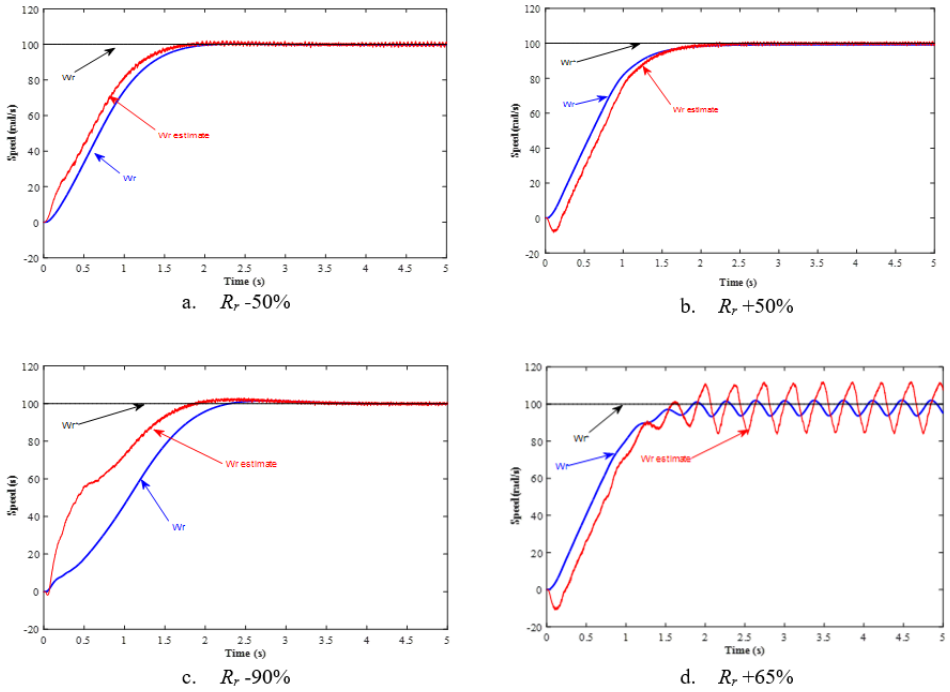

a. R_r -50% b. R_r +50%

c. R_r -90% d. R_r +65%

Figure 6. Simulation result with the variation of R_r parameter values

The condition for the change in the value of R_s is almost the same as the condition for the change in the value of R_r, as shown in Figure 6. The figure shows that when the value of R_r in the controller is reduced to 90% (Figures 6.a and c), the actual speed can reach the reference speed, namely 100 rad/s, although there is a difference in the transient conditions. In addition, when the R_r value is reduced, overshoot will occur (Figure 6.c), although the overshoot percentage is only slightly. When R_r is enlarged by 50% (Figure 5.b), the actual speed can reach the reference speed. However, if the value of R_r is enlarged again by 65%, the estimated speed and the actual speed oscillate (Figure 6.d). Thus, to get a good response, the difference in the value of R_r that can be applied is a maximum of 50%.

International Journal of Applied Sciences and Smart Technologies

Volume 4, Issue 1, pages 59-74

p-ISSN 2655-8564, e-ISSN 2685-9432

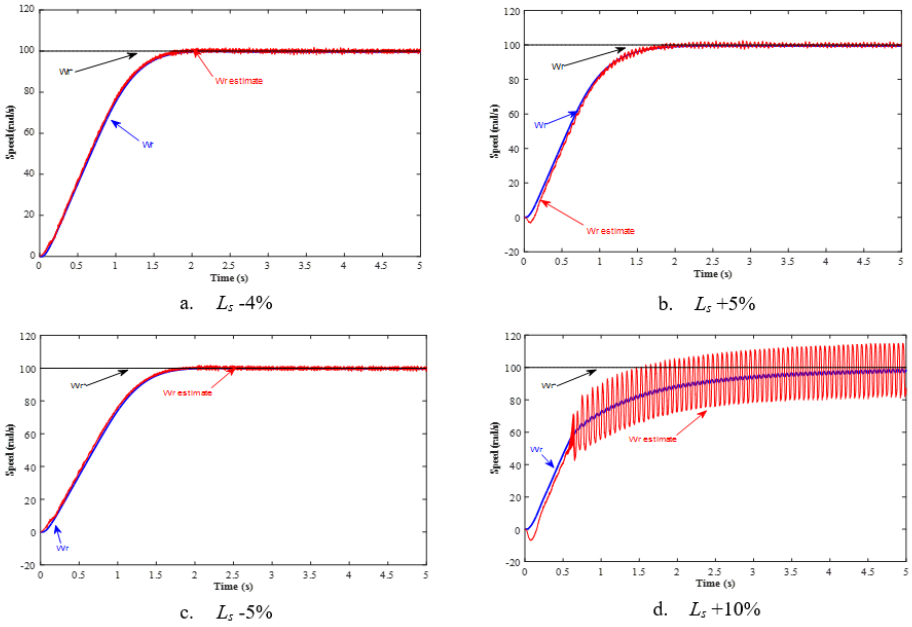

a. L_s -4% b. L_s +5%

c. L_s -5% d. L_s +10%

Figure 7. Simulation result with the variation of L_s parameter values

The effect of differences in resistance values is different from differences in inductance values, as illustrated in Figures 7 - 9. In the three figures, to get a good response, the difference in inductance values between the inductance values in the controller and the actual is very small. The difference in the values of L_s (Figure 7) and L_r (Figure 8) is between -5% to +5% (Figure 7.a - c and Figure 8.a -c). When the difference gets bigger, i.e. 10%, the estimation speed oscillates (Figs 7.d and 8.d). In the two figures, it appears that the actual speed time to achieve stability (settling time) is longer than before.

International Journal of Applied Sciences and Smart Technologies

Volume 4, Issue 1, pages 59-74

p-ISSN 2655-8564, e-ISSN 2685-9432

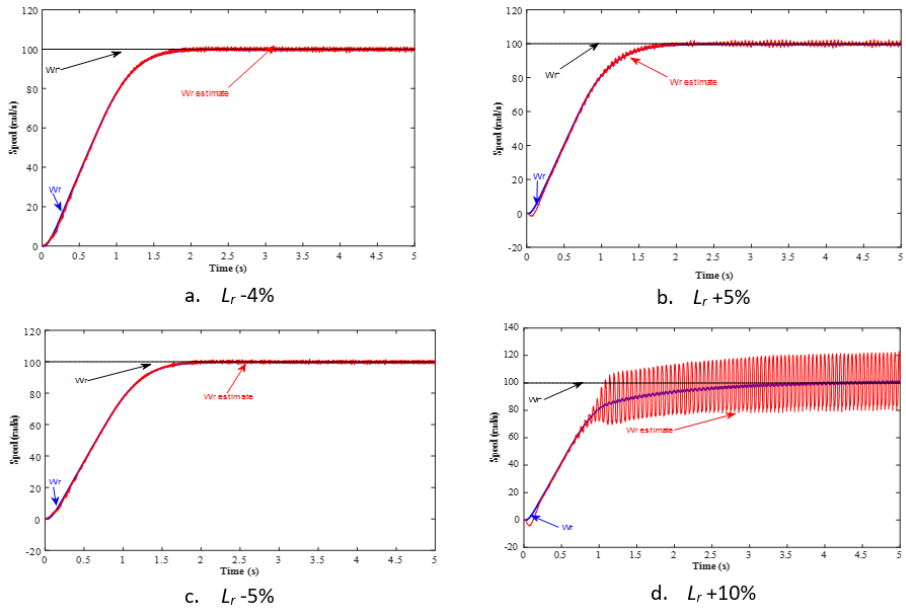

Figure 8. Simulation result with the variation of L_r parameter values

The small differences in the value of mutual inductance (L_m) between the controller and the actual value of the motor parameters have greatly affected the system response, as illustrated in Figure 9. It appears that to get a good response, the differences in the inductance value between the inductance value in the controller and the actual is smaller than L_s and L_r. The difference in L_m values that can be applied is between -3% to +3% (Figure 9.a, c, d, f). As the difference gets bigger, the estimation speed oscillates (Figs 9.b and d). In the two figures, it appears that the actual speed time to achieve stability (settling time) is longer than before. When the L_m value is enlarged (more than +3%) the system becomes an error. Therefore, the recommended L_m differences value is -3% to +3%.

International Journal of Applied Sciences and Smart Technologies

Volume 4, Issue 1, pages 59-74

p-ISSN 2655-8564, e-ISSN 2685-9432

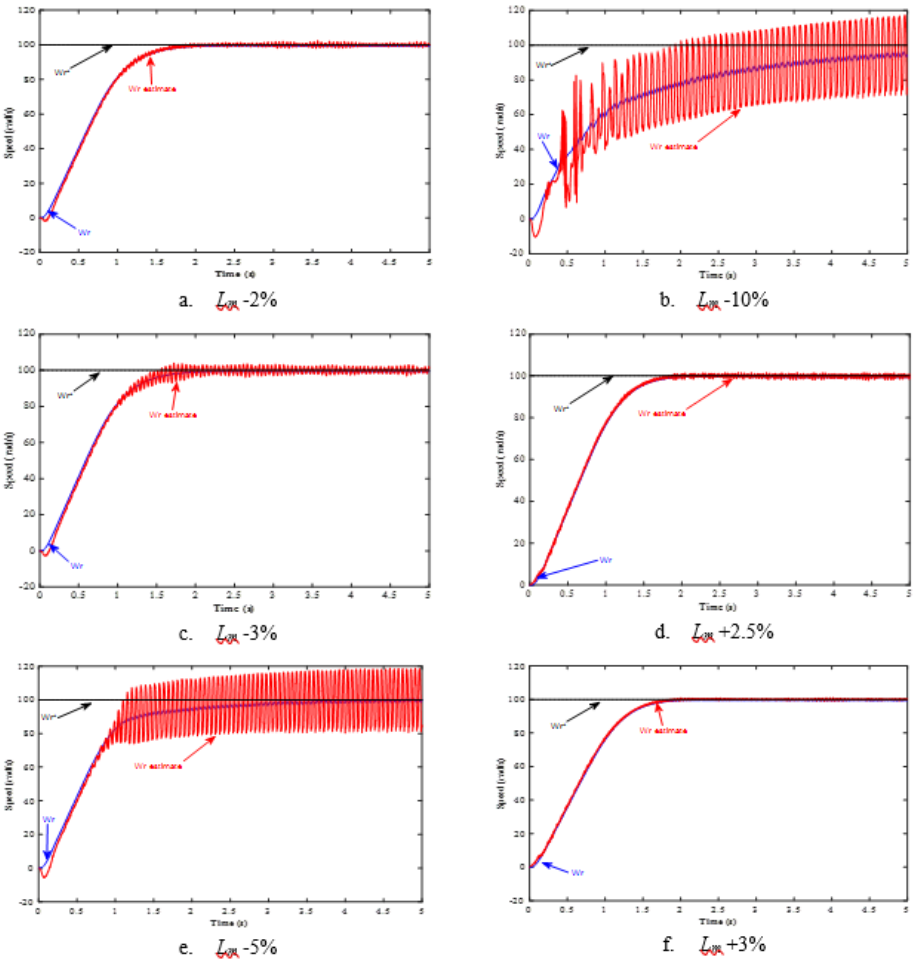

Figure 9. Simulation result with the variation of L_m parameter values

4 Conclusion

The differences in induction motor parameters between the controller and the actual value affect the system response. The value differences of R_r and R_s that can be applied are a maximum of 50%. However, the small differences in the inductance value greatly affect the system response. To get a good response, the value differences of L_s and L_r are between -5% to +5%, while the difference in the value of L_m is between -3% to +3%.

References

[1] Z. Alpholicy X., S. S. Bhandari, P. P. Dsouza, and D. C. Raina, "Personal Assistant Robot," *Int. J. Appl. Sci. Smart Technol.*, **3**(2), 145–152, 2021.

[2] Y. E. Loho, D. Lestariningsih, and P. R. Angka, "Alarm System and Emergency Message from Wheelchair User Emergency Condition," *Int. J. Appl. Sci. Smart Technol.*, **3**(2), 171–184, 2021.

[3] B. W. Harini, F. Husnayain, A. Subiantoro, and F. Yusivar, "A synchronization loss detection method for PMSM speed sensorless control," *J. Teknol.*, **82**(4), 47–54, 2020.

[4] P. Vas, Sensorless Vector and Direct Torque Control. Oxford Uviversity Press, 1998.

[5] O. Avalos, E. Cuevas, and J. Gálvez, "Induction motor parameter identification using a gravitational search algorithm," *Computers*, **5**(2), 2016.

[6] A. C. Megherbi, H. Megherbi, K. Benmahamed, A. G. Aissaoui, and A. Tahour, "Parameter identification of induction motors using variable-weighted cost function of genetic algorithms," *J. Electr. Eng. Technol.*, **5**(4), 597–605, 2010,

[7] S. Yamamoto and H. Hirahara, "Effect of Parameter Tuning on Driving Performance of a Universal-Sensorless-Vector-Controlled Closed-Slot Cage Induction Motor," *2019 22nd Int. Conf. Electr. Mach. Syst. ICEMS 2019*, 2019.

[8] Bernadeta Wuri Harini, "Pengaruh Parameter Motor pada Sistem Kendali tanpa Sensor Putaran," *J. Nas. Tek. Elektro dan Teknol. Inf.*, **10**(3), 236–242, 2021.

[9] A. Glumineau and J. de León Morales, Sensorless AC electric motor control. Springer, 2015.

[10] F. Yusivar and N. Avianto Wicaksono, "Simulasi Mesin Induksi Tanpa Sensor Kecepatan Menggunakan Pengendali Orientasi Vektor," *J. Nas. Tek. Elektro dan Teknol. Inf.*, **4**(4), 2016.

[11] R. Ridwan, E. Purwanto, H. Oktavianto, M. R. Rusli, and H. Toar, "Desain Kontrol Kecepatan Motor Induksi Tiga Fasa Menggunakan Fuzzy Pid Berbasis Idirect Field Oriented Control," *J. Integr.*, **11**(2), 146–155, 2019.

[12] J. Agrawal and S. Bodkhe, "Low speed sensorless control of PMSM drive using

Volume 4, Issue 1, pages 59-74
p-ISSN 2655-8564, e-ISSN 2685-9432

high frequency signal injection," *12th IEEE Int. Conf. Electron. Energy, Environ. Commun. Comput. Control (E3-C3), INDICON 2015*, 4–9, 2016.

[13] F. Semiconductor, "3-Phase AC Induction Motor Vector Control Using a 56F8300 Device," *Memory*, 2005.

[14] R. Gunawan and F. Yusivar, "Reducing estimation error due to digitizing problem in a speed sensorless control of induction motor," *IECON Proc. (Industrial Electron. Conf.*, **2005**(1), 1677–1682, 2005.

[15] F. Yusivar, H. Haratsu, T. Kihara, S. Wakao, and T. Onuki, "Performance comparison of the controller configurations for the sensorless IM drive using the modified speed adaptive observer," *IEE Conf. Publ.*, **475**, 194–200, 2000.

[16] F. Yusivar and S. Wakao, "Minimum requirements of motor vector control modeling and simulation utilizing C MEX S-function in MATLAB/SIMULINK," *Proc. Int. Conf. Power Electron. Drive Syst.*, **1**, 315–321, 2001.

Volume 4, Issue 1, pages 59-74

p-ISSN 2655-8564, e-ISSN 2685-9432

This page intentionally left blank

International Journal of Applied Sciences and Smart Technologies

Volume 4, Issue 1, pages 75–88

p-ISSN 2655-8564, e-ISSN 2685-9432

Characteristics of Wooden Furniture Drying Machine

Petrus Kanisius Purwadi[1, *], A. Prasetyadi[1]

[1]*Department of Mechanical Engineering, Sanata Dharma University, Paingan, Maguwoharjo, Depok, Sleman, Yogyakarta 55282, Indonesia*
[*]*Corresponding Author: pur@usd.ac.id*

(Received 20-05-2022; Revised 27-05-2022; Accepted 28-05-2022)

Abstract

This study aims to determine the characteristics of the electric energy drying machine used to dry wooden furniture. Furniture made of mahogany. The research was conducted experimentally in the wood furniture industry. The size of the wood drying room is 8 m x 6 m x 3 m. The dryer works with a vapor compression cycle using R134a freon and several fans placed in the drying chamber. The drying process uses a closed air system. The total volume of dried wooden furniture is 12.9 m^3. The initial moisture content in the wood ranges from 18% to 23%. Wooden furniture is considered dry if the moisture content in the wood furniture is less than 12%. Research gives satisfactory results. The performance of the drying machine or *COP* is 10.85. The drying time for wooden furniture is about 72 hours.

Keywords: COP, wooden furniture, dryer, vapor compression

1 Introduction

Drying wood furniture in the wood furniture industry with wood fuel still has many shortcomings. Apart from being energy-intensive, it is also impractical, unsafe, uncomfortable, environmentally unfriendly and takes a long time. Economically, the

Volume 4, Issue 1, pages 75–88
p-ISSN 2655-8564, e-ISSN 2685-9432

drying process with wood fuel requires a large amount of money. Drying wood furniture referred to here is the process of drying wooden furniture that only relies on high temperature air to dry all wooden furniture. In general, the air temperature in the wood furniture drying room is not more than 70^{o}C. If the air temperature of the drying chamber is more than that, the air will damage wooden furniture and flammable wood. The air used in the drying process of wood furniture is air heated by a heat exchanger which has a much higher working temperature. By means of air passed through a heat exchanger, then the hot air produced is used to dry wooden furniture. In the heat exchanger flows a mixed gas (air and gas resulting from the fuel combustion process) which has a much higher temperature.

The use of fuel with wood wastes energy because the mixed gas resulting from the fuel combustion process that is discharged into the environment still has a high temperature. As is known, high-temperature exhaust gases have high energy as well. The process of drying with wood fuel is quite a hassle. It's a hassle, because the industry must provide wood fuel every time it will carry out the process of drying wood furniture, prepare for the combustion process, burn wood fuel, maintain and oversee the drying process of wood furniture from start to finish. Based on information from workers in the wood furniture industry, drying wood furniture takes more than 7 days. The drying process with wood fuel is considered unsafe. If the drying process is not maintained and controlled properly, the possibility of a fire is quite large. The process of drying wooden furniture also does not provide comfort. Not comfortable, because after the drying process is finished, the air in the drying room still has a high temperature (about 35^{o}C). Actually, the industry can still reduce the air condition to close to the outside air condition, but it takes a long time to get the same air temperature as the outside air temperature. The industry can't wait to immediately take out and import wooden furniture with the air condition in the drying chamber still quite high. This condition makes workers uncomfortable when loading and removing wooden furniture from the drying room. The drying process with wood fuel is not environmentally friendly. Not environmentally friendly because burning wood fuel produces dust, and exhaust gases that pollute the environment. It also produces soot that makes the walls of the drying room for wood furniture black. The drying time of wooden furniture is also relatively long. The duration

Volume 4, Issue 1, pages 75–88
p-ISSN 2655-8564, e-ISSN 2685-9432

depends on the volume of the wood being dried, the thickness of the wood, the type of wood, the type of furniture, and so on.

Many researches and applications related to the drying process have been carried out by experts [1-14] although with different objects being dried and the drying system chosen is also different. Research and application with fish objects has been carried out by A. Aryadillah and A. Mursadin [1], M. Nur Alam, et al, [2]. Research with briquette objects was carried out by P.K. Purwadi, et al [3]. Research with the object of corn chips has been carried out by D. Purwadianto [4]. Research with the object of towels has been carried out by K. Wijaya [5], and clothes by P.K. Purwadi and W. Kusbandono [6,7,8,9], Balioglu [10], T. Mitsunori [11], Bison [12]. Research and application with wooden planks has been carried out by W. Kusbandono and P.K. Purwadi [13], Purwadi, P.K., et al 14]. The research method used is a simulation and some is experimental. Apart from aiming to get good performance or better efficiency of the dryer, there is also a goal to get a dryer that can replace the drying process by drying directly under the hot sun. The dryer can work during the rainy season or can be done at night or can be done whenever needed. From the results of several studies that have been carried out, some researchers use a drying machine that works with a vapor compression cycle. Drying machines that work with a vapor compression cycle, in addition to providing good performance, also provide a fast-drying process.

The dryer is made and used in drying wood furniture, working with a vapor compression cycle. With the vapor compression cycle, air that is dry and quite hot can be produced. Dry air means that the water content in the air is quite low, with the resulting relative humidity (*RH*) of less than 35%. The air produced is quite hot, which causes the air condition in the drying chamber to be no more than 35^{o}C.

A. Vapor compression cycle

The main components of a vapor compression machine include: compressor, condenser, capillary tube and evaporator. Figure 1 presents a series of main components of a steam compression engine and Figure 2 presents the vapor compression cycle on the P-h diagram, which is accompanied by a further cooling and further heating process. There is no need for superheating and subcooling. The further cooling process is carried out so that the condition of the refrigerant when it enters the capillary tube is actually in

International Journal of Applied Sciences and Smart Technologies

Volume 4, Issue 1, pages 75–88

p-ISSN 2655-8564, e-ISSN 2685-9432

the liquid phase. The further heating process is used so that when the refrigerant enters the compressor, it is actually in the gas phase. Both processes are used to increase the performance of the refrigeration engine and facilitate the function of the compressor to circulate the refrigerant flowing in the vapor compression cycle system. Compressor work becomes light and not easily damaged.

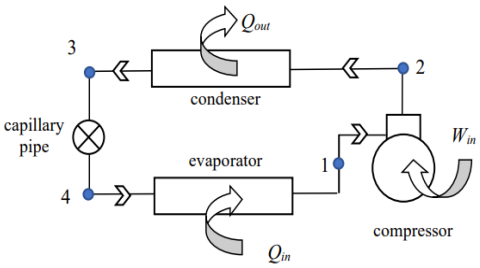

Figure 1. Vapor compression cycle component circuit

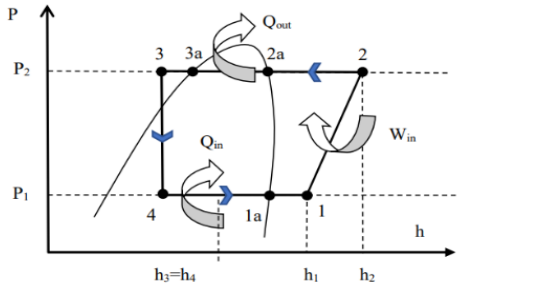

Figure 2. Vapor compression cycle on P-h diagram

The amount of heat absorbed per unit mass-refrigerant by the evaporator *(Q_{in})* can be calculated by Equation (1)

$$Q_{in} = h_1 - h_4 \quad (kJ/kg) \tag{1}$$

The amount of heat released per unit mass-refrigerant by the condenser *(Q_{uot})* can be calculated by Equation (2)

$$Q_{out} = h_2 - h_3 \quad (kJ/kg) \tag{2}$$

Compressor work per unit refrigerant-mass *(Win)* can be calculated by Equation (3).

$$W_{in} = h_2 - h_1 \quad (kJ/kg) \tag{3}$$

The performance of the steam compression cycle engine can be expressed by Equation (4). *COP* is the ratio between the amount of useful energy and the energy supplied to the dryer

$$COP = (Q_{in} + Q_{out})/W_{in} \tag{4}$$

The variables h_1, h_2, h_3 and h_4 in Equation (1) to (3), are the enthalpy of refrigerant entering the compressor, enthalpy of refrigerant leaving the compressor, enthalpy of refrigerant leaving the condenser and enthalpy of refrigerant entering the evaporator, respectively. The enthalpy that enters the evaporator is equal to the amount of enthalpy

Volume 4, Issue 1, pages 75–88

p-ISSN 2655-8564, e-ISSN 2685-9432

that leaves the condenser or enters the capillary tube. This is because the process that occurs in the capillary tube takes place with a constant enthalpy value

B. Wood Furniture Drying Process

The medium used for drying wood furniture is air. The air system used is a closed air system. During the wood furniture drying process, no outside air is entered or removed from the building which is used for the wood furniture drying process. The building for the wood drying process consists of a wood furniture drying room and a drying machine room. The thermodynamic processes experienced by air during the wood drying process include the following processes: cooling, cooling and dehumidifying, heating and cooling and humidifying. When the air passes through the evaporator, the air first undergoes a cooling process, then the air undergoes a cooling and dehumidifying process. After the air leaves the evaporator, the air undergoes a heating process as it passes through the condenser. When air is blown into the drying chamber by the condenser fan the air passes through the wooden furniture to be dried. In this process the air undergoes a cooling and humidifying process. Inside the drying room, several fans are installed. One of the functions of the fan is so that the cooling and humidifying process can run optimally. Figure. 3 presents a schematic of the wood furniture drying process carried out in this study.

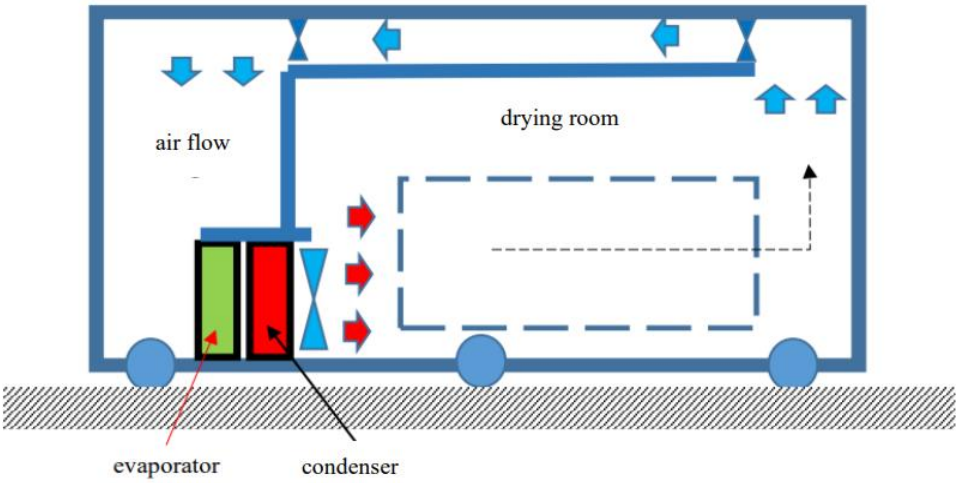

Figure 3. Schematic of wood furniture drying machine with closed air system

International Journal of Applied Sciences and Smart Technologies

Volume 4, Issue 1, pages 75–88

p-ISSN 2655-8564, e-ISSN 2685-9432

2 Research Methodology

The research was conducted experimentally in the wood furniture industry, with a drying room size of 8m x 6m x 3m. The dryer works with a source of electrical energy. The drying machine works by using a vapor compression cycle, using a refrigerant R134a working fluid. The main components of the drying machine include: compressor, evaporator, condenser and capillary tube. The dried object is wooden furniture. Figure 4 shows some examples of dried wood furniture.

Figure 4. Some examples of wood furniture being dried in a drying room

In the process of drying wood furniture, the evaporator serves to get dry air, while the condenser functions to get hot enough air. When the dryer works, the air used to dry the wooden furniture is passed through the evaporator and condenser before being used to dry the wood furniture. The total electric power required to drive the compressor is about 3 HP, and the total electric power to drive the evaporator fan and condenser fan is about 80 watts. In the wooden furniture drying room, 6 fans are provided with a uniform fan power of @ 250 watts. In addition to functioning to accelerate air flow, the fan also functions so that all wooden furniture flows through the air. The dried wood furniture has a volume of 12.9 m^3, with various forms of wood furniture. Mahogany wood furniture. The initial condition before the drying process was carried out, the moisture content in the wood furniture was in the range of 18-23%. The drying process is stopped when all wooden furniture has a moisture content of less than 12% or below 12%. The process of

Volume 4, Issue 1, pages 75–88
p-ISSN 2655-8564, e-ISSN 2685-9432

drying wood furniture is carried out with a drying machine that works continuously without stopping.

3 Results and Discussion

The results of the research in the form of data are presented in Tables 1 to 4. Apart from the direct measurement results, data are also taken from the P-h diagram and tables of the refrigerant properties used (such as: enthalpy, condenser working temperature, evaporator working temperature). The data collection from this research was carried out with several assumptions, such as:

a. The compression process in the compressor that occurs in the vapor compression cycle takes place isentropically
b. The process of decreasing refrigerant pressure in the capillary tubes that occurs in the vapor compression cycle takes place isentalpically
c. The process of desuperheating and condensation or condensation of refrigerant in the condenser that occurs in the vapor compression cycle takes place at a constant pressure (P_2)
d. The refrigerant evaporation process in the evaporator that occurs in the vapor compression cycle takes place at a constant pressure (P_1).
e. The superheating and subcooling processes are ignored

From Table 3, it can be seen the characteristics of the dryer used for drying wood furniture in the industry where this research was conducted. The amount of heat absorbed by the evaporator per unit mass of refrigerant from the air is 126.43 kJ/kg. The heat absorbed by the evaporator causes the air to decrease in dry bulb air temperature and undergo a process of condensation of water vapor in the air. In other words, the air undergoes a cooling and cooling and dehumidifying process. The process of cooling and dehumidifying the air takes place at a relative humidity (*RH*) of 100%. The air becomes dry, because the water content in the air decreases. The value of the specific humidity of the air decreases. The amount of heat released by the condenser per unit mass of refrigerant into the air is 152.11 kJ/kg. This heat causes the air temperature to rise again, and the relative humidity of the air (*RH*) decreases by 19%. With dry air conditions, and relatively low humidity, the drying process of wooden furniture can be carried out

Volume 4, Issue 1, pages 75–88

p-ISSN 2655-8564, e-ISSN 2685-9432

successfully. In this drying process, the compressor work per unit mass of refrigerant required is 25.68 kJ/kg and the resulting drying machine performance is 10.85.

Table 1. Working pressure and temperature on vapor compression cycle machine

Researched machine	Evaporator working pressure (P_1)	Working pressure Condenser (P_2)	Evaporator working temperature (T_{evap})	Condenser working temperature (T_{kond})
	(kPa)	(kPa)	(°C)	(°C)
Vapor compression cycle machine of wood furniture dryer	414.61	1455.50	10	54

Table 2. Enthalpy values in the vapor compression cycle

Researched machine	h_1	h_2	h_3	h_4
	(kJ/kg)	(kJ/kg)	(kJ/kg)	(kJ/kg)
Vapor compression cycle machine of wood furniture dryer	404.32	430.00	277.89	277.89

Table 3. Characteristics of the vapor compression cycle machine of the dryer

Researched machine	Q_{in}	Q_{out}	W_{in}	$COP=(Qi+Qout)/(Win)$
	(kJ/kg)	(kJ/kg)	(kJ/kg)	
Vapor compression cycle machine of wood furniture dryer	126.43	152.11	25.68	10.85

Table 4. Air conditions in the drying process of wood furniture

Researched machine	The condition of the air entering through the evaporator		Air temperature out of the evaporator	Condenser exit air temperature		Drying time
	$T_{db,A}$	RH	$T_{db,C}=T_{wb,C}$	$T_{db,D}$	RH	t
Vapor compression cycle machine of wood furniture dryer	30ºC	68%	16ºC	44	19%	72 hours

The air conditions in the air-drying process are not only presented in Table 4, but also presented in Figure 5. The A-B-C-D-A process in Figure 5 presents the air-drying process. The A-B and B-C processes in Figure 5 occur when the air passes through the evaporator, the C-D process occurs when the air passes through the condenser, and the D-A process

Volume 4, Issue 1, pages 75–88

p-ISSN 2655-8564, e-ISSN 2685-9432

when the air passes through the wooden furniture. The A-B process is the air-cooling process, the B-C process is the cooling and dehumidifying process, the C-D process is the heating process and the D-A process is the cooling and humidifying process. The cooling and humidifying process is assumed to run at a constant enthalpy value, so the process is also known as evaporative cooling. The evaporative cooling process experienced by the air, when the air carries out the process of drying wooden furniture. The evaporative cooling process takes place at a constant wet bulb air temperature.

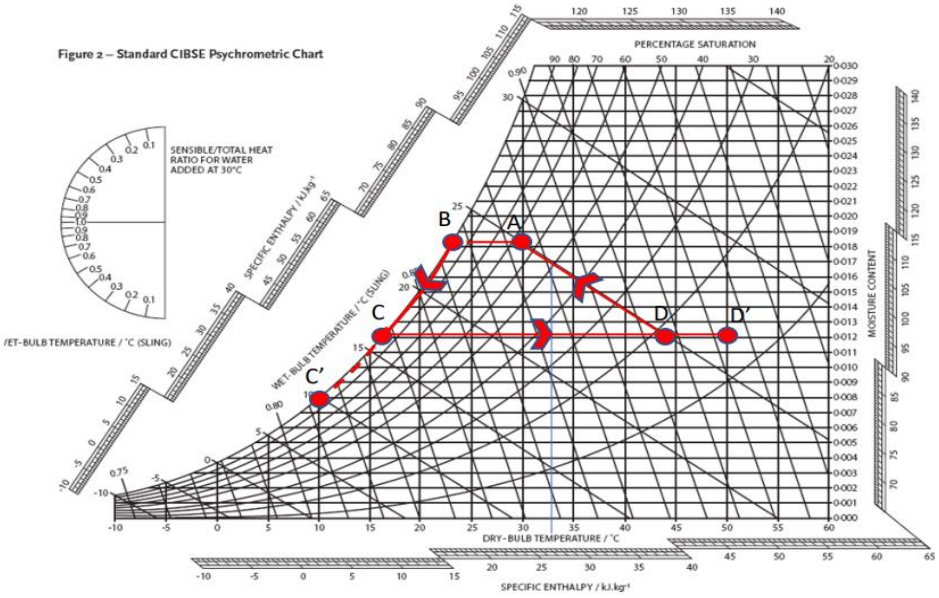

Figure 5. Air conditions in the drying process of wood furniture

In the A-B process, the air undergoes a cooling process. The dry bulb air temperature decreases in temperature until it reaches the dew point temperature of the water vapor in the air (point B in Figure 5). The air releases heat, and the enthalpy of the air decreases. The heat released by the air is used to vaporize or boil the refrigerant flowing in the evaporator pipe. In the A-B process, the process runs at a fixed specific humidity value, because there is no addition or reduction of water content in the air. The relative humidity of the air increases, as the dry bulb air temperature decreases. In the A-B process, the dry bulb air temperature and the wet bulb air temperature decreased until they reached the dew point temperature of the water vapor in the air (point B in Figure 5). The dry-bulb

Volume 4, Issue 1, pages 75–88
p-ISSN 2655-8564, e-ISSN 2685-9432

air temperature at point B is equal to the wet-bulb air temperature and the same as the dew point temperature of the water vapor in the air.

In the B-C process, the air is cooling and dehumidifying. In addition to the decrease in air temperature, dry bulb air also experienced a decrease in specific humidity. In this process the air releases heat, which causes the enthalpy of the air to decrease. The heat released by the air is used for the evaporation or boiling process of the refrigerant flowing in the evaporator pipe. As is known, the evaporator sucks heat from the air that passes through the evaporator pipe to be used to change the refrigerant phase from liquid to gas. The specific humidity of the air decreases because in this process there is a reduction in the water content in the air. The decrease in water content is caused because some of the water vapor in the air condenses. The B-C process runs at 100% relative humidity. During the process, the dry bulb air temperature is the same as the wet bulb air temperature.

In the C-D process, the air undergoes a heating process. The air temperature has increased in temperature, both dry bulb air temperature and wet bulb air temperature. This is because the air gets the heat released by the condenser. As is known, in the vapor compression cycle, the condenser releases heat to the air passing through the condenser. The heat released by the condenser comes from the desuperheating process and the refrigerant condensation process when the refrigerant flows in the condenser pipe. In this process the enthalpy of air increases. The process runs at a constant specific humidity, because there is no additional water content in the air, but the relative humidity of the air decreases as the air temperature increases.

In the D-A process, the air undergoes an evaporative cooling process. The air undergoes a cooling process and the addition of specific humidity. The dry-bulb air temperature decreases, but the wet-bulb air temperature remains the same. This is because some of the energy in the air is sucked in by the wooden furniture to evaporate some of the water in the wood furniture. As it is known that the evaporation process requires latent heat. With the process of evaporation of water in wooden furniture, it causes the water content in the wood to decrease. Over time, the wood will dry out. In this process, water is transferred from the wood to the air. This causes the water content per unit mass of air to increase, which causes the specific humidity of the air to increase.

Volume 4, Issue 1, pages 75–88
p-ISSN 2655-8564, e-ISSN 2685-9432

Unlike drying wood furniture using wood fuel, drying wood furniture with a steam compression cycle is not energy-intensive. The electrical energy used to drive the compressor and drive the fans are all useful for the drying process. Relatively no energy is wasted. The energy absorbed by the evaporator causes the air to dry out and the energy released by the condenser causes the air to increase in temperature. The resulting air condition provides benefits for the drying process of wood furniture. The electrical energy required by the condenser fan and evaporator fan is also useful in increasing the air flow rate required for the drying process. Likewise, the electrical energy used to drive the fans in the drying room. Even if there is a leakage of electrical energy that turns into heat, as happens in compressors or in electric motors from fans, then this heat energy will not go to waste. In the process of drying wood furniture, the air used also passes through the compressor and passes through the electric motor of the fans. In other words, the heat from the leak will be accepted by the air and cause an increase in the temperature of the air. The higher the air temperature, the faster the drying process. As is known, the position of the compressor and fans are placed in the building room. Because the system used in the drying process for wood furniture is not energy-intensive, it is only natural that the drying machine has a high performance (*COP* of the dryer is 10.85).

One of the characteristics of this wood furniture dryer with a vapor compression cycle is that it is practical. Practical because it does not bother the user. To run the dryer, the user just presses on from the on-off button which causes the compressor and fans to work. If you want to turn it off, just press the off button. Users are not bothered by having to maintain and control the drying process of wooden furniture. During the drying process of wooden furniture, users can leave the drying process area, because they are not required to be in the drying location.

The process of drying wood furniture with a vapor compression cycle can run safely and comfortably. Small chance of fire. The air condition in the drying chamber does not allow a fire to occur. There is no fire and no embers that allow a fire to occur. Unlike when using wood fuel, in the presence of fire, the temperature produced in the fuel combustion process can exceed 200^{o}C. By using a machine that works with a vapor compression cycle, there is no air condition that has a temperature above 50^{o}C. The air temperature in the wood furniture drying room is safe, the air temperature is only around

Volume 4, Issue 1, pages 75–88
p-ISSN 2655-8564, e-ISSN 2685-9432

30^{o}C. With such air conditions, workers can put wooden furniture in the drying room or take out wooden furniture, at any time. Workers do not feel hot, because the air temperature is not much different from the outside air temperature. More comfortable than the air condition when using the drying process with wood fuel. The air condition in the drying room is also relatively clean. No soot is produced from the drying process with this system.

Drying using a vapor compression system is relatively more environmentally friendly. Does not cause environmental pollution, both air pollution and noise pollution. The refrigerant used in the vapor compression cycle is selected which is environmentally friendly. Does not cause social problems for the surrounding community. No exhaust gas is produced from the process of using this electrical energy. All of the electrical energy used in this drying process is converted into work and heat.

With the high performance of the machine, the drying system used is able to carry out the drying process relatively quickly. To get the moisture content of all wooden furniture below 12%, the time needed is only about 76 hours or about 3 days. With a note, the machine works continuously without stopping. This can be done, because the drying process can be left behind. The drying process can be carried out continuously during the day and night. With fast drying time, the production capacity of wood furniture can be increased

4 Conclusion

Research on wood furniture drying machine using the vapor compression cycle has been successful. The process of drying wooden furniture can run as expected: it does not waste energy, is practical, safe, comfortable, environmentally friendly, and quickly dries wooden furniture. The dryer has a high performance, with a *COP* of 10.85. The drying process for wooden furniture takes about 72 hours (3 days).

Acknowledgements

The author, Petrus Kanisius Purwadi as a grantee, expresses his gratitude for the support and grants provided by LPPM Sanata Dharma University Yogyakarta so that this

research can run well and be completed. Research contract number with LPPM USD is No: 007/Penel./LPPM-USD/II/2022. The author also does not forget to thank the owner of the wood furniture industry in Sragen and the staff where this research was conducted.

References

[1] A. Aryadillah, A. Mursadin, "Analisis perbandingan kinerja sistem distribusi panas pada variasi ruang mesin pengering ikan", *SJME Kinematika*, **1(**1), 27-36, 2016.

[2] M. Nur Alam, Sukarti, F.I. Lisanty, "Penerapan teknologi alat pengering ikan bagi kelompok pengusaha ikan teri kering di Kecamatan Ponrang Kabupaten Luwu", *Prosiding Seminar Nasional Hasil Pengabdian Kepada Masyarakat (SNP2M)*, 225-229, 2018.

[3] P.K. Purwadi, Y.B. Lukiyanto, S. Mungkasi, "Mengembangkan industri briket dengan mempergunakan mesin pengering briket energi listrik", *Abdimas Altruis Jurnal Pengabdian Kepada Masyarakat*, **1**(2), 52-61, 2018.

[4] D. Purwadianto, P.K. Purwadi, "Karakteristik mesin pengering emping jagung energi listrik", *Prosiding Seminar Nasional Universitas Respati Yogyakarta*, **1**(2), 116-123, 2019.

[5] K. Wijaya, P.K. Purwadi, "Mesin pengering handuk dengan energi listrik", *Majalah Ilmiah Teknik Mesin Mekanika*, 15(2), 31-35, 2016.

[6] P.K. Purwadi, "Mesin pengering kapasitas limapuluh baju sistem tertutup", *Jurnal Ilmiah Widya Teknik*, **16**(2), 91-96, 2017

[7] P.K. Purwadi, W. Kusbandono, "Mesin pengering pakaian energi listrik dengan mempergunakan siklus kompresi uap", *Proceeding Seminar Nasional Tahunan Teknik Mesin XIV (SNTTM XIV)*, MT 61, 2015

[8] P.K. Purwadi, W. Kusbandono, "Pengaruh kipas terhadap waktu dan laju pengeringan mesin pengering pakaian", *Teknoin Jurnal Teknologi Industri*, **22**(7), 514-523, 2016

[9] P.K. Purwadi, W. Kusbandono, "Inovasi mesin pengering pakaian yang praktis, aman dan ramah lingkungan", *Jurnal Ilmiah Widya Teknik,* **15**(2), 106-111, 2016.

[10] Balioglu, "Heat Pump Laundry Dryer Machine", *Patent Application Publication*, Pub. No: US 2013/0047456 A1, 2013

[11] T. Mitsunori, "Dehumidifying and heating apparatus and clothes drying machine using the same", *European Patent Specification*, EP 2 468 948 B1, 27.11.2013, 2013.

Volume 4, Issue 1, pages 75–88

p-ISSN 2655-8564, e-ISSN 2685-9432

[12] Bison, "Heat Pump Laundry Dryer and a Method for Operating a Heat Pump Laundry Dryer", *Patent Application Publication*, Pub. No: US 2012/0210597 A1, 2012.

[13] W. Kusbandono, P.K. Purwadi, "Effects of the Existence of Fan in the Wood Drying Room and the Performance of the Electric Energy Wood Dryer", *International Journal of Applied Sciences and Smart Technologies*, **3**(1), 83–92, 2021.

[14] P.K. Purwadi, S. Mungkasi, Y.B. Lukiyanto, "Peningkatan pemahaman proses pengeringan kayu di SMK Pangudi Luhur Muntilan", *Jurnal Abdimas Dewantara*, **3**(2), 16-29, 2020.

International Journal of Applied Sciences and Smart Technologies

Volume 4, Issue 1, pages 89–96

p-ISSN 2655-8564, e-ISSN 2685-9432

Shrinkage of Biocomposite Material Specimens [HA/Bioplastic/Serisin] Printed using a 3D Printer using the Taguchi Method

Felix Krisna Aji Nugraha[1,*]

[1]*Department of Mechanical Design Technology, Sanata Dharma University, Yogyakarta, Indonesia*

[*]*Corresponding Author: felix@pmsd.ac.id*

(Received 15-05-2022; Revised 25-05-2022; Accepted 26-05-2022)

Abstract

The Fused Deposition Modeling in the rapid prototyping technique was modified using a paste-shaped material with biocomposite material. One of the correction factors for the printed test specimen results is shrinkage. The paste material used is hydroxyapatite [CA5(PO4)6(OH)2] and tapioca bioplastic. Besides these materials, sericin is added, which is produced from extracts from silkworm cocoons. The composition of the biocomposite paste used with the ratio of hydroxyapatite and bioplastic was 40:50, 50:50, 60:40, by adding 0.3% sericin to the hydroxyapatite solution. The parameters used in the printing process of the test specimens are the perimeter speed of 60 mm/s, the infill speed of 10 mm/s, and the layer height of 0.45 mm. The design in this test has dimensions of 100mm long, 25mm wide, and 3mm thick. The optimal shrinkage of the test specimens was analyzed using the Taguchi method. Specimen printing is done by using additive manufacturing method. The process is carried out using a Portabee three-dimensional printing machine that uses a FDM system modified to an Aqueous-Based Extrusion Fabrication (ABEF) system. The results obtained that the optimum

Volume 4, Issue 1, pages 89–96
p-ISSN 2655-8564, e-ISSN 2685-9432

composition for shrinkage of the biocomposite material was 50:50 with the addition of 0.3% sericin to the hydroxyapatite solution.

Keywords: shrinkage, biocomposite, three-dimensional printer, taguchi

1 Introduction

Many researches on biocomposite materials have been carried out. The research used examined the composition of biocomposite materials consisting of [hydroxyapatite/bioplastic/sericin]. The materials in this study were hydroxyapatite from Sigma Aldrich, tapioca starch bioplastic, and sericin extracted from caterpillar cocoons (Bombyx morii). Biomaterials can be divided into two types, namely natural and artificial biomaterials. Examples of natural biomaterials are collagen, elastin, and chitin, while artificial biomaterials are made of metals, polymers, ceramics, and composites [1]. The highest biocompatibility properties of ceramic biomaterials compared to other biomaterials. Ceramic materials in biomaterials are known as bioceramics [2].

Composite is a material formed from a non-homogeneous combination of two or more constituent materials. Due to the different characteristics of the material, it will produce a new material (composite) that has different properties from the constituent materials [3]. In the study of composite scaffold specimens using biocomposite materials with nanohydroxyapatite (nHA) and tapioca flour (bP) bioplastics. The ratio of nHA/bP biocomposite materials varied at 0, 20, 40, 60, and 80% (w/w), respectively. The tensile strength of the scaffold material was tested with the Diameter Tensile Strength (DTS) test, the highest tensile strength of the nanobiocomposite material was obtained with an nHA/bP ratio of 60% (w/w) [4]. The addition of 2.7% Camphorquinone and the use of ultraviolet light on [hydroxyapatite/bioplastic] biocomposite with a ratio of hA/bP = 47.86%/52% resulted in the fastest solidification time = 408 seconds, and resulted in a DTS test for 2576.74 KPa [5].

Zirconia content at 40% and higher can increase the porosity of the biocomposite material, then cause a decrease of 0.039 MPa in the compressive strength of the hydroxyapatite-zirconia [6].

Volume 4, Issue 1, pages 89–96
p-ISSN 2655-8564, e-ISSN 2685-9432

Rapid prototyping is a method of rapidly creating three-dimensional objects from digital data. Rapid prototypes are different from conventional manufacturing processes which have the principle of making a product with a workpiece by using a cutting tool to get a three-dimensional slice of an object that fits the desired shape, instead using an additive principle that adds material to the already formed layer. Because it uses the additive principle, rapid prototyping is also known as additive manufacturing [7]. In general, the working principle of FDM is based on the deposition of melted thermoplastic filaments onto the workbench to create a layer-by-layer structure with the movement of the extrusion nozzle on the X, Y, and Z axes [8]

Basically, ABEF has a similar working principle to FDM. However, the ABEF method uses a material in the form of a semi-liquid paste for the construction of three-dimensional objects. The paste material is extruded from the container to the nozzle using the screw extrusion principle [9]. In this study, modifications were made to a three-dimensional printer-Portabee machine to modify its working principle from FDM to ABEF system. Modification of the ABEF system by using a single screw extruder.

2 Research Methodology

The ingredients in this study were hydroxyapatite (catalog no. 04328, Sigma-Aldrich) and commercial tapioca flour. Sericin is extracted from the cocoons of the silkworm (Bomix morii) by hydrothermal processing. The citric acid and glycerin materials used are technical grade materials. Biocomposite material is made by wet process or using distilled water. The hydroxyapatite suspension with a percentage of 20% (w/v) was prepared by dispersing HA powder in distilled water with a percentage of citric acid of 10% (w/w). Citric acid is used as a dispersant. The suspension material was mixed using a rotation of 1000 RPM, at a temperature of 250C for 20 hours to obtain a homogeneous suspension.

A suspension of 20% (w/v) tapioca flour was prepared by dispersing tapioca flour powder in distilled water with 3.25% (v/v) glycerin. The tapioca flour suspension was transformed into bioplastic by stirring at 600 RPM at 500C for 15 minutes. The biocomposite paste material was carried out by mixing the HA suspension with bioplastic

Volume 4, Issue 1, pages 89–96

p-ISSN 2655-8564, e-ISSN 2685-9432

at various mass percent ratios (w/w), as shown in Table 1. Sericin was added to each composition in a ratio of 0.3% (w/w) to the mass of the HA suspension.

Table 1. Variations in the composition of biocomposite materials

Level Factor	% mass ratio (w/w)	
	HA suspension	Bioplastic
1	40	60
2	50	50
3	60	40

The creation of a three-dimensional image of a specimen with dimensions of 100 mm x 25 mm x 3mm was created using the Solidworks software, as shown in Figure 1. A three-dimensional image file is an image saved with the 'stl' format type. . File format derived from 'stl'. converted into G-code programming language using Slic3r software. The results of the G-Code program language are entered into a three-dimensional printing machine, and the parameter settings for the material filler setting on the Portabee machine are 10 mm/s, print speed 60 mm/s, and layer height 0.45 mm. This biocomposite paste material is filled into the working material container of the Portabee three-dimensional printing machine. By using a three-dimensional Printing Portable machine that has been modified, the test specimen printouts are obtained by three-dimensional printing using the ABEF system. The process of printing specimens using a modified three-dimensional printer-machine is shown in Figure 2.

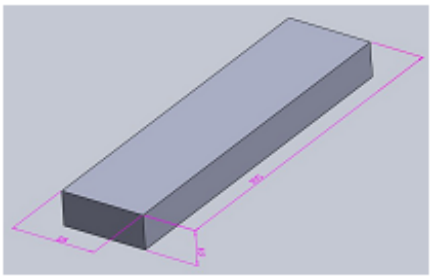

Figure 1. Test specimen design drawing

International Journal of Applied Sciences and Smart Technologies

Volume 4, Issue 1, pages 89–96

p-ISSN 2655-8564, e-ISSN 2685-9432

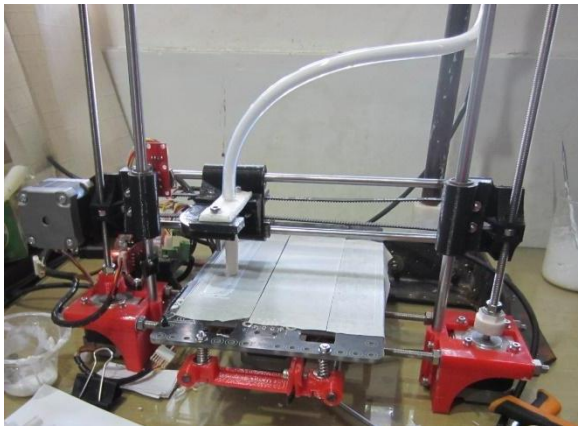

Figure 2. The process of printing test specimens using a three-dimensional printing machine

The dimensions of the test specimens were measured using a digital caliper with an accuracy of 0.01mm. After the results of measuring the dimensions of the test specimens in the form of length, width, and thickness are obtained, the measurement results are then collected. The results of the specimen measurement, the dimension value is the average of the dimension values measured at three different measuring points. Measurement of the dimensions of the specimen is illustrated in Figure 3. The shrinkage of the test specimen is carried out by calculating the final volume of the object from the results of measuring the dimensions of length, width, and thickness.

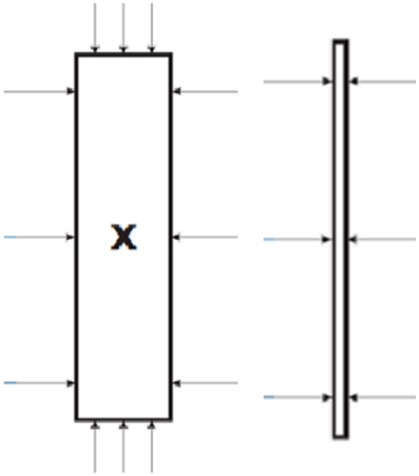

Figure 3. Test specimen measurement point

International Journal of Applied Sciences and Smart Technologies

Volume 4, Issue 1, pages 89–96

p-ISSN 2655-8564, e-ISSN 2685-9432

3 Results and Discussion

The results of the measurement of the dimensions of the test specimens are shown in Table 2. The results of these measurements were analyzed using the Taguchi Method with "smaller is better" characteristics.

Table 2. Measurement results of test specimens

Komposisi		DIMENSI AKHIR SPESIMEN			VOLUME
HA	BP	PANJANG	LEBAR	TEBAL	
40	40	113.09	29.34	2.58	8560.596
40	50	113.97	30.31	1.52	5250.735
40	60	115.86	34.35	2.37	9432.105
50	40	108.5	25.45	1.07	2954.618
50	50	112.75	27.09	1.14	3482.013
50	60	112.91	25.98	1.29	3784.088
60	40	120.07	25.75	1.47	4544.95
60	50	110.32	22.29	1.82	4475.44
60	60	116.24	32.74	1.29	4909.35

3.1. Mean analysis of response parameters

Calculation analysis to determine the smallest value using the mean function. This is because the characteristics of smaller is better in finding the value of the smallest discrepancy/error. In Figure 4 is shown at the smallest shrinkage at the level of 2.

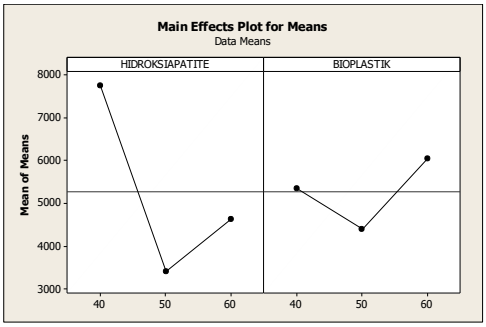

Figure 4. Graph of the analysis of the mean of the parameters affecting the response parameters

3.2. SNR analysis of response parameters

Signal to Noise Ratio (SNR) is useful for knowing the factors that influence the response. The characteristics of the SNR used are the smaller is better function. With

Volume 4, Issue 1, pages 89–96

p-ISSN 2655-8564, e-ISSN 2685-9432

these characteristics, the largest SNR value indicates the smallest error rate. Figure 5 shows the smallest shrinkage response at level 2.

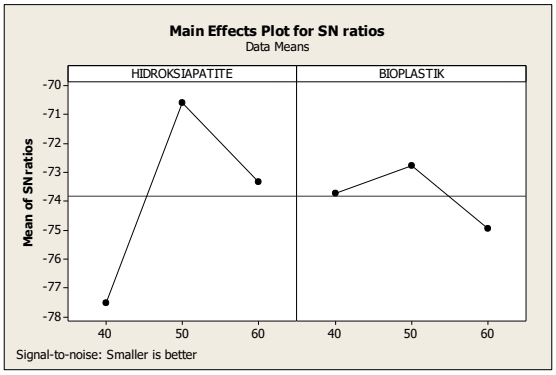

Figure 5. Graph of SNR analysis of parameters affecting response parameters

4 Conclusion

From the research process, it was found that the optimal composition of biocomposite material with the lowest shrinkage was the ratio of HA/bP 50/50 (w/w). In this study, only the composition of the biocomposite paste material for the smallest shrinkage was produced. Further research is needed on the machine process parameters during the specimen printing process.

References

[1] M. Vallet-Regi, Ceramics for Medical Applications. *Journal of Chemical Society*, 97-107, 2001.

[2] H.E. Davis, and J.K Leach, Hybrid and Composite Biomaterials in Tissue Engineering. *Multifunctional Biomaterials and Devices*, 1-26, 2013.

[3] F. Gapsari, P.H. Setyarini, Pengaruh Fraksi Volume Terhadap Kekuatan Tarik dan Lentur Komposit Resin Berpenguat Serbuk Kayu. *Jurnal Rekayasa Mesin*, **1**(2), 59-64, 2010.

[4] A.E. Tontowi, D.P. Perkasa, A. Mahulauw, Erizal, Experimental Study on NanoBiocomposite of [nHA/Bioplastic] for Building a Porous Block Scaffold. Conference NANOCON, Pune, India, 2014.

Volume 4, Issue 1, pages 89–96

p-ISSN 2655-8564, e-ISSN 2685-9432

[5] A.E.Tontowi, D. I. Shafiqy., J.Triyono., Study On A Layered Photo Composite Of Hydroxyapatite-Bioplastic-Camphorquinone Composed By Response Surface Method, *International Journal of Applied Engineering Research*. **10**. Research India Publications, 2015.

[6] E. Pujiyanto., A.E.Tontowi., M.W.Wildan., W. Siswomihardjo., Porous Hydroxyapatite–Zirconia Composites Prepared by Powder Deposition and Pressureless Sintering, *Advanced Materials Research*, **445**, 463-468, Trans Tech Publications, Switzerland, 2012.

[7] M. Heynick, and I.Stotz, Tiga dimensi CAD, CAM and Rapid Prototyping, *LAPA Digital Technology Seminar*,**1**(1), 2006.

[8] A Bagsik, and V. Schoppner, Mechanical Properties of Fused Deposition Modeling Parts Manufactured with ULTEM*9085, ANTEC, Boston, 2011.

[9] M.S. Mason, T. Huang, R.G. Landers, M.C. Leu, G.E. Hilmas, M.W. Hayes, Aqueous-Based Extrusion Fabrication of Ceramics on Demand, *Proceedings of Solid Freeform Fabrication Symposium*, Austin, TX, 124-134, 2007.

International Journal of Applied Sciences and Smart Technologies

Volume 4, Issue 1, pages 97-108

p-ISSN 2655-8564, e-ISSN 2685-9432

Comparison of Static Signature Identification using Artificial Neural Networks Based on Haar, Daubechies and Symlets Wavelet Transformations

R. A. Kumalasanti[1,*]

[1]*Department of Informatics, Faculty of Science and Technology, Sanata Dharma University, Yogyakarta, Indonesia*

[*]*Corresponding Author: rosaliasanti@usd.ac.id*

(Received 21-05-2022; Revised 28-05-2022; Accepted 29-05-2022)

Abstract

Signature is a biometric attribute that is quite important for each individual that can be used as self-identity. Until now, the signature is still used as a sign of legal approval and is agreed upon by everyone. This makes the signature worthy of attention from a security aspect. Various approaches have been proposed in the development of signature identification to minimize signature forgery. This study will discuss the identification of signatures by using the image of the signature on paper. This identification consists of two processes, namely training and testing by utilizing Artificial Neural Networks Backpropagation and Wavelet Transform. Optimal results are obtained by using ANN which has learning rate 0,09, two hidden layers, each 20 and 10 nodes with the most superior Wavelet Haar reaching 94.44%

Keywords: signature, ANN, identification, backpropagation, wavelet

International Journal of Applied Sciences and Smart Technologies

Volume 4, Issue 1, pages 97-108

p-ISSN 2655-8564, e-ISSN 2685-9432

1 Introduction

The rapid development of technology in this era has changed the lifestyle in society. The need for proof of the validity of a transaction or document is important because of the increasing number of diverse activities. Proof of validity in the form of personal data such as signatures is still used as personal data and the validity of a document. Nowadays, many self-data recognition using electronics have been developed, such as iris recognition, fingerprints, facial recognition, and so on, but until now the conventional method in the form of signatures is still very much needed. Signatures are considered a fairly easy way and without expensive costs so that in this modern era, signatures are still considered valid proof of legal use. Personal data is an attribute of each individual whose validity needs to be protected. A signature is a biometric attribute that has ownership which is physiologically the hallmark or character of each individual. Biometrics is the science of automatic recognition of individuals. Biometrics depends on a person's physiology and behavior, so this attribute is attached to an individual with its own uniqueness and characteristics. This proves that the signature is a very important individual attribute and the need for ownership protection. Visually, it is difficult for the human eye to compare signatures that look similar even with the same pattern. This limitation makes signatures often misused by irresponsible parties. Solo Pos once published news in the media that there had been fraudulent acts committed by CPNS applicants. The fraud that occurred in Solo was an act of falsifying signatures on diplomas or important documents contained in the application files of Candidates for Civil Servants (CPNS) by falsifying signatures on documents as much as 40% and this number is not a small number [1]. The news shows that many acts of forging signatures have been carried out and as if it is considered normal. Of course this is detrimental to the owner of the signature and the recipient of the fake document.

Systems with artificial intelligence are needed to help humans compare signatures. Optimal accuracy is the goal of system development in order to minimize signature forgery. The system built will be able to reduce human work in comparing similar signatures with physical visual limitations. A system with advantages in the field of pattern recognition will be built using an artificial neural network and wavelet

Volume 4, Issue 1, pages 97-108
p-ISSN 2655-8564, e-ISSN 2685-9432

switching. ANN consists of neurons that can communicate between network layers. There are four types of wavelets to find optimal accuracy. The input data used is a static signature (offline) with paper media and then scanned with a scanner. In this study, wavelets are used to perform pre-processing. Wavelet is a mathematical function that offers high temporal in high frequency images, while low frequencies will be better frequencies [2]. This advantage is expected to provide quality information so that it can support the learning process in the network.

2 Research Methodology

Handwriting is an interesting object challenging pattern recognition. There are also studies that use handwriting as an object for optical character recognition. The system can be used to recognize English characters (A-A,a-z), numbers (0-9) as well as special characters or symbols (x,$,%,^,&,*). The research was conducted by training a neural network using the Backpropagation algorithm. The results of handwriting pattern recognition using neural networks achieve very high accuracy [3].

Other research related to signatures was also carried out by using Backpropagation ANN. Identification of the signature is expected to provide a sense of security for the owner of the signature. The system is able to recognize the signature and the owner of the signature to reduce the act of forging signatures. This system produces signature identification in the form of accuracy and the face of the signature owner [4].

The next research is about speech signal pattern recognition using wavelet switching and artificial intelligence. Speech signal is biometric data such as handwriting, fingerprint, iris and so on. Biometric is data owned by individuals and has a unique character. The pattern recognition phase of the system built with a neural network design has provided a fairly high recognition accuracy. The accuracy obtained from the speech signal pattern recognition is 81.96% [5]

2.1 Handwriting Signature

A signature is an individual identity that has its own characteristics and patterns. The uniqueness of the signature is often used as an attribute or a marker of the validity of a document. Until now, signatures are still often used anywhere and anytime to mark the

Volume 4, Issue 1, pages 97-108
p-ISSN 2655-8564, e-ISSN 2685-9432

validity of every transaction, even on important documents. Visually, it is difficult for the human eye to compare existing signatures. At first glance, the signature looks similar, but it could be that the signature was forged by an irresponsible person. Human physical limitations (eye disorders, fatigue and focus) can affect the results of interpretation so that it can result in someone's inaccuracy in seeing and even comparing signatures. Based on these problems, a system is needed that can assist in comparing signatures that look the same but can be forged. The system is expected to ease human work in determining the authenticity of signatures. The signature itself is divided into two techniques, namely offline (static) and online (dynamic). A signature with an offline technique is a signature that is done on a piece of paper and scanned for processing, while a signature with an online technique is a signature that is done on a digitizer device. Basically there are three types of forgery, namely random forgery, a signature that is done accidentally because forgers only know the name of the owner of the signature and use his name with his own pattern to forge, while simple forgery is a signature made by someone who has absolutely no practice or even has no previous experience in imitating signatures, and skilled forgery is a sign hand made by someone who has experience in copying signatures [6].

2.2 Artificial Neural Network

Artificial Neural Network (ANN) is one of the reliable networks in recognizing an object. ANN is a mathematical model by analogizing how the human brain works in processing an object. Humans can recognize objects by starting with data collection as memory input so that when they meet the object at a different time, someone will remember the object. The workings of neurons in the human brain have the power to collect signals obtained from adjacent neurons through dendrites. Electrical activity will be transmitted by neurons through axons consisting of thousands of branches. Neurons will work when they get stimuli from outside to be conveyed to neighboring neurons so they can give the correct response. The network is interconnected through several stages or processes and has parallel distributed processing [7]. In ANN, neurons are referred to as nodes and the parts are divided into three parts, namely the input layer, hidden layer and output layer. The number of nodes and the number of layers depends on the needs of the system, so in the ANN learning phase requires some simulation to get the most

Volume 4, Issue 1, pages 97-108

p-ISSN 2655-8564, e-ISSN 2685-9432

appropriate and optimal ANN architecture. ANN characteristically has a layer consisting of a number of nodes (Input layer, Hidden layer and Output layer) which holds the activation function. ANN with input layer, hidden layer and output layer can be seen in Figure 1 below.

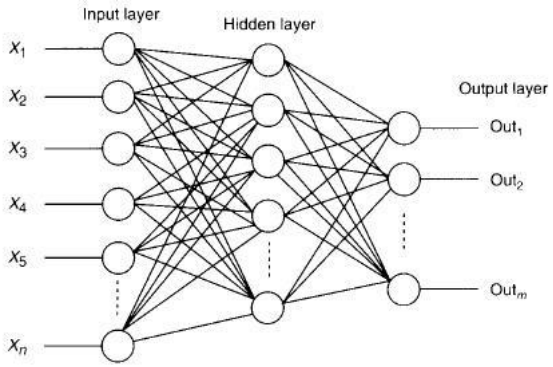

Figure 1. Artificial Neural Network Representation [**8]**

2.3 Backpropagation

In this study, ANN was collaborated with the Backpopagation algorithm in identifying signature patterns. The way the Backpropagation algorithm works is by utilizing an error condition in the output layer, it will change the weight by means of back propagation after the forward propagation process is complete [9]. The backpropagation algorithm cycle consists of two stages, namely forward pass (forward propagation) and backward pass (backward propagation). The backpropagation algorithm is a guided learning approach because the desired result is already known. After finishing processing, there may be differences in the predicted results. If this happens, the network will immediately be subjected to backward propagation to get a smaller error tolerance. A smaller error will also provide an optimal percentage of the identification results.

2.5. Wavelet Transform

Preprocessing in this study utilizes wavelet transfer in preprocessing to represent the time and shape frequency signal. Wavelet switching is one of the mathematical tools that has a transfer layer function so that it can produce coefficients that represent the characteristics of the signal [10]. Wavelet has advantages, namely in terms of signal analysis. The wavelet's signal analysis is multi-resolution so that it provides better signal

Volume 4, Issue 1, pages 97-108
p-ISSN 2655-8564, e-ISSN 2685-9432

accuracy and analysis. The advantages of wavelets are because of their advantages in providing multi-resolution signals. It aims to analyze features that may not be detected by one resolution so that they will still be detected using another resolution [11] [12]. Discrete Wavelet Transform (DWT) is an option as an efficient method that can be used to retrieve information in the image in the form of discrete data. In utilizing wavelets, it is also necessary to determine the level of decomposition to obtain optimal accuracy. Low resolution image is decomposed by DWT into different subbands, namely low-low (LL), low-high (LH), high-low (HL), and high-high (HH). Figure 2 is a decomposition image on wavelet level 2.

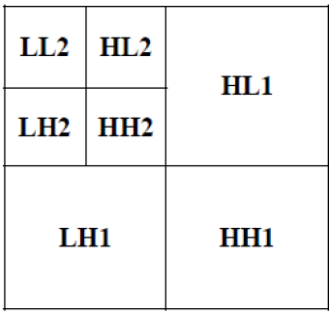

Figure 2. Level 2 decomposition on Wavelet **[10]**

3 Results and Discussion

Identification of the signature image is divided into two phases, namely training and testing. This image data is obtained from 15 individuals where each individual will write as many as 6 signatures as input data. The signature image sample with a size of 256x256 pixels will be subjected to preprocessing. The static signature image is scanned using a scanner to reduce limitations on rotation, and shooting distance. This digital image is then cut into a size of 256x256 pixels and then converted into a black and white image (threshold). Black and white images will make it easier for the system to learn image patterns and provide a lighter computing load than Greyscale or RGB. The black and white image will then be subjected to some predetermined wavelets.

This study uses several kinds of wavelets to obtain optimal accuracy. Normalization is done before training using Backpropagation ANN. In this training phase, the results will be weighted. Each weight according to its respective ID will be stored in the data

Volume 4, Issue 1, pages 97-108
p-ISSN 2655-8564, e-ISSN 2685-9432

store. The results of this training are in the form of weights that will be stored in the data store. This stored weight will be input data which will later be seen for its ability to produce pattern characteristics. This input data is then tested on several existing wavelets. The signature image identification flow can be seen in Figure 3.

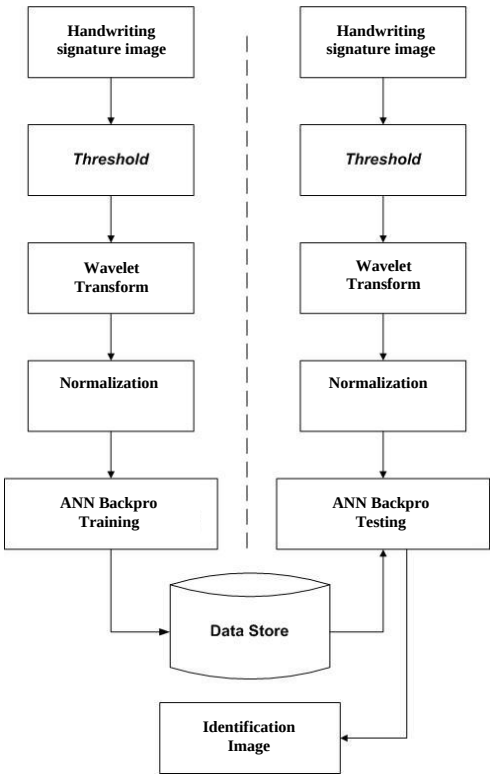

Figure 3. Flow Diagram

Each signature image is resized to 256x256. If the image size is smaller, the computational load will be lighter, but the pattern characteristics will also decrease. The size of 256x256 is an option in implementing signature identification. The simulation carried out has the aim of getting optimal accuracy from the existing wavelets. The wavelets being tested are Haar Wavelets, Daubechies 2, Daubechies 3, and Symlets 3. The selection of these four wavelets refers to previous studies which obtained a fairly high accuracy in pattern recognition identification. The wavelet decomposition used is level 4 in obtaining information. The choice of level or decomposition is also related to the amount of information. The higher the level on the wavelet, the less information will be obtained. So in this study is expected to provide optimal identification results as well.

Volume 4, Issue 1, pages 97-108

p-ISSN 2655-8564, e-ISSN 2685-9432

The learning rate used is 0.9 with two hidden layers of 20 and 10 nodes, respectively. Figure 4 shows the process of image signature training, and the simulation of the four wavelets can be seen in Figure 5. The figures below also shows the MSE and epoch results for each wavelet.

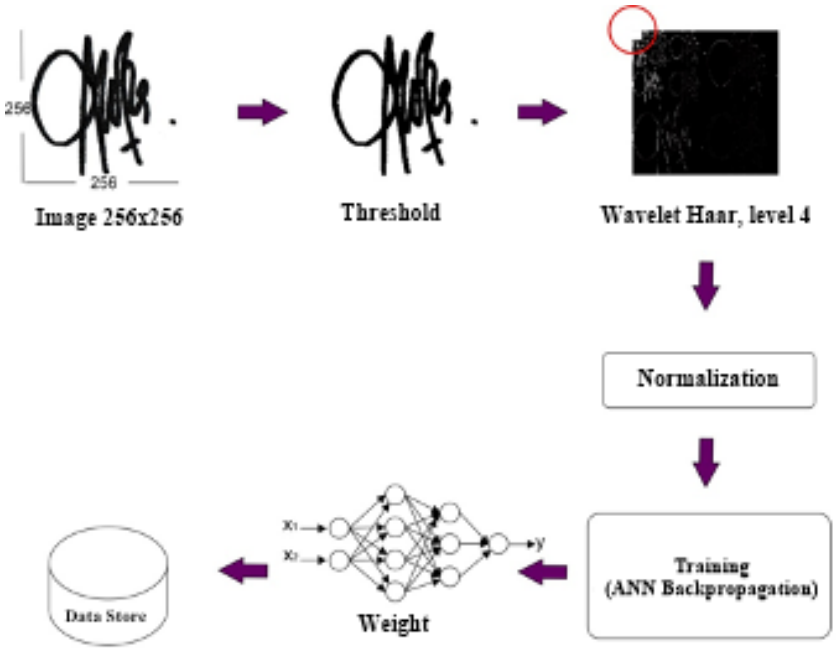

Figure 4. Training on the Identification process

Table 1. Image Identification Comparison Results with level 4 wavelet switching, learning rate 0.09.

Wavelet	Epoch	MSE	Accuracy
Haar	100000	0,0909	94,44%
Db2	100000	0,0634	87,78%
Db3	1382	0,0858	91,11%
Sym3	16724	0,1022	87,78%

International Journal of Applied Sciences and Smart Technologies

Volume 4, Issue 1, pages 97-108

p-ISSN 2655-8564, e-ISSN 2685-9432

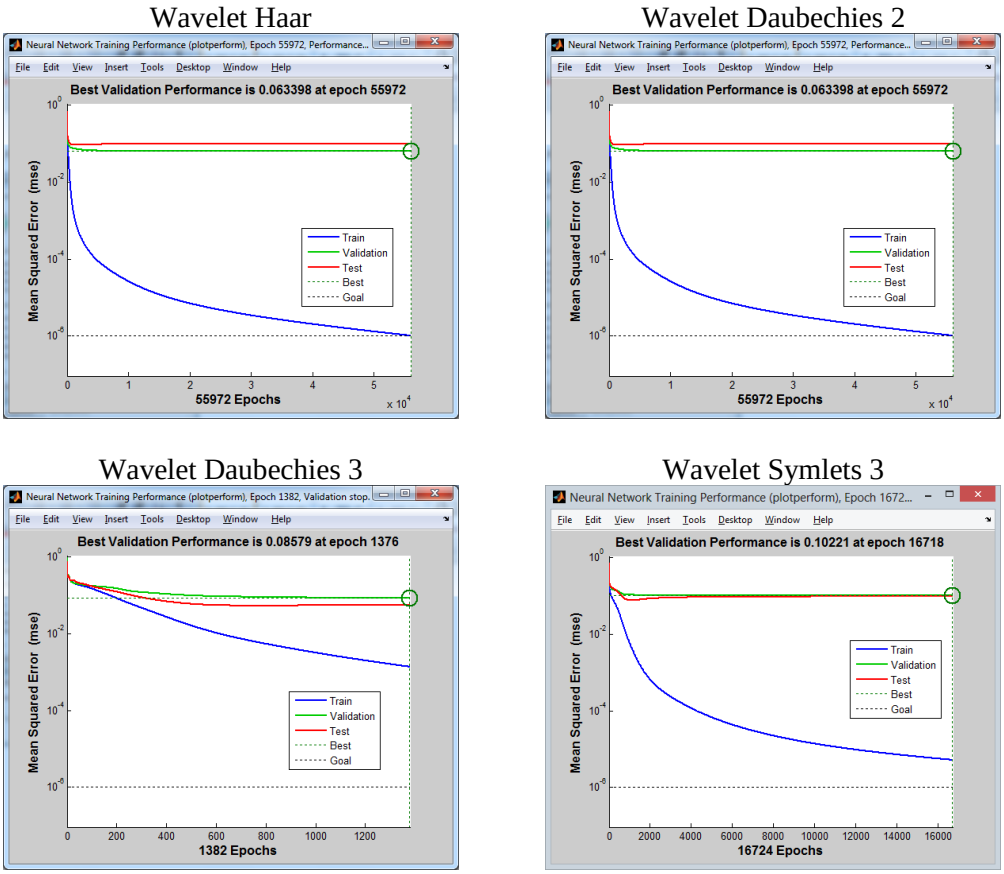

Figure 5. ANN Performance Results using wavelet

The accuracy results from Table 1 show that each wavelet has its own reliability in providing accuracy. Wavelet Haar, epoch 100000, MSE 0.0909 is the most superior by getting an accuracy of 94.44%. Backpropagation ANN achieves optimal results in performing static signature pattern recognition by utilizing the advantages of wavelets in preprocessing

4 Conclusion

The identification of the signature image has been successfully applied by involving two processes, namely training and testing. Based on the simulation that has been done, it can be concluded that the comparison of signature identification using wavelet switching and ANN has been successfully constructed. Image size 256 x 256 by scanning using a scanner and preprocessing several simulations have been carried out to get optimal results. Simulations have been carried out on several types of wavelets,

namely Haar, Daubechies 2, Daubechies 3, Symlets 3, with 4 levels of decomposition and a learning rate of 0.09. The simulations carried out resulted in the most superior accuracy being 94.44% using the Haar wavelet transformation.

References

[1] M. Khamdi, "Solo Pos," 20 October 2013. [Online]. Available: www.solopos.com. [Accessed 13 August 2021].

[2] M. G. Haleem, L. E. George and H. M. Bayti, "Fingerprint Recognition Using Haar Wavelet Transformation and Local Ridge Attributes Only," *International Journal of Advanced Research in Computer Science and Software Engineering*, **4** (1), 122-130, January 2014.

[3] S. S. Kharkhar, H. J. Mali, S. S. Gandhari, S. S. Shrikande and D. K. Chitre, "Handwriting Recognition Using Neural Network," *International Journal of Engineering Development and Research*, **5**(4), pp. 1179-1181, December 2017.

[4] P. Sovia, M. Yanto and W. Nursany, "Implementation of Signature Recognition Using Backpropagation," *Journal of Computer Science and Information Technology*, **1**(1), 30-44, December 2016.

[5] O. Rangel, D. Amaya and O. Ramos, "Pattern Recognition of Speech Signals Using Wavelet Transform and Artificial Intelligence," *International Journal of Applied Engineering Research*, **12**(21), 11088-11093, August 2017.

[6] Y. Y. Munaye and G. B. Tarekegn, "Signature Recognition System Using Artificial Neural Network," *European Journal of Computer Science and Information Technology*, **6**(2), 42-47, April 2018.

[7] N. Z. Zacharis, "Predicting Student Academic Performance in Blended Learning Using Artificial Neural Network," *International Journal of Articial Intelligence and Applications*, **7**(5), 17-29, September 2016.

[8] P. G. Patil and R. S. Hegadi, "Offline Handwritten Signature Classification Using Wavelet and Support Vector Machines," *International Journal of Engineering Science and Innovative Technology*, **2**(3), 37-42, May 2013.

[9] I.P.B.D. Purwanta, C.P.Kuntor Adi,N.P.N.P. Dewi, “Backpropagation Neural Network for Book Classification Using the Image Cover” *International Journal of Applied Sciences and Smart Technologies*, **2**(2), 179-196, December 2020.

[10] Suma'inna, "Detection of Cardiac Abnormalities Based on ECG Pattern Recognition Using Wavelet and Artificial Neural Network," Pushpa Publishing House, **76**(1), 111-122, May 2013.

[11] P. Meibner, H. Watschke, J. Winter and T. Vietor, "Artificial Neural Network Based Material Parameter Identification for Numerical Simulations of Additively Manufactured Parts by Material Extrusion," *MDPI*, **12**(2949), 1-28, December 2020.

[12] J. M. Castillo, J. M. Cspedes and H. E. Cuchango, "Water Level Prediction Using Artificial Neural Network Model," *International Journal of Applied Engineering Research*, **13**(19), 14378-14381, July 2018.

International Journal of Applied Sciences and Smart Technologies

Volume 4, Issue 1, pages 97-108

p-ISSN 2655-8564, e-ISSN 2685-9432

This page intentionally left blank

International Journal of Applied Sciences and Smart Technologies

Volume 4, Issue 1, pages 109–120

p-ISSN 2655-8564, e-ISSN 2685-9432

The influence of artificial aging on tensile properties of Al 6061-T4

Freddy. S. R. Taebenu[1], Heryoga Winarbawa[1], Rines[1], Budi Setyahandana[1] and I. M. W. Ekaputra[1, *]

[1]*Mechanical Engineering Department, Faculty of Science and Technology, Sanata Dharma University, Yogyakarta*

[*]*Corresponding Author: made@usd.ac.id*

(Received 22-05-2022; Revised 27-05-2022; Accepted 28-05-2022)

Abstract

This paper presents an explanation related to experimental testing in the form of the tensile properties of Al 6061. Al 6061 was heat treated by the precipitation hardening method. The precipitation hardening consisted of T4 and T6 treatment. Al 6061 samples were heat-treated at a temperature of 430°C for 2 hours, then cooled slowly at room temperature. The T4 was conducted at a temperature of 530°C for 2 hours, followed by rapid cooling in a water medium and natural ageing at a temperature of 70°C for six days. Temperature T6 is the final process of applying precipitation hardening treatment to Al 6061. Temperature T6 is carried out at 530°C for 2 hours, then cooled rapidly in a water medium and continued with artificial ageing at 190°C with a variation of ageing time for 3 hours, 5 hours, and 7 hours. The effect of the applied treatment was observed to increase the maximum strength value of the tensile test of Al 6061.

Keywords: Al 6061, precipitation hardening, ultimate tensile strength

International Journal of Applied Sciences and Smart Technologies

Volume 4, Issue 1, pages 109–120

p-ISSN 2655-8564, e-ISSN 2685-9432

1 Introduction

For over fifty years, aluminium (Al) alloy has ranked second after iron and steel, widely supplied in the metal market. The rapid growth in demand for Als is attributed to the attractive characteristics of these alloys [1]. Aluminium alloy has been used in aircraft construction since the 1930s. As the industrial sector with the most use of Al materials, the aerospace industry relies heavily on Al types 2024 and 7075. Considerations for using Al 6061 are based on the properties of the alloy, namely low weight, good strength, formability, weldability, and durability. High corrosion resistance and low cost [2]. Although generally more expensive than ferrous metal, the applicability of Al has increased in use and has become competitive with ferrous alloys [3, 4]. Various heat treatment studies on Al 6061 were selected to improve the properties of the alloy's mechanical structure. Heat treatment is a series of processes that involve heating and cooling metallic materials in their solid-state.

The applied heat treatment aims to cause desired changes in the mechanical structure and the properties of the metal parts. By applying heat treatment, metals can be made tougher, stronger, and more resistant to impact. Under the same conditions, heat treatment can also make metal materials softer and more elastic [5]. In particular, the effect of solution heat treatment and artificial ageing has been studied on the mechanical properties of Al 7030 and 7108. The obtained results were the relationship between the decrease in the peak strength value of the mechanical properties of Al 7030 and 7108 on the widening of the size distribution of the deposits. It is further explained that differences in the type, volume fraction, size and distribution of the deposited particles regulate the properties and changes that occur due to time and temperature, which is based on the initial state of the structure. The initial structure of a wrought material can vary depending on the structure of the material not undergoing crystallization to recrystallization so that these conditions, as well as the time and temperature of the precipitation heat treatment, affect the final structure and the resulting mechanical properties [6, 7, 8, 9]. The metastable precursor of the equilibrium phase 6061 is precipitated in a process involving one or more combinations of complex elements. Chemical content, heat treatment parameters, and casting conditions significantly affect

Volume 4, Issue 1, pages 109–120
p-ISSN 2655-8564, e-ISSN 2685-9432

the extrusion ability and determine the combined microstructure. These results show that the properties of some Al can be increased through a specific heat-treatment process. Heat treatment can be done either by heating the solution or artificial ageing. In the process of heating the solution, the alloy is heated to a temperature range of 400°C to 530°C and then rapidly cooled in an aqueous medium to room temperature. Especially for the Al 6xxx group, the artificial ageing treatment is carried out at a temperature of 200 °C, while the average ageing hardening temperature is usually 160°C to 200°C [9, 10].

Aluminium alloy subjected to a solution heating treatment is believed to have varying mechanical properties, affecting the machining capabilities to which the Al is applied. Some of the mechanical properties possessed by Al 6061 are associated with the type of treatment, such as solution treatment, ageing time, and temperature applied to the alloy [11]. Al 6061 has an intermetallic phase structure composed of Si and generally alloys composed of AlMgSi elements and related alloys. Maximum strength can be achieved by precipitation hardening, but the alloy's ductility is reduced. Conversely, the ductility can be increased by using an annealing process, but this process causes the strength of the alloy to decrease [12, 13] into the artificial ageing treatment for 98 hours at 175°C. Based on the results studied, the microstructural and mechanical properties of the specimens were not affected by the artificial ageing treatment applied as a result of the previous precipitation strengthening process [14, 15]. Based on the research literature that has been conducted [16, 17], the T6 tempering process in alloy 6061 involves the formation of very thin deposits. The precipitate formed represents β", which is oriented to the three sequences of deposits formed in the alloy's matrix. The size of the alloy matrix formed is on a nanometric scale and is coherent. From the considerations carried out, several studies provide further details showing the order in detail of the composition of the phases contained in the Al-Mg-Si alloy. The general compositions for deposits formed on Als are listed in Table 1.

The study presented includes experimental observations of tensile tests using a universal testing machine with 200 kN capacity and investigated Al 6061-T4 to characterize tensile test properties under T6 temper ageing conditions. From the observations made in the test, it is possible to determine the distribution of the tensile

Volume 4, Issue 1, pages 109–120
p-ISSN 2655-8564, e-ISSN 2685-9432

properties experienced by the alloy. The initial condition is shown as a thermal loading process, namely the application of annealing or normalizing treatments, temper T4, and temper T6. The thermal loading process applied to alloy 6061 is limited to the solid-state of the alloy. Therefore, the maximum temperature to be used is under the solidus temperature of 582°C. After the thermal loading process is applied, it is followed by observing the tensile test results through computerization. From the review of the cited literature, it was observed that there was no work on artificial ageing or the response to precipitation hardening of 6061 Als applying T4 and T6 temper heat treatment by varying the time of artificial ageing, as well as their effect on the tensile behaviour of 6061-T4 Als. Therefore, the study focused on the variation of the ageing time of temper T6 on the tensile strength behaviour of 6061-T4.

Table 1. Compositions of the precipitates contained in Al-Mg-Si alloys.

Phase	Composition
GP zone	Mg_1Si_1
β"	Mg_5Si_6
β′	Mg_9Si_5
β	Mg_2Si

2 Research Methodology

2.1 Specimen preparation

Cylindrical specimens with a length of 100 mm and a specimen diameter of 22 mm are supplied in the form of extruded rods which are then subjected to conventional machining processes to reduce the specimen diameter to 17 mm. In the following process, the specimen is formed by the standard dimensions specified in the form of ASTM E8 for tensile strength testing. After going through various heat treatments given to each specimen, the specimen is then reconstructed through conventional machining. For the tensile test, the specimens formed by conventional machining for each variation amount to two specimens with four variations, so the total number of specimens provided is eight. Several specimens of Al 6061-T4 prepared for tensile strength testing are shown in Figure 1 based on the ASTM E8 standard. Based on the time variations in the artificial ageing treatment of temper T6 applied to Al 6061-T4, the specimens are sequentially categorized into several groupings in Table 2.

International Journal of Applied Sciences and Smart Technologies

Volume 4, Issue 1, pages 109–120

p-ISSN 2655-8564, e-ISSN 2685-9432

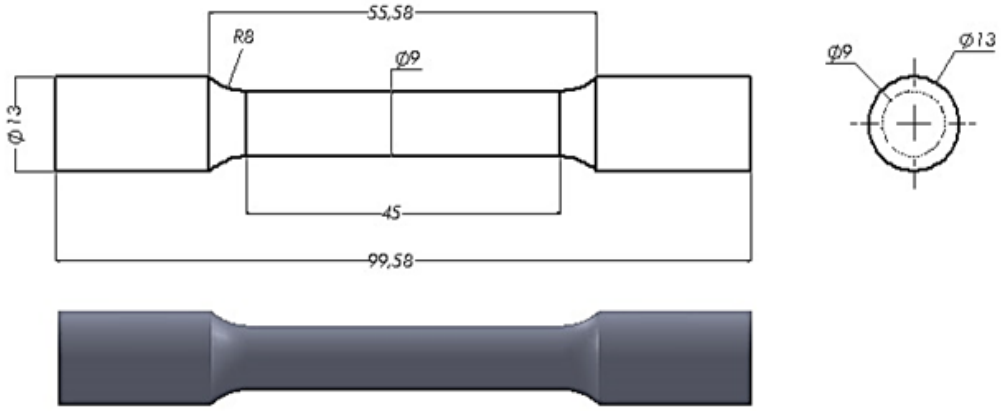

Figure 1. Tensile test specimen

Table 2. Categorization of specimens

Specimen category	Condition of specimen
a	Base metal without treatment
b	SHT 530°C for 2 h and AA 190°C for 3 h
c	SHT 530°C for 2 h and AA 190°C for 5 h
d	SHT 530°C for 2 h and AA 190°C for 7 h

2.2 Heat Treatment

In metallurgical components, several processes affect the hardening mechanism of the mechanical structure of a material. The processes applied to Al 6061 include the annealing or normalizing processes, temper T4, and temper T6. In the primary process, specimens were given normalizing heat treatment at a temperature of 430°C and held for 2 hours. Then, the specimens were cooled slowly at room temperature. Furthermore, the specimens were heated for 2 hours at 530°C to obtain a solid solution phase before being rapidly cooled in water media to room temperature. Then in the following process, the specimens are left at room temperature for six days or 144 hours. This process is a series of T4 tempering treatment processes. The heat treatment of solid solution T6 and selected artificial ageing for Al 6061 is the final process of hardening the alloy's structure. First, the alloy was heat-treated for 2 hours at a temperature of 530°C and then cooled in a water medium at room temperature before being heated again with a variation of 3, 5, and 7 hours at a temperature of 190°C.

Volume 4, Issue 1, pages 109–120

p-ISSN 2655-8564, e-ISSN 2685-9432

2.3 Tension Test

The tensile test is one of the most commonly used mechanical stress-strain tests. The tensile testing process begins with fixing the specimen on the holding grip, then continuously and simultaneously measuring the applied load occurs instantly. The output of the tensile strength test is recorded as the relationship of the load or force applied to the cross-sectional area of the specimen surface. The specimens, with and without additional heat treatment, were tested under uniaxial loads with high static and load loading rates. Tensile strength tests on specimens were determined using a universal testing machine with a capacity of 200 kN with a deformation rate of 0.01mm per second.

3 Results and Discussion

3.1. Tensile Test Data

Based on the tensile test result, the mechanical properties of the 6061-T4 Al specimen were obtained, shown in Table 3. Investigation of the effects of artificial ageing time variation applied to Al 6061-T4 is reported in this analysis. The behaviour of the tensile properties is analyzed in a tensile test cycle, the maximum tensile strength and the limit of tensile strength before the material fracture, elastic strength, plastic character, and the relationship to the stress-strain cycle. It is shown visually in Figure 2 that the maximum strength value of the highest tensile test on Al 6061-T4 is obtained at the ageing time condition of 3 hours, and then sequentially followed by the ageing time conditions of 5 and 7 hours and finally, normal conditions.

Tabel 3. Mechanical properties of the specimens aluminium alloy 6061-T4.

Specimen category	a	b	c	d
Ultimate tensile stress (MPa)	102.36	264.73	219.74	199.51
Fracture stress (MPa)	66.11	204.10	162.34	111.07
Yield stress (MPa)	48.164	217.19	177.67	175.31
Modulus elasticity (MPa)	2305.76	3086.40	2003.60	2712.85
Strain hardening exponent	0.19	0.031	0.088	0.048

International Journal of Applied Sciences and Smart Technologies

Volume 4, Issue 1, pages 109–120

p-ISSN 2655-8564, e-ISSN 2685-9432

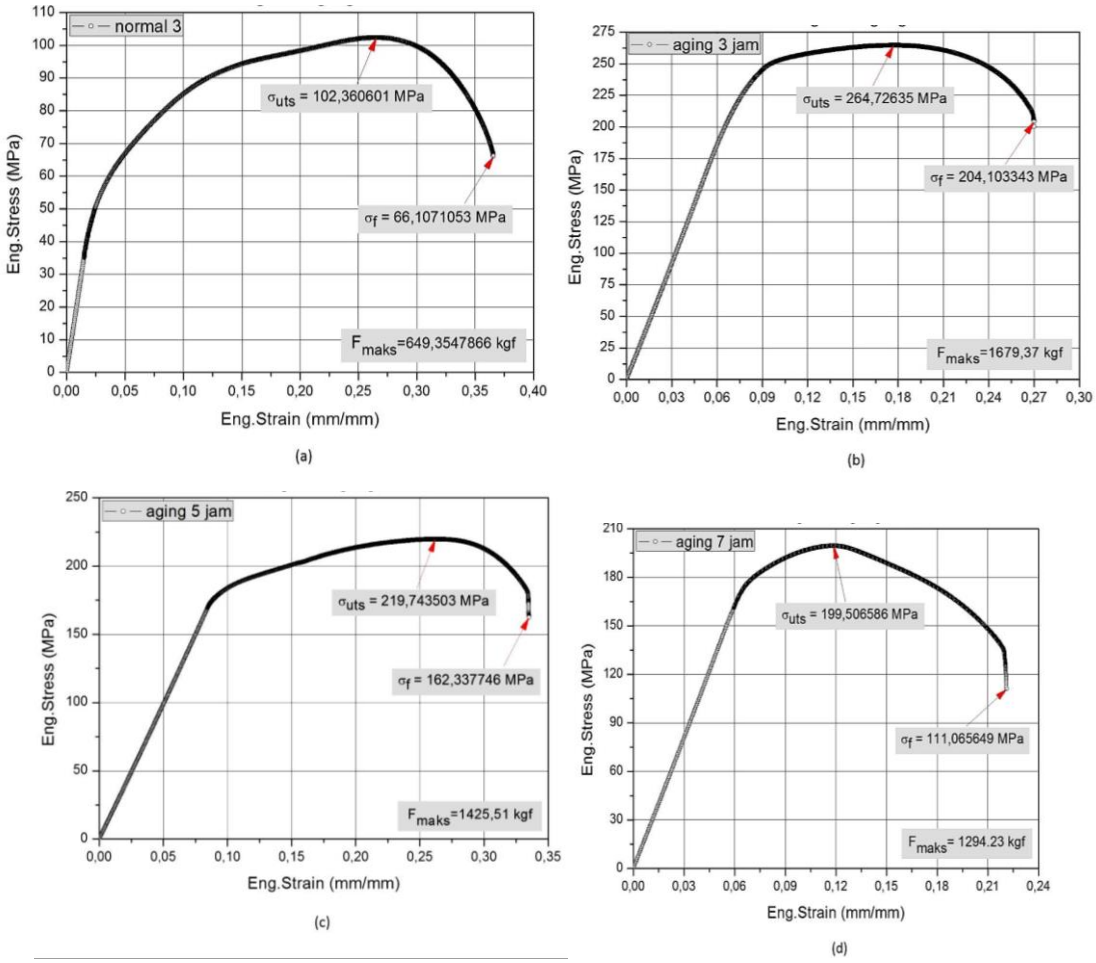

Figure 2. Tensile test result with various aging time

Inversely proportional to the maximum tensile strength, the highest durability in Al 6061-T4 starts under normal conditions and then continues with the ageing time conditions of 5, 3, and 7 hours. Durability, or can be referred to as the mechanical resistance of a material, is a condition in which the material can maintain the structure of the atomic particles in the material matrix in a non-loading state until it reaches a weakening state and finally experiences final failure. The increase in change in the shape of the material structure is represented by the increase in the data points shown in Figure 2. Figure 3 shows that the highest maximum tensile strength value starts from the condition 3 hours ageing time of 264,73 MPa. Then, the 5 hours ageing time condition

Volume 4, Issue 1, pages 109–120
p-ISSN 2655-8564, e-ISSN 2685-9432

is 219.74 MPa, followed by 7 hours ageing time of 199.51 MPa, and finally, the normal condition is 102.36 MPa.

In addition to the maximum tensile strength value, Figure 2 also shows the value of the endurance limit or mechanical resistance of Al 6061-T4, which is shown as the value of fracture stress. Based on the Figure, the value of each fracture stress is shown as follows, starting from the normal condition of 66.11 MPa with the resulting stretch range reaching ± 0.35 mm/mm, then the 5-hour ageing time condition is 162.34 MPa with The resulting stretch range is ± 0.30 mm/mm, then the 3 hours ageing condition is 204.10 MPa with a range of ± 0.27 mm/mm stretch, and finally the 7 hours ageing time condition is 111.07 MPa with the resulting stretch range of ± 0.21 mm/mm. The results obtained in the analysis of Figure 3 show that there are differences in data values between fracture stress and stretch range; the basis of the comparison between the two mechanical resistance parameters lies in the object seen from the behaviour of the 6061-T4 Al structure, namely the characteristics of ductile and brittle properties. Specifically, based on the theory, the characteristics of ductile and brittle materials can be determined by comparing the value of the maximum tensile strength to the yield stress. Furthermore, the comparison is limited by specific value criteria, which are factors of the ductility and brittle characteristics of the material. The resulting value of the comparison is also known as the stretch hardening ratio value. Based on the theory, it is explained that if the stretch hardening ratio value is > 1.4, the alloy material will experience cyclically softening. At the same time, for the stretch hardening ratio value > 1.2, the alloy material will experience cyclic hardening. Through Table 4, the highest comparative value for the stretch hardening ratio is obtained under normal conditions. In order, the value of the stretch hardening ratio obtained is as follows, namely, under normal conditions, the yield hardening ratio value is 2.13, the condition for 5 hours of ageing is 1.24, the condition for 3 hours the ageing time is 1.22, and the ageing time condition 7 hours of 1.14.

These results show that under normal conditions, the 6061-T4 experiences softening in a cycle, as evidenced by the stretch hardening ratio value more significant than the reference factor in theory, namely 1.4. This proves that the stretch hardening ratio value under normal conditions describes the tensile properties of Al 6061-T4, which is

Volume 4, Issue 1, pages 109–120
p-ISSN 2655-8564, e-ISSN 2685-9432

cyclically softened. Conversely, in the conditions of variation in artificial ageing, the structure of the Al 6061-T4 material undergoes cyclical hardening, which is evidenced by the hardening ratio obtained in the range of reference factors. Thus, the conditions for artificial ageing variations meet the established standards that the resulting value is between the range 1,2 to 1,4. Furthermore, the calculations showed that the highest value achieved in the stretch hardening ratio values is produced at the ageing time condition of 5 hours. Therefore, the ageing time condition is 3 hours, and the ageing time condition is 7 hours. From another point of view, it can also be seen that the stretch hardening exponential value is for the stretch hardening exponential value > 0.2. Therefore, the alloy material will harden cyclically. In contrast, in the condition of the stretch hardening exponential value > 0.1, the alloy material will experience softening on a cycle basis. For average conditions, the stretch hardening exponent's value is equal to 0.19372 > 0.1 so that the material is softened cyclically.

4 Conclusion

Al 6061 can experience an increase in strength by applying T4 and T6 temper treatment with ageing time variations of 3, 5, and 7 hours. A decrease follows an increase in the strength properties of the alloy in ductility. The highest strength value was achieved at 3 hours ageing time of 264.73 MPa with a reduction in ductility of 10% in terms of a decrease in the stretch value to normal conditions. From the results shown, it is also explained that each variation of ageing time that is applied successfully increases the strength of aluminum 6061-T4 alloy significantly while maintaining the ductility and elasticity of the alloy with a reduction in value that is not too far. Investigations on the stretch hardening ratio value and the stretch hardening exponent proved that the increase in strength of the Al 6061-T4 occurred due to the structure of the alloy matrix successfully hardening or strengthening with the formation of an intermetallic phase, namely Si in the alloy matrix structure.

Volume 4, Issue 1, pages 109–120

p-ISSN 2655-8564, e-ISSN 2685-9432

References

[1] C. F. Tan, M. R. Said, "Effect of hardness test on precipitation hardening Al 6061-T6", *Chiang Mai Journal of Science*, **36**(3), 276-286, 2009.

[2] M.F.I.A. Imam, dkk, "Influence of Heat Treatment on Fatigue and Fracture Behavior of Aluminium Alloy", *Journal of Engineering Science and Technology*, **10**(6), 730 – 742, School of Engineering: Taylor's University, 2015.

[3] J.E. Hatch, ed, "Aluminium: Properties and Physical Metallurgy", ASM Metals Park, OH, 231-32, 1984

[4] Lehmus D, and Banhart J, "Materials Science and Engineering A", **349**, 98, 2003

[5] J. Ridwan, dkk, "Effect of Heat Treatment on Microstructure and Mechanical Properties of 6061 Aluminium Alloy', **Journal of Engineering and Technology, 5**(1), 2014

[6] Fahrettin Ozturk, "Effects of aging parameters on formability of 6061-O alloy", *Journal of materials and design*, **31**, 487-4852, 2010.

[7] H.R. Shahverdia, "Effects of time and temperature on the creep forming of 7075 Al Springback and mechanical properties", *Journal of material science and engineering*, **A 528**, 8795-8799, 2011.

[8] G.E. Totten, C.E. Bates, N.A. Clinton, *Handbook of Quenchants and Quenching Technology*, ASM International, **62**, 140-144, 1993

[9] G.E. Totten, Howes, Maurice A.H, *Steel Heat Treatment Handbook*, Marcel Dekker, Inc, 1997.

[10] D. Maisonnette, M. Suery, D. Nelias a, P. Chaudet, T. Epicier, "Effects of heat treatments on the microstructure and mechanical properties of a 6061 aluminium alloy", *Materials Science and Engineering*, Elsevier, **528**(6), 2718-2724, 2018

[11] H. Demir, S. Gunduz, "The effect of aging on machinability of 6061 aluminium alloy", *Materials & Design*, **30**(5), 1480-1483, 2009.

[12] Lehmus D, Banhart J, and Rodriguez-Perez MA, "Materials Science and Technology", **18**, 474, 2002.

[13] S. Kalpakjian dan S.R. Schmid, "Manufacturing Engineering and Technology", Sixth Edition, Prentice Hall, New York, 2009

Volume 4, Issue 1, pages 109–120

p-ISSN 2655-8564, e-ISSN 2685-9432

[14] G. Mro´wka-Nowotnik, "Influence of chemical composition variation and heat treatment on microstructure and mechanical properties of 6xxx alloys", *Archives of Materials Science and Engineering*, **46**(2), 98-107, 2010.

[15] Shatha M. Raja, Hassan A. Abdulhadi, Khairallah S. Jabur, Ghusoon R. Mohammed, "Aging Time Effects on the Mechanical Properties of Al 6061-T6 Alloy", *Engineering, Technology & Applied Science Research*, **8**(4), 3113-3115, 2018.

[16] N. R. Prabhu Swamy, C. S. Ramesh, T. Chandrashekar, "Effect of heat treatment on strength and abrasive wear behavior of Al6061-SiC composites", *Bulletin of Materials Science*, **33**(1), 49-54, 2010.

[17] K. Matsuda, S. Ikeno, T. Sato, "HRTEM Study of Nano-Precipitation Phases in 6000 Series Als", Science, *Technology and Education of Microscopy: an Overview*, 152–162, 2003.

International Journal of Applied Sciences and Smart Technologies

Volume 4, Issue 1, pages 109–120

p-ISSN 2655-8564, e-ISSN 2685-9432

This page intentionally left blank

International Journal of Applied Sciences and Smart Technologies

Volume 4, Issue 1, pages 121–122

p-ISSN 2655-8564, e-ISSN 2685-9432

AUTHOR GUIDELINES

Author guidelines are available at the journal website:
http://e-journal.usd.ac.id/index.php/IJASST/about/submissions#authorGuidelines

International Journal of Applied Sciences and Smart Technologies

Volume 4, Issue 1, pages 121–122

p-ISSN 2655-8564, e-ISSN 2685-9432

This page intentionally left blank